CATALYTIC DEOXYGENATION OF HEPTANOIC ACID TO α-OLEFINS OVER SUPPORTED Pt CATALYSTS

PATCHAREE JUTALIKITWONG

A THESIS SUBMITTED IN PARTIAL FULFILLMENT

OF THE REQUIREMENT FOR THE DEGREE OF MASTER OF SCIENCE IN

PETROCHEMICALS AND HYDROCARBON CHEMISTRY

DEPARTMENT OF CHEMISTRY

FACULTY OF SCIENCE

KING MONGKUT'S INSTITUTE OF TECHNOLOGY LADKRABANG

2017

KMITL-2017-SC-M-015-001

Thesis Title	Catalytic deoxygenation of heptanoic acid to α-olefins over supported Pt catalysts
Student Name	Patcharee Jutalikitwong
Student ID	58605038
Degree	Master of Science (Petrochemicals and hydrocarbon chemistry)
Department	Chemistry
Year	2017
Thesis Advisor	Assoc. Prof. Dr. Tawan Sooknoi
Thesis Co-advisor	Asst. Prof. Dr. Tosapol Maluangnont

Abstract

In this work, the catalytic deoxygenation of *n*-heptanoic acid to 1-hexene was conducted as a model reaction for the production of α-olefins from fatty acids. Several Pt catalysts (0.5 wt%) supported on SiO_2 (or TiO_2), including the bimetallic Pt-M catalysts with different metal promoters M such as Fe (0.2 wt%), Ga (0.2 wt%), and Sn (0.2-0.5 wt%) were synthesized by incipient wetness impregnation. The catalysts were reduced *in-situ* at 400 °C prior to the catalytic activity evaluation at 320-400 °C under atmospheric pressure of H_2 in a fixed bed flow reactor. It was found that the 0.5Pt/SiO_2 catalyst was active in several reactions including (i) decarbonylation (to produce hexene, via the *n*-heptanal intermediate) and (ii) decarboxylation, and (iii) hexene hydrogenation (the latter two producing *n*-hexane). In contrast, the bimetallic Pt-M catalysts (M = Fe, Ga and Sn) significantly suppressed the hydrogenation activity. So, as high as 50% selectivity to hexene (at 50 % conversion of *n*-heptanoic acid) was obtained over 0.5Pt-0.5Sn/SiO_2 at 400 °C. In addition, the increase of Sn content (0.2 to 0.5 wt%) resulted in the formation of several bimetallic Pt-Sn phases (PtSn, Pt_2Sn_3 and $PtSn_2$), which helped to suppress the hydrogenation of hexene, leading to the high hexene selectivity.

On the other hand, the low activity but high selectivity to the ketonization product (7-tridecanone, 91% selectivity) over 0.5Pt-0.2Sn/TiO_2 was obtained and ascribed to the Lewis acid character of the oxygen vacancy site in TiO_2. The strong adsorption of *n*-heptanoic acid to the metal active sites could hinder H_2 adsorption and dissociation, resulting in the decreased catalytic stability when H_2 partial pressure was limited. From these results, the deoxygenation of fatty acids over the 0.5Pt-0.5Sn/SiO_2 catalyst has high potential to selectively produce the respective α-olefin.

Keywords : Bimetallic Pt-M catalysts, Deoxygenation, Heptanoic acid, α-Olefins

Acknowledgement

The author wishes to gratefully thank to my advisors, Assoc. Prof. Dr.Tawan Sooknoi and Asst. Dr. Tosapol Maluangnont, for their supports, supervisions, inspiration, suggestions and encouragements throughout this thesis.

I wish also thanks to Dr. Amnat Permsubscul, Dr. Natthida Numwong and Assoc. Prof. Dr. Joongjai Panpranot for serving as the chairperson and the committee, and valuable comments.

I would like to acknowledge the financial support from the Thailand Research Fund, granted to Assoc. Prof. Tawan Sooknoi (BRG5680007) and Asst. Dr. Tosapol Maluangnont (TRG5780160). I also appreciate the supports from the Department of Chemistry, Faculty of Science, King Mongkut's Institute of Technology Ladkrabang for the equipments, chemicals and facilities.

I would like to extend my thanks to Mr. Boonyawat Wuttitham and Mr. Ayut Witsuthammakul for their help and advices in working the data analysis, support and encouragement.

I would like to extend my sincere appreciation to all of my teachers, my friend and my CCR research group for their constant guidance advice, support and encouragement.

Sincerely thanks to Mr. Thanasak Solos, for his advice, suggestion and kindness.

Finally, I deeply appreciate and thank my parents and my family for their constant supports and encouragements.

Patcharee Jutalikitwong

Table of Contents

Table of Contents (Continued)

List of Tables

List of Figures

List of Schemes

Chapter 1

Introduction

1.1 Motivation

Long chain α-olefins have been used as an important raw material to produce various chemicals commonly found in everyday life, such as detergent alcohols, plasticizers, polymers, surfactants and synthetic lubricants. However, a conventional supply for long chain α-olefins, crude oil, is becoming shortfall [1]. The limited supply certainly will not meet the increasing demand for long chain α-olefins due to a rapid growth in human population [2]. Therefore, researchers have extensively searched for alternative sources of petrochemicals, including natural oil and fat derivatives [3-8].

Triglyceride, which can be easily obtained from vegetable oils or animal fats, can potentially be a renewable source for major petrochemicals. It can be hydrolyzed into glycerol and a mixture of fatty acids. The fatty acids obtained can be further converted to long chain α-olefins via the catalytic deoxygenation. This reaction includes decarbonylation/decarboxylation that removes the carboxylic group without breaking the hydrocarbon chains. It is typically promoted by supported noble metal catalysts, commonly Pt [9-12]. Unfortunately, several early works have shown that aliphatic carboxylic acids are selectively decarboxylated to long chain saturated hydrocarbons over supported Pt catalyst, instead of the desirable long chain α-olefins [13-17]. In order to prevent catalyst deactivation, either a high total pressure or a high hydrogen partial pressure is generally required. Hence, the alkene formed will be immediately hydrogenated to the alkane.

Therefore, the challenge is to search for a catalyst exhibiting high selectivity to alkene products (especially long chain α-olefins), while maintaining activity with minimal deactivation. Incorporation of a metal promoter, i.e. tin, gallium or iron as metal alloys, to supported Pt catalysts is a promising route [18]. In addition to the metal promoters, the product distribution could well be influenced by the nature

of the support, including their chemistry, specific surface area, pore size distribution, acidity, etc [19]. Accordingly, these effects, toward the deoxygenation performance, particularly the selectivity towards long chain α-olefins would be investigated in this work.

1.2 Objectives

1. To obtain long chain α-olefins from the deoxygenation of a fatty acid over supported Pt catalysts.

2. To understand the influence of several types of supported Pt catalysts, including the type of metal promoter and alloys, toward the deoxygenation activity and the selectivity to long chain α-olefins.

3. To obtain appropriate reaction conditions for the deoxygenation of model fatty acids, heptanoic acid, to long chain α-olefins with reasonable catalyst stability.

1.3 Scopes of study

1. Preparation of Pt-supported catalysts by impregnation over different types of supports and with various metal promoters, including Pt/SiO_2, Pt/TiO_2, $Pt\text{-}Sn/SiO_2$, $Pt\text{-}Fe/SiO_2$ and $Pt\text{-}Ga/SiO_2$

2. Characterization of Pt-supported catalysts by the following techniques:

   2.1 Powder X-ray diffraction (PXRD)

   2.2 Temperature-programmed reduction (TPR)

   2.3 Surface area measurement and pore size distribution analysis

   2.4 Thermogravimetric analysis (TGA)

   2.5 Inductively coupled plasma-mass spectroscopy (ICP-MS)

   2.6 Transmission Electron Microscopy (TEM)

3. Catalytic activity testing of Pt-supported catalysts using a fixed bed flow reactor under atmospheric pressure for

3.1 The effect of the type of supports and the metal promoters

3.2 The effect of the contact time (W/F) from 1-8 $g \cdot h \cdot mol^{-1}$

3.3 The effect of the reaction temperature ranging from 320 to 400°C

3.4 The effect of the partial pressure of hydrogen as carrier gas

4. Analysis and quantification of products from the reaction by gas chromatography

1.4 Expected results

It is expected that a new technology for the conversion of medium- to long-chain carboxylic acids to value-added petrochemicals will be obtained. This technology could potentially be developed into an industrial process for the production of long chain α-olefins and other related petrochemicals from the renewable sources.

Chapter 2

Theory and Literature Reviews

2.1 Fatty acids

Fatty acids or derivatives of fatty acids are used in a wide variety of applications. The demand for fatty acids has been growing by about 4% per year over the past 10 years and has reached about 3,000,000 metric tons per year. Fatty acids are typically present in the raw materials used for the production of biodiesel. The natural fatty acids are obtained from the hydrolysis of hard animal fats (tallow), coconut, palm kernel and soybean oils and from the fractional distillation of crude tall oil (a byproduct of Kraft pulping of pine wood). These acids are almost entirely straight chain, even-numbered monocarboxylic acids containing from 4 to 22 carbon atoms. Most new plants have been built in Southeast Asia which is the major source for coconut, palm and palm kernel oils. The market is dominated by two producers, the Uniquema group and the Henkel group representing about 50% world market share. Other fatty acids are derived from petroleum [20].

About 100,000 metric tons of the natural fatty acids are consumed in the preparation of various fatty acid esters. The simple esters with lower chain alcohols (methyl-, ethyl-, *n*-propyl-, isopropyl- and butyl esters) are used as emollients in cosmetics and other personal care products and as lubricants. Esters of fatty acids with more complex alcohols, such as sorbitol, ethylene glycol, diethylene glycol and polyethylene glycol are consumed in foods, personal care, paper, water treatment, metal working fluids, rolling oils and synthetic lubricants [20]. Common saturated and unsaturated fatty acids are shown in **Table 2.1** and **2.2** respectively.

Table 2.1 Common saturated fatty acids [21].

Number of Carbon Atoms	Formula	Common Name	Source
4	$CH_3(CH_2)_2COOH$	Butyric acid	Butter
6	$CH_3(CH_2)_4COOH$	Caproic acid	Butter
8	$CH_3(CH_2)_6COOH$	Caprylic acid	Coconut oil
10	$CH_3(CH_2)_8COOH$	Capric acid	Coconut oil
12	$CH_3(CH_2)_{10}COOH$	Lauric acid	Palm kernel oil
14	$CH_3(CH_2)_{12}COOH$	Myristic acid	Oil of nutmeg
16	$CH_3(CH_2)_{14}COOH$	Palmitic acid	Palm oil
18	$CH_3(CH_2)_{16}COOH$	Stearic acid	Beef tallow
22	$CH_3(CH_2)_{20}COOH$	Beheric acid	Sesame oil

Table 2.2 Common unsaturated fatty acids [21].

Number of Carbon Atoms	Formula	Common Name	Source
16	$CH_3(CH_2)_5CH=CH(CH_2)_7COOH$	Palmitoleic acid	Whale oil
18	$CH_3(CH_2)_7CH=CH(CH_2)_7COOH$	Oleic acid	Olive oil
18	$CH_3(CH_2)_4CH=CHCH_2(CH_2)_7COOH$	Linoleic acid	Soybean oil
18	$CH_3CH_2(CH=CHCH_2)_3(CH_2)_6COOH$	Linolenic acid	Fish oils
20	$CH_3(CH_2)_4(CH=CHCH_2)_4(CH_2)_2COOH$	Arachidonic	Liver

2.1.1 Heptanoic acid

Heptanoic acid (**Figure 2.1**), also called enanthic acid, is the acid with seven carbon atoms. It is the oily liquid with unpleasant, rancid odor. It contributes to the odor of some rancid oils. Heptanoic acid is slightly soluble in water, but very soluble in ethanol and ether, and has been naturally found in oily seed [22]. Alternatively, heptanoic acid can be derived from the methyl ester of ricinoleic acid (which is a constituent of caster bean oil) from a process comprising of hydrolyzation and oxidation [23]. The bio-transformation of ricinoleic acid has also been studied by

a multi-step enzymatic activation [24]. Heptanoic has been employed as a model chemical in the ketonization study over oxides of Mn, Ce and Zr depositing on supports such as alumina, silica or titania [25]. It has been used as a building block for the synthesis of an industrial lubricant, flavor, fragrance for cosmetics, and cigarette additive. Additionally, the salts of heptanoic acid (i.e., heptanoates) are a corrosion inhibitor, and are a representative precursor for drugs such as esterify steroid [26].

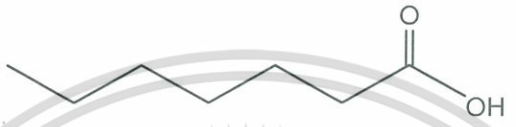

Figure 2.1 Molecular structure of heptanoic acid

2.1.2 Fatty acid reactions

2.1.1.1 Deoxygenation

Deoxygenation is a chemical reaction involving the molecular oxygen (O_2) removal from reaction mixtures or from a molecule. It is a novel technique for the production of diesel-like fuel from renewable resources like vegetable oils and animal fats. This method is being investigated and developed in several laboratories. It has recently been demonstrated that renewable feedstock over various heterogeneous catalysts in liquid-phase tends to decarboxylate. This leads to the new reactions called decarboxylation and decarbonylation.

2.1.1.2 Decarboxylation

Decarboxylation is a chemical reaction involving the removal of carboxyl group from the substrate via carbon dioxide release. It has been found that decarboxylation for simple carboxylic acids is limited and does not occur easily. However, esters or carboxylic acids with a carbonyl group at the 3- (or b-) position readily undergo thermal decarboxylation [27]. The reaction pathway proceeds via cyclic transition state with enolate forming as an intermediate. In the case of

dicarboxylic acids, the tautomerization occurs to give the final carbonyl (carboxylic acid) product as shown in **Scheme 2.1**;

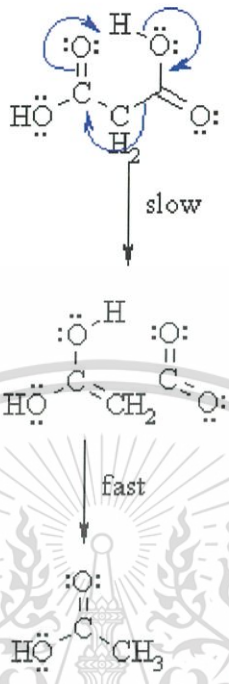

[27]

Scheme 2.1 The decarboxylation of a typical dicarboxylic acid via tautomerization

In the case of simple carboxylic acids, the final product would be an alkane and a carbon dioxide. An easy demonstration could be the observation from the conversion of linear fatty acids to linear hydrocarbon fuels via decarboxylation as shown in **Scheme 2.2**;

Scheme 2.2 The decarboxylation of a carboxylic acid

2.1.1.3 Decarbonylation

Decarbonylation is a chemical reaction that is mostly similar to decarboxylation except that instead of releasing carbon dioxide as the by-product, carbon monoxide and water will be released. This reaction is usually observed by

the transformation of aldehydes via metal complex catalysts [28]. The pathway for decarbonylation also proceeds via cyclic transition state with enolate formed as an intermediate and the rest is almost identical to that of decarboxylation.

Compared to the decarboxylation, the final product of decarbonylation from the same carboxylic acid would be an alkene instead of an alkane. This is crucial to the industries as alkene is one of the most important feedstock that is currently being employed [29]. For example, alkenes could be applied as a monomer for the production of various polymers in a large-scale application.

An easy demonstration could be the observation from the conversion of linear fatty acids to linear hydrocarbon fuels via decarbonylation as shown in **Scheme 2.3**;

Decarbonylation

Scheme 2.3 The representative decarbonylation reaction of a carboxylic acid

2.1.1.4 Ketonization

Ketonization or ketonic decarboxylation is a reaction involving the formation of symmetric ketone from two equivalents of carboxylic acid via decarboxylation. In addition of releasing carbon dioxide, one water molecule is also released as well. This reaction is essentially important for the production of symmetric ketones such as acetone or fatty ketones. Not only this reaction produces non-polluting by-product but the need of solvent or another reagent could also be neglected [30]. The method itself has been reported for a long time since 1858 [31]. One of the major report suggests that the ketonization might be involved in deoxygenation as the intermediate step and could be further converted to other fine chemicals under the presence of transition metals [32]. A representative example for the ketonization is demonstrated in **Scheme 2.4** taking heptanoic acid as an example.

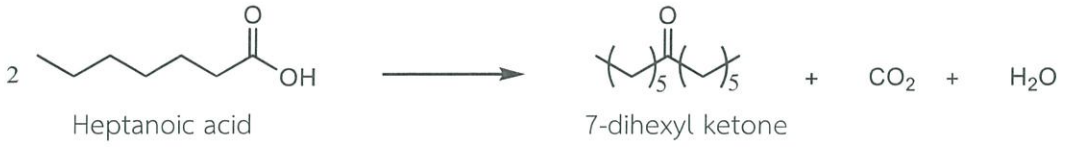

Scheme 2.4 The ketonization of heptanoic acid

2.2 Platinum and platinum alloy

Platinum or Pt is a chemical element with atomic number 78. It belongs to the group 10 of the periodic table of elements as a transition metal and belongs to the group of precious metal. Its high density makes it one of the densest metals after osmium and iridium [33]. Platinum becomes useful in industries due to its sky-high resistance to corrosion even at high temperature. Also, platinum would not be oxidized in air regardless of the temperature. Moreover, platinum itself is considered to be one of the least reactive metals and does not tarnish. Due to these properties, platinum is currently being employed in various industrial applications [34].

One of the major use of platinum is as a catalyst in chemical reactions. Platinum catalysts are being used in various applications such as the catalytic converter in automobile, a catalyst in separation processes in the petroleum industry, in the catalytic reforming of straight-run naphtha into higher-octane gasoline, as well as the use in fuel cells as an oxygen reduction catalyst [35].

Platinum could also be used in the hydrogen-involved processes due to its high affinity to hydrogen [36]. It has been proposed as a promising catalyst for the hydrogenation of heterocyclic compounds such as pyridine and furan under an elevated pressure. Furthermore, platinum has high affinity to carbon monoxide such that carbon monoxide would be adsorbed over Pt surface with 1:1 ratio [37]. This is proved to be useful in some chemical reactions that involves carbonyl-group such as decarboxylation and decarbonylation.

The final goal of catalytic studies with alloys is easy to formulate: (i) by using alloy catalysts one should learn more about the functioning of metals as catalysts;

this is the fundamental aspect: and (ii) one should be able to find empirically or to design rationally catalysts having better activity, selectivity and stability. Matters relating to the second point are already documented in the patent and scientific literature. So, for example, the platinum-iridium alloy catalyst used in naphtha reforming is several times more active per unit volume of reactor than the platinum catalysts originally used. These catalysts have been rationally designed on the basis of knowledge concerning the reactions of hydrocarbons on the individual metals. The most successful combination, namely platinum-rhenium, was found empirically and shows superior selectivity and stability in the sulfided state. The same holds for platinum alloys used in the pharmaceutical industry for reactions such as trans-alkylation and hydrogenation of molecules with hetero-atoms, or for palladium alloys used in selective hydrogenation of acetylene, etc. However, the more intriguing for a scientist is point (i) above. One keeps asking questions concerning the relation of the activity and the selectivity; the latter being more and more important, to the chemisorption and thus to the surface structure and composition. It is interesting to see if alloying would change the chemisorption bond strength, a factor which influences the activity of the catalysts [38].

2.3 Support

2.3.1 TiO_2

Titanium dioxide, titania or titanium(IV) oxide, is the naturally occurring oxide of titanium with chemical formula TiO_2. Titania has long been used as a support for metal catalysts in many chemical processes. This is because titania itself provides promising surface area which leads to satisfactory metal surface distribution [39]. However, there is a major discovery where the interaction between noble metals such as platinum and titanium oxide results in an excessive change in the chemisorption properties of the noble metals. The term "Strong Metal-Support Interaction" was introduced [40] to describe this phenomena.

Further studies have found that the lack of adsorption might be due to the Ti migration [41, 42]. Titanium oxide can migrate onto fresh metal surfaces and form a thick cover film, changing the surface properties and morphology. It is likely that the transformation occurs via hydrogen spill-over mechanism [43]. Due to these facts, the oxygen vacancies are created on catalyst surfaces and consequently, the catalytic activity is modified [44].

2.3.2 SiO_2

Silica (SiO_2) is an amorphous solid where its internal surface area can be reach 500 m^2/g [45]. The silica surface is nearly inert. The most reactive groups are the –OH groups (called silanol groups) that terminate the primary particles; these are weakly acidic, comparable to alcohols. The bulk may be terminated entirely by –OH groups, which can be removed by dehydroxylation. Two types of silanol groups are usually distinguished, isolated groups and neighboring (vicinal) groups that may be hydrogen bonded to each other. Fully hydrated samples, when heated in air (i.e., calcined) at temperatures < 200 °C, also contain germinal groups, $Si(OH)_2$. The complete removal of silanol groups requires temperature higher than 700 °C and results in significant changes in surface morphology. The aprotic sites present after dehydroxylation at 600-800 °C have been suggested to be primarily highly strained Si-O-Si linkages.

2.4 Linear alpha olefins

The term 'olefins', also known as alkenes, refers to a large number of compounds that contain carbon and hydrogen and have at least one double bond in their structure. Short-chain olefins, like ethylene, are cracked from naphtha or natural gas. Ethylene is then oligomerized into longer chain linear alpha olefins, ranging from 6 to 30 carbons in length. Alpha olefins are characterized by their high purity, high degree of linearity, and a double bond uniformly positioned between the first and second carbon. For drilling fluid applications, alpha olefins in the C_{14} to C_{18} range are used because they have the right mix of physical properties like viscosity, pour point and

flash point. Internal olefins are then produced from linear alpha olefins by catalytically moving the double bond to different locations in the molecule. As a result, the pour point of the fluid decreases significantly, thus enabling these materials to be used successfully in deep-water applications. Internal olefins used as base fluids for drilling mud typically have carbon chain lengths in the C_{15} to C_{18} range [46].

Linear Alpha Olefins (LAO) or Normal Alpha Olefins (NAO) are olefins or alkenes with a chemical formula C_xH_{2x}, distinguished from other mono-olefins with a similar molecular formula by linearity of the hydrocarbon chain and the position of the double bond at the primary or alpha position. A typical example of an alpha olefin, i.e., *1*-hexene, is shown in **Figure 2.2**.

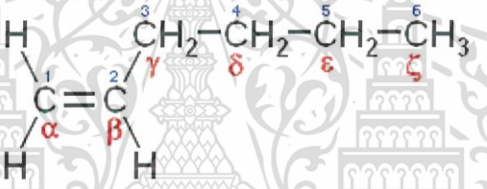

Figure 2.2 *1*-hexene, a typical linear alpha-olefin

Linear alpha olefins are industrially important alpha-olefins, including *1*-butene, *1*-hexene, *1*-octene, *1*-decene, *1*-dodecene, *1*-tetradecene, *1*-hexadecene, *1*-octadecene and higher blends of C_{20}-C_{24}, C_{24}-C_{30}, and C_{20}-C_{30} ranges.

2.4.1 Synthesis

Industrially, linear alpha olefins are commonly manufactured by a few main routes: (i) oligomerization of ethylene, and (ii) by Fischer-Tropsch synthesis followed by purification. Another route to linear alpha olefins which has been used commercially on small scale is (ii) dehydration of alcohols. Prior to about 1970's linear alpha olefins were also manufactured by thermal cracking of waxes, whereas linear internal olefins were also manufactured by chlorination/dehydrochlorination of linear

paraffin. There are six commercial processes which oligomerize ethylene to linear alpha olefins. Four of these processes produce wide distributions of linear alpha olefins. These are the Ethyl Corporation (Ineos) process, Gulf (Chevron Phillips Chemical Company) process.

2.4.1.1 Ineos (Ethyl) Process

Ethyl linear alpha olefin process is commonly called stoichiometric Ziegler process. It is a two-step process. In the first step, a stoichiometric quantity of triethyl aluminium in olefin diluents is reacted with excess ethylene at high pressure (above 1000 psig) and relatively low temperature (below 400 °F). On the average, nine moles of ethylene are added per mole of triethyl aluminium, resulting in, on average, trioctyl aluminium. The distribution of alkyl chains on the aluminium is determined by statistical bell curve distribution except for some smearing to the light side due to the kinetic phenomena and some smearing to the heavy side due to some incorporation of heavier olefins into the chain. Excess ethylene and olefin diluent are flashed off. The heavy aluminium tri-alkyls are reacted with ethylene again in a displacement or a *tran*-alkylation reaction, but at high temperature (over 400 °F) and at low pressure (less than 1000 psig) to recover triethyl aluminium and a statistical distribution of linear alpha olefins, which serve as the olefin diluents in the chain-growth step [47].

2.4.1.2 CP Chemicals (Gulf) Process

The Gulf linear alpha olefin process is commonly called a catalytic Ziegler process. Triethyl aluminium is used as a catalyst, but in catalytic amounts and the process is a single-step process. Triethyl aluminium and excess ethylene are fed to a plug flow-reactor. The reaction is conducted at high pressure and high temperature. Excess ethylene is flashed off. The triethyl aluminium catalyst is washed out of the product with caustic and the linear alpha olefins are separated. The product distribution is a Schultz-Flory distribution typical of catalytic processes.

2.4.2 Applications

The terminal double bonds of linear alpha olefins react readily with a wide variety of chemicals. Linear alpha olefins can be used to synthesize any derivative requiring an even-numbered, straight carbon chain.

2.4.2.1 Polymers

Homopolymers & Copolymers Other than Polyethylene

Certain linear alpha olefins can be used to prepare homopolymers and copolymers other than polyethylene. Linear alpha olefin *1*-butene can be polymerized to *1*-polybutene (PB), a homopolymer that is ideal for many engineering applications because of its excellent long-term mechanical properties.

PB is extremely creep resistant and behaves similarly to a cross-linked plastic. It features a unique combination of unusually high tensile strength and good tear properties. PB shows no signs of cracking, crazing or fracturing when stressed below its short-time failure stress value for long periods of time. In addition, its tear strength increases rapidly as the tear rate escalates. PB's benefits broaden the commercial applications for polymers.

Linear alpha olefins C_6, C_8, C_{10}, C_{16}, C_{18}, C_{20-24} and C_{24-28} are used for the production of copolymers. Using per-esters as initiators, copolymers of maleic anhydride and linear alpha olefins can be formed.

The maleic copolymer made from linear alpha olefin C_{18} is a product known as PA-18, which has been used successfully as a release agent in tapes and paper templates for PVC curtains, and in water-resistant sunscreen formulas.

The copolymers produced from other linear alpha olefin fractions are normally converted to acid amides, half esters or diesters for use as lube-oil additives and pour-point depressants. They are also effective curing agents for epoxy resins and act as unique thermo-set resin compositions in liquid monoepoxides. In addition, linear alpha olefins C_6, C_8 and C_{10} have been co-enter polymerized with vinyl acetate and vinyl chloride.

Polyethylene Copolymers

With the evolution of increasingly sophisticated polyethylene technology, alpha olefins 4, 6 and 8 have become even more valuable co-monomers for the production of a wide range of polyethylene resins.

High-density polyethylene (HDPE) is principally used for the manufacture of high-performance pipe, blow-molded household and industrial bottles, oil bottles, injection-molded food containers, consumer durables and disposable goods and film goods such as grocery sacks and merchandise bags. HDPE possesses high flex stiffness (flexural modulus) but low environmental stress cracking resistance (ESCR). Lowering the melt index (high melt viscosity) can help to alleviate the low ESCR, but the processibility of the polymer suffers, due to lower flow rates. The addition of Chevron Phillips Chemical's alpha olefins 4, 6 or 8 as a co-monomer increases the resulting polymer short chain branching, thereby improving the flow properties while greatly increasing the ESCR.

In addition, HDPE polymers made with alpha olefins 6 or 8 as a co-monomer have much higher ESCR than those made with *1*-butene. For a given polymerization process at a polymer density of 0.950 g/cc and melt index ranges of 0.2 to 0.3 g/10 minutes, *1*-butene copolymers had ESCR values of 50 to 310 hours, and 1-hexene copolymers exhibited ESCR values of 800 to more than 1,000 hours. Copolymerizing with Chevron Phillips Chemical's alpha olefin 8 rather than *1*-hexene produces polymers with even better ESCR values.

Linear low-density polyethylene (LLDPE) is made by incorporating an even higher level of co-monomer (*1*-butene, *1*-hexene or *1*-octene) into the product to reduce the density of the resulting polyethylene. Conventional Ziegler-Natta catalysts as well as more recent metallocene technologies are being used today to produce LLDPE. LLDPE provides significantly greater stiffness than low-density polyethylene (LDPE) polymers, which are typically produced in high-pressure processes. Because the melt index of LLDPE can be raised to values much higher than that of LDPE (while

maintaining equivalent or superior physical properties), processing cycle times can be reduced. In addition, many products made with LLDPE can be significantly down-gauged to save on raw material costs.

For the greatest possible strength and tear resistance, the density can be reduced even further using emerging metallocene technologies to produce what is referred to as very low-density polyethylene (VLDPE). Among other benefits, VLDPE has a higher heat-seal temperature than LDPE, yet provides equivalent seal strength.

Regardless of the application, Chevron Phillips Chemical's *1*-hexene performs exceptionally well under the most stringent polymerization conditions. This is particularly important with the emergence of sophisticated metallocene technology for the production of LLDPE and VLDPE where high purity co-monomers are critically important to maintain high catalyst activity and resulting product performance.

2.4.2.2 Surfactants

Alpha Olefin Sulfonate (AOS)

Linear alpha olefins are excellent intermediates for producing alpha olefin sulfonate (AOS) surfactants. These surfactants provide outstanding detergency, high compatibility with hard water, and good wetting and foaming properties. AOS is free of skin irritants and sensitizers, and it biodegrades rapidly. It is used in high-quality shampoos, light-duty liquid detergents, bubble baths, and heavy-duty liquid and powder detergents. It is also used in emulsion polymerization. C_{14}-C_{16} AOS blends are frequently used in liquid hand soaps.

To make AOS, linear alpha olefins are first sulfonated in a continuous thin film reactor to produce a mixture of alkene sulfonic acids and sultones (cyclic sulfonate esters). The mixture is neutralized with aqueous sodium hydroxide and then hydrolyzed at elevated temperatures to convert the remaining sultones to alkene sulfonates and hydroxy sulfonates. This results in an aqueous solution of alpha olefin

sulfonate. (If a solid anhydrous product is desired, it can be easily obtained by neutralizing and hydrolyzing the solution in isopropanol instead of water).

Detergent Alcohols

Linear alpha olefins are easily converted to primary alcohols via oxo chemistry. By reaction with ethylene oxide, the alcohols form a variety of nonionic ethoxylates, which may themselves serve as surfactants or be further derivatized. Anionic alkyl ether sulfates can be derived from the sulfation of the ethoxylates. These are widely used in the cosmetics and toiletries industries. Alternatively, the alcohols may be directly sulfated to produce alkyl sulfates.

Linear Alkyl Benzene Sulfonates

Linear alpha olefins react with benzene via Lewis acid catalysis to form linear alkyl benzenes (LABs). Sulfonation and subsequent neutralization of LAB result in linear alkyl benzene sulfonates, which are commonly used in dishwashing liquids, laundry detergents, all-purpose cleaners, and lube-oil additives. Similarly, phenol or naphthalene will react with olefins, producing other types of detergents and wetting agents upon sulfonation/neutralization.

Amine Derivatives

Linear alpha olefins are also suitable for manufacturing alkyl dimethyl amines (ADMAs), which are precursors to a number of surface-active derivatives. Amine oxides produced via hydrogen peroxide oxidation of ADMAs are excellent foam boosters and are typically used in shampoos, bubble baths, and dishwashing detergents.

Quaternary ammonium halides or "Quats," which result from reaction of ADMAs with alkyl or benzyl halides, are highly effective biocides and antistatic agents. Betaines, which are mild amphoteric surfactants, feature good foam boosting and stabilizing properties. They are readily derived from ADMAs by reaction with sodium chloroacetate.

Alkane Sulfonates

Sodium bisulfite will react with linear alpha olefins via a free-radical mechanism to produce alkane sulfonates. Alkane sulfonates with chain lengths of C_{12} or higher have limited water solubility, suggesting their application in synthetic detergent bars. Shorter alkane sulfonates like C_8, however, are hydrotropic.

2.4.2.3 Synthetic Fluids

Poly alpha olefins

Synthetic base fluids for high-performance lubricants and functional fluids can be prepared by oligomerizing Chevron Phillips Chemical's alpha olefins, particularly alpha olefins 10 and 12. The resulting oligomers, consisting of dimers, trimers, tetramers and so on, are typically hydrogenated and then formulated with appropriate additives.

For more than two decades, Chevron Phillips Chemical has been a leader in the development and production of PAOs. Our original products, which are produced from *1*-decene, consist of PAOs 2, 4, 6 and 8cSt and C10 dimer. In the mid-1990s, Chevron Phillips Chemical developed unique PAO products, which are synthesized from *1*-dodecene. They are PAOs 2.5, 5, 7 and 9cSt as well as the C_{12} dimer.

Now our comprehensive range of PAOs provides our customers with a greater range of physical properties from which to choose, giving them more flexibility and versatility in developing products better suited to their individual applications.

2.4.2.4 Additives

Plasticizer Alcohols

C_8 through C_{10} linear alpha olefins are used to produce primary C_9 through C_{11} plasticizer alcohols via hydroformylation or oxo chemistries. The phthalate plasticizers produced from these alcohols gave superior properties to those made from *2*-ethyl *1*-hexanol. The same chemistry is used to produce C_{13} to C_{15} synthetic detergent alcohols from C_{12} and C_{14} linear alpha olefins.

Alkenyl Succinic Anhydrides

Alkenyl succinic anhydrides (ASAs) are prepared by heating linear alpha olefins and maleic anhydride to approximately 200 °C. Some ASAs are used as dispersants in lube oils and automatic transmission fluids, and as pour-point depressants in lube and crude oils. Others are converted to acid amides, half esters, and diesters. One of the largest applications for ASA is as the paper sizing agent in alkaline media. For this use, linear alpha olefins C_{16} or C_{18} are isomerized to a thermodynamic distribution of internal olefins, which are then reacted with maleic anhydride to produce the desired liquid ASA.

Polyvinylchloride Lubricants & Stabilizers

Heat and pressure are applied during the extrusion of polyvinylchloride (PVC) as it moves through the die. Lubricants (waxes) are compounded into the PVC to ensure proper lubrication in the extruder and to control fusion of the PVC compound. Linear alpha olefin C_{30+} is the preferred lubricant for this application.

During the extrusion process, PVC often begins to decompose. Various materials are used to retard this degradation, including dibutyl or dioctyl tin oxides and/or dioctyl tin mercaptides. These compounds are made using tin (IV) chloride and the corresponding aluminum alkyls, which in turn are derived from linear alpha olefins. The mercaptans used to make the tin mercaptides are usually made from linear alpha olefins.

2.4.2.5 Specialty Chemicals

Epoxides

Treatment of alpha olefins with peracids forms epoxides, which find use as modifiers for epoxy resins. Epoxides may also serve as polyether ingredients in polyurethanes. Almost all carbon number fractions of our alpha olefins find some application in the epoxide market.

Halogenated Linear Alpha Olefins

Chlorinated linear alpha olefin 20-24 (C_{20}-C_{24} alpha olefin) may be used as a secondary plasticizer in PVC formulations. Chlorinated alpha olefin (40 wt% chlorine)

based plasticizer formulations have been evaluated against chlorinated paraffins (42 wt% chlorine) and alkyl-aryl hydrocarbon plasticizer formulations. The evaluation of the mechanical properties of these formulations shows that the chlorinated alpha olefin is equivalent in plasticizing efficiency to the two other secondary plasticizers, while having adequate heat stability and volatility properties. Polychlorinated *1*-dodecene, *1*-tetradecene, and *1*-hexadecene perform well as stable high temperature metalworking fluid additives.

Additional Applications

Chevron Phillips Chemical's alpha olefins are used in many other applications including the production of mercaptans, ketones, ester, pyrazines, alkylphosphines, alkyl silanes, and as a substitute for paraffins and paraffin waxes.

Sulfur-hydrogen bond containing compounds may be added to alpha olefins, under the proper conditions, to form sulfur-containing hydrocarbons. Mercaptans, produced from the reaction between alpha olefin and hydrogen sulfide, are successfully used in rubber additives, ore flotation, and specialty chemical applications.

Alpha olefins may be converted to internal olefins through olefin isomerization or higher carbon number internal olefins by metathesis or dimerization reactions. Chevron Phillips Chemical's blend of isomerized C_{16} and C_{18} alpha olefins is an excellent synthetic fluid for use in offshore drilling muds. The blend has outstanding physical and ecotoxicological properties for this application. In fact, the EPA has selected this product as an ecotox standard for fluids used in offshore drilling muds.

Trialkylphosphine and trialkylphosphine oxides, silylhydrocarbons, alkyl silanes, and some organometallic compounds are produced commercially from linear alpha olefins for a wide variety of end products.

Derivatives of Chevron Phillips Chemical's alpha olefins with carbon numbers above C_{20} find uses in lube oils, transmission fluids, and as pour-point

depressants in lube and crude oil. These wax fractions may also be chemically modified to simulate more expensive carnauba or Montan waxes used to make polishes and candles.

The high molecular weight of linear alpha olefins is primary raw material in the chemical industry [48, 49] as shown in **Table 2.3**.

Table 2.3 Application of linear alpha olefins

Linear alpha olefins	Application
1-Decene ($C_{10}H_{20}$)	Detergent alcohols, poly alpha-olefins, alkyl aromatics, plasticizer alcohols, epoxides, di-/poly- halides, personal care, flavors and fragrances
1-Dodecene ($C_{12}H_{24}$)	Detergents, plasticizer alcohols, poly alpha-olefins, alkyl aromatics, ADMA, ASA, epoxides, mercaptans, di-/poly-halides, alkyl silanes, personal care, flavors and fragrances
1-Tetradecene ($C_{14}H_{28}$)	Maleic anhydride copolymers, AOS, alkyl aromatics, ADMA, detergent alcohols, ASA, epoxides, metal working fluids, di-/poly- halides, alkyl silanes, personal care, flavors and fragrances
1-Hexadecene ($C_{16}H_{32}$)	Maleic anhydride copolymers, AOS, alkyl aromatics, ADMA, ASA, lube oil additives, epoxides, metal working fluids, di-/poly- halides, alkyl silanes, personal care, flavors and fragrances
1-Octadecene ($C_{18}H_{36}$)	Maleic anhydride copolymers, AOS, alkyl aromatics, ADMA, ASA, lube oil additives, epoxides, metal working fluids, di-/poly- halides, alkyl silanes, personal care, flavors and fragrances
Alpha Olefin C_{20-24}	Lube oil additives, personal care, epoxides, alkyl aromatics, drilling fluids, maleic anhydride copolymers, pour point depressants
Alpha Olefin C_{24-28}	Epoxides, di-/poly- halides, candles, pour point depressants, personal care

2.5 Literature reviews

Recent work on decarbonylation and decarboxylation of carboxylic acids over transition metal catalysts is often performed in the presence of hydrogen to inhibit catalyst deactivation. However, the reactions are highly selective towards the production of paraffins because of the rapid hydrogenation of any alkenes formed in the process [50, 51]. Terminal alkenes formed by decarbonylation are attractive organic materials because of their application in the polymer industry. Therefore, an effective catalyst for decarbonylation should prevent both hydrogenation of α-olefin product as well as the double bond isomerization to form internal olefins.

Limited studies have been reported on the conversion of fatty acids to olefins [50, 52]. In 1982, Maier *et al.* studied the decarboxylation of carboxylic acids for production of fuel-like hydrocarbons [53]. In their work, they showed that supported Pd and Ni catalysts were highly selective towards deoxygenation products. However, the use of hydrogen in the reaction was necessary. Murzin and co-workers studied several other supported metals such as ruthenium (Ru), platinum (Pt), iridium (Ir), osmium (Os), and rhodium (Rh), and it was concluded that the most promising transition metals are Pd and Pt, which achieved more than 90% selectivity towards alkane and alkene production when supported on carbon [54]. Nickel has also been extensively studied for deoxygenation, but it is not an attractive metal because it particularly favors alkane production and cracking [3, 55-57]. Since studies performed by different groups were run at different concentrations of H_2, conversion levels, amounts of catalyst, time on stream, results such as turnover frequency (TOF), conversions, and product selectivities were not always reported. So, it is still unclear which metals are more selective towards the formation of alpha-olefins.

For the effect of support, Snåre *et al.* showed that Pt, Rh, and Pd nanoparticles displayed very different activity and product distribution when supported on alumina instead of carbon during liquid-phase operation [50]. Ford *et al.* showed that when Pd nanoparticles were supported on carbon instead of silica, the turnover frequency of

the reaction increased an order of magnitude, from 0.055 to 0.206 s^{-1}, for the liquid-phase deoxygenation of succinic acid at 573 K [58]. Moreover, Lugo-José *et al.* showed an increased turnover frequency from 0.0002 to 0.0053 s^{-1} when Pd nanoparticles were supported over carbon instead of silica, for the gas-phase deoxygenation of propanoic acid at 573 K.

Most of the experiments with carboxylic acid deoxygenation over Pd catalysts involved a long chain hydrocarbon as a solvent [55, 57-66] and co-feeding H_2 [58, 60, 62-66] to enhance the TOF and the stability of the catalyst. Under these conditions, liquid-phase TOF values reported over Pd ranged from 0.01 to 0.96 s^{-1} for batch reaction at 573 K [60, 62, 63] and from 0.027 to 0.004 s^{-1} for fixed-bed operation at 543 K [67, 68].

For the effect of feed concentration, Mäki-Arvela *et al.* showed that when the concentration of lauric acid decreases from 0.44 to 0.22 mol/L, the steady state reaction rates did not change [68]. Similarly, Snåre *et al.* reported a zero-order regime at concentrations between 0.15 and 1.5 mol/L [59]. However, Bartosz *et al.* showed that the reaction rate increases when the concentration of fatty acid decreases from 0.6 to 0.15 mol/L [69]. Furthermore, Immer *et al.* showed that as the concentration of fatty acid decreases, the decarboxylation rate decays rapidly whereas the decarbonylation rate increases [63]. This led to a switchover in product selectivity from paraffins and CO_2 (typical of decarboxylation) to olefins and CO (typical of decarbonylation).

A recent study showed that ketonization can play an important role in upgrading fatty acids into fine chemicals or fuels [30]. This reaction involves the coupling of two carboxylic acids to produce a symmetrical ketone with the simultaneous removal of oxygen in the form of CO_2 and H_2O. Gaertner *et al.* [32] theorized that ketonization might be an intermediate step in the deoxygenation reaction and, in the presence of a transition metal, the ketone could further convert to olefins. The ketonization reaction is also referred to as ketonic decarboxylation.

As mentioned above, hydrogenation is an important side reaction that can also take place over supported metal catalysts. Because hydrogenation of α-olefins forms less valuable paraffins, sources of hydrogen in the reaction need to be minimized. Snåre *et al.* showed that reaction under low H_2 conditions lead to coke formation [59].

Furthermore, regarding the effect of Pt-alloying, Pt-containing bimetallic catalysts have attracted much attention because of their enhanced performance in comparison to monometallic Pt catalysts. The enhanced catalyst activity, selectivity, and stability may be attributed to geometric (ensemble) and electronic (ligand) effects of bimetallic catalysts. $PtSn_x$ has been studied both experimentally and theoretically [70-74]. Thermodynamic investigations of the $PtSn_x$ alloys (x = 0 – 4) show that a $PtSn_x$ bulk alloy is expected to be the stable phase below 540 °C. Experiments showed that $PtSn_x$ improved selectivity to olefin formation [72, 73]. Theoretical studies suggested that the lowering of the d-band center of $PtSn_x$ in comparison to Pt resulted in a lower binding energy of an olefinic adsorbate to the catalyst surface [70, 71]. Additionally, coke precursors may not be poisoning for a Sn-modified Pt surface due to an increased carbon mobility [75]. $PtSn_x$ has also exhibited the ability to transform paraffinic methyl esters into olefins in organic solvents [76]. The ability of $PtSn_x$ to tolerate alkenes and coke suggests that $PtSn_x$ may be better suited for deoxygenation of fatty acids to olefin as compared to Pt catalysts.

Chapter 3

Research Methodology

3.1 Reagents

Details on the reagents used in this thesis are summarized in **Table 3.1**.

Table 3.1 A list of reagents

Chemical	Grade of purity	Manufacturer
10% Hydrogen in argon gas	99.99%	PRAXAIR
Air zero gas	99.99%	PRAXAIR
Chloroplatinic acid hexahydrate	99.90%	SIGMA-ALDRICH
($H_2PtCl_6 \cdot 6H_2O$)		
Distilled water	-	-
Gallium (III) nitrate hydrate	99.99%	SIGMA-ALDRICH
($Ga(NO_3)_3 \cdot xH_2O$)		
Helium gas	99.99%	PRAXAIR
Heptanaldehyde	95.00%	ACROS
Heptanoic acid	98.00%	ACROS
Hydrogen gas	99.99%	PRAXAIR
Iron (III) nitrate nonahydrate	>98.50%	QRëC
($Fe(NO_3)_3 \cdot 9H_2O$)		
Liquid nitrogen	-	Linde
Nitrogen gas	99.99%	PRAXAIR
n-octane	>99.99%	CARLO ERBA
Titanium dioxide (P25)	>99.70%	Degussa
Quartz wool	-	Grace

Table 3.1 A list of reagents (continued)

Chemical	Grade of purity	Manufacturer
Silicon dioxide	99.99%	CARLO ERBA
Tin(II) chloride dihydrate	≥98.5%	QRëC
($SnCl_2 \cdot 2H_2O$)		

3.2 Apparatuses

1. Alumina crucible
2. Agate mortar
3. Glass bead
4. Glass wool
5. Glass tube
6. Gas-tight syringe 25 mL, SGE Analytical Science
7. Syringe 10 µL, SGE Analytical Science
8. Graduate pipette and red bulb
9. Hot air oven, UM500, Memmert
10. Box furnace, Controller P 320, Nabertherm
11. Laboratory glassware
12. Protector laboratory hood, Science Technology
13. Mass flow controller, Brooks Instrument
14. Quartz wool
15. Quartz tube
16. Syringe pump, KDS-100, KD-scientific
17. Tube furnace, VCTF4, Vecstar
18. Powder X-ray diffractometer, a DMAX2200 Ultima+, Rigaku
19. Surface area and pore size analyzer, Autosorb-1, Quantachrome
20. Thermogravimetric analyzer, Pyris, Perkin Elmer

21. Scanning electron microscope, EVO®MA10, ZEISS 23. X-ray photoelectron spectrophotometer, AXIS ULTRA, KRATOS ANALYTICAL
22. Wavelength dispersive X-ray fluorescence spectrophotometer, Bruker, Tiger
23. Thermal conductivity detector, TCD2-c, Valco Instrument
24. Gas chromatography, Hewlett Packard 6890

3.3 Preparation and characterization of catalysts

3.3.1 Preparation of Pt-supported catalysts

The platinum was introduced into the supports by sprayed-incipient wetness impregnation method. 0.0664 g of $H_2Cl_6Pt{\cdot}6H_2O$ was dissolved in 20 mL deionized water to make a solution with a concentration of 6 mmol/L. The prepared metal precursor solution was partially sprayed onto 5 g of a supports until the support is wet. After that, the wet sample was left to dry in oven at 80 °C. The process was repeated until the desired volume was used up, at which point it is assumed that the desired metal loading (~0.5 wt%) is reached. After that, the impregnated Pt catalyst was dried in oven under static air at 110 °C overnight. Finally, the catalyst was kept in dried plastic container at room temperature.

3.3.2 Preparation of Pt-metal alloyed catalysts

The Pt-metal alloyed catalysts were similarly prepared by a sprayed-impregnation method. The platinum precursor (0.0664 g) was first dissolved in 20 mL of deionized water. Separately, the other desired metal precursors (0.0475 g for $SnCl_2 \cdot 2H_2O$, 0.0721 g for $Fe(NO_3)_3 \cdot 9H_2O$, and 0.0392 g for $Ga(NO_3)_3 \cdot xH_2O$) were dissolved in 20 mL of 1.0 M HNO_3. The two precursor solutions (Pt and another metal) were subsequently mixed, then deionized water was added into volume 50 mL. The solution was slowly sprayed to 5 g of support as described in **3.3.1**. Thereafter, the sample were dried in oven at 110 °C overnight. Lastly, the sample were stored in dried plastic bottle at ambient temperature.

3.3.3 Characterization of Pt-supported catalysts

3.3.3.1 Powder X-ray diffraction

The data on phase identification, including the determination of unit cell parameters and the crystallite size can be obtained by Powder X-ray diffraction (PXRD). The PXRD patterns were recorded on a DMAX2200 Ultima+ (Rigaku) diffractometer using CuKα radiation. The 2θ covered was 5-90° with a scan step of 0.040°/step.

3.3.3.2 Temperature-programmed reduction

The H_2 consumption of a catalyst (i.e., the reducibility of the metal/ alloyed metal) can be determined by a temperature-programmed reduction by H_2 gas (H_2-TPR). The measurement was performed in a quartz tube connected with a thermal conductivity detector (VICI). Prior to an analysis, the sample (approximately 0.1 g) was activated in nitrogen (flow rate of 30 mL/min) from room temperature to 200 °C at a heating rate of 10 °C/min, followed by an isothermal treatment at 200 °C for 1 h. Subsequently, the system was naturally cooled down to room temperature. Then, the temperature reduction profile was recorded using 10% H_2 in Ar at the heating rate of 10 °C/min, from 50 to 900 °C. The TCD signal was calibrated employing a known mass of CuO as a standard, considering that CuO is reduced stoichiometrically and completely to Cu and H_2O. The reduction profile of CuO and the calculation of the hydrogen consumption can be found in **Appendix A**. The H_2 consumption was present as mmol H_2 per gram of a catalyst.

3.3.3.3 Surface area measurement and pore size distribution

Specific surface area of a catalyst was measured by an Autosorb-1 (Quantachrome) instrument. Each sample (weighed approximately 0.1 g) was degassed at 300 °C for 12 hours prior to analysis. After that, nitrogen gas was adsorbed on the surfaces of the sample at -196 °C. The adsorbate pressure was fixed at 1 torr, the equilibration time of 3 min at each point, and the scaled tolerances were set at zero. The surface area was analyzed employing BET equation [77]. The BJH pore size distribution was also calculated [78].

3.3.3.4 Thermal stability

The thermal stability of a catalyst was measured by thermogravimetric analyzer (Pyris). The sample was manually grinded in a mortar to homogeneous fine particles. Then, approximately 10 mg of the sample was put into a platinum pan. The measurement was conducted under 20 mL/min of nitrogen atmosphere, from 30 to 900 °C with heating rate of 5 °C/min. The mass of the sample as the function of temperature was recorded.

3.3.3.5 Morphology

For transmission electron microscopic study (TEM), the sample was crushed in a mortar with few drops of acetone, and the suspended powder was dispersed on a carbon-coated copper TEM grid. Electron micrographs are acquired in the magnification range of 3,000-1,500,000×.

3.3.3.6 Elemental analysis

Elemental analysis of the metal-supported catalyst is performed by inductively coupled plasma/mass-spectroscopy (ICP/QMS). An accurate 100 mg of catalyst was weighed and then digested with 1 mL of nitric acid for 3 hours on a hotplate at 90 °C. After the complete dissolution of the powder, this solution was filtrated and washed by deionized water. The liquid was transferred into a 50 mL plastic volumetric flask. Then, the metal concentration is reduced by diluting with deionized water to 0.5 ppm. The diluted solution was measured by ICP/QMS against the blank. Finally, the metal content is calculated using calibration curves. Calibration curves were prepared with the concentration range of 0.2-1 ppm for Pt (chloroplatinic acid solution), Sn (Tin(II) chloride solution), Fe (Iron (III) nitrate solution), and Ga (Gallium (III) nitrate solution).

The chemical composition of catalysts can be also determined by a wavelength-dispersive X-ray fluorescence spectrometry (WD-XRF). The sample is prepared by mixing 4.5 grams of boric acid and 0.5 grams of catalyst followed by manual grinding. The mixture is packed onto the sample holder and then compressed at 150 kN. The sample is placed in the sample chamber. CuKα is employed as a source for the measurement at 50 kV, 60 mA.

3.4 Catalytic activity testing

The catalysts were pressed, crushed, and sieved into 250-450 μm diameter. The catalyst was packed into the glass reactor and sandwiched by glass wool and glass bead. The schematic diagram of the reactor is shown in Figure 3.1. The reactor is positioned at the center of a vertical tube furnace. Nitrogen is used as a carrier gas, where its flow rate was controlled by a mass flow controller and was checked by a bubble flow meter. Before activity testing, the catalyst was reduced by heating from room temperature to 400 °C (5 °C/min) and held at 400 °C for 2 hours under the stream of H_2 (100 mL/min). Then, heptanoic acid in *n*-octane (15 wt%) was fed into the reactor under a 100 mL/min flow of H_2 by a syringe pump at a flow rate of 1.2-5.0 mL/h. These flow rates and mass of the catalyst (0.01 g) corresponds to the contact time (W/F) of 1-8 $g \cdot h \cdot mol^{-1}$. The catalytic testing was continued for at least 3 hours on stream. The reacted gaseous mixture flew out of the reactor was passed on-line through a gas sampling loop of a gas chromatograph. In order to prevent condensation of the products, the transfer line after the reactor was heated by the heating tape at 230 °C. The products were analyzed on-line by an HP6890 gas chromatograph equipped with a DB-1 column (30 m × 0.32 mm) and FID detector. The products were analyzed every 30 minute.

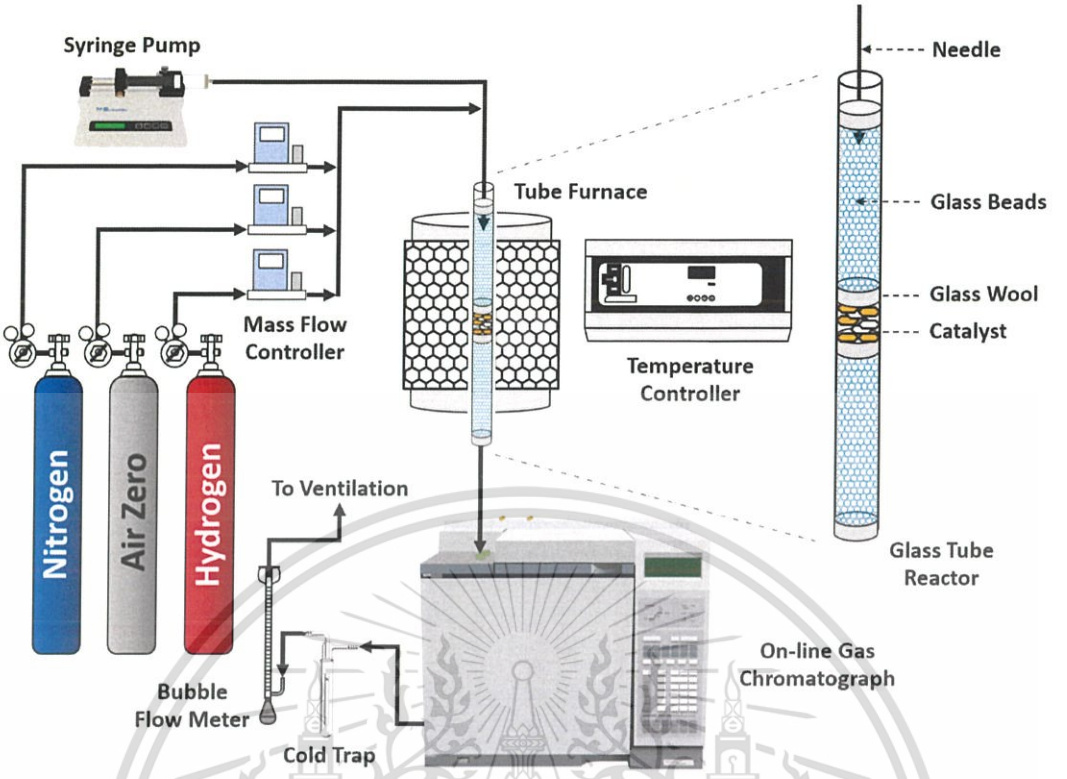

Figure 3.1 Schematic diagram of catalytic testing rig

The catalytic activity testing using heptanal as the substrate was also performed similarly at the contact time of 1-5 g·h·mol^{-1} employing the same reaction conditions for heptanoic acid.

The standard for the quantitative analysis was prepared by mixing *n*-hexane, *1*-hexene, *n*-heptane, heptanal, heptanoic acid, *1*-heptanol, and *2*-decanone (2 wt% each) in *n*-octane solvent. Examples of the chromatogram of the standard, including the summary of the retention time for some runs are shown in **Appendix B**.

Chapter 4

Results and Discussion

4.1 Characterization of the catalyst

4.1.1 Metal loading and BET surface area

The physicochemical properties of different catalysts are summarized in Table 4.1. The metal content in the catalysts was determined by inductively coupled plasma mass spectroscopy (ICP/MS). However, since the dissolution protocol for ICP/MS analysis may not completely dissolve Sn species into the medium, the Sn content was separately analyzed by energy dispersive X-ray spectroscopy (EDX). Results are shown in Table 4.1. It was found that the platinum loading was approximately 0.5 wt%, as anticipated for all samples. The experimentally-determined amount of other metal promoters is also in reasonable agreement with the amount loaded.

Table 4.1 The physical properties of the catalysts.

	Metal loading (wt%)				S_{BET}
Sample	Pt[a]	Fe[a]	Ga[a]	Sn[b]	(m^2/g)
SiO_2	-	-	-	-	300
TiO_2	-	-	-	-	50
0.5Pt/SiO_2	0.58	-	-	-	290
0.5Pt-0.2Fe/SiO_2	0.54	0.28	-	-	275
0.5Pt-0.2Ga/SiO_2	0.56	-	0.26	-	272
0.5Pt-0.2Sn/SiO_2	0.55	-	-	0.29	278
0.5Pt-0.3Sn/SiO_2	0.54	-	-	0.33	263
0.5Pt-0.5Sn/SiO_2	0.55	-	-	0.50	254
0.5Pt-0.2Sn/TiO_2	0.54	-	-	0.28	48

[a] *ICP/MS*

[b] *EDX*

The specific surface area (S_{BET}) of all catalysts is determined via the nitrogen adsorption/desorption isotherm fitted with a Brunauer-Emmet-Teller (BET) equation. The S_{BET} of the silica support is as high as 300 m^2/g, which is 6 times larger than that of titanium oxide (50 m^2/g). The specific surface area of the catalysts only slightly decreased upon impregnation of the Pt or bimetallic Pt-M (e.g., M = Fe, Sn, or Ga). Considering such small decrease, it can be safely assumed that these promoters (Pt, or bimetallic Pt with Fe, Sn and Ga) are highly dispersed on the supports.

The dispersion of Pt onto SiO_2 was confirmed by TEM. After the deposition, the catalyst was reduced under hydrogen at 400 °C for 2 h. The TEM images in Figure 4.1 show the presence of several Pt particles with 1-3 nm in diameter. It is clear that the monometallic Pt nanoparticles were highly dispersed on the silica support. This high dispersion could be the reason that the S_{BET} of 0.5Pt/SiO_2 is not much different from that of SiO_2.

Figure 4.1 TEM images of 0.5Pt/SiO_2 after the reduction at 400 °C.

4.1.2 Reducibility of the catalyst

The temperature-programmed reduction (TPR) profiles of Pt and bimetallic Pt-M (Pt-Fe, Pt-Sn, and Pt-Ga) supported on SiO_2, and also the bimetallic Pt-Sn supported on TiO_2, are shown in Figure 4.2.

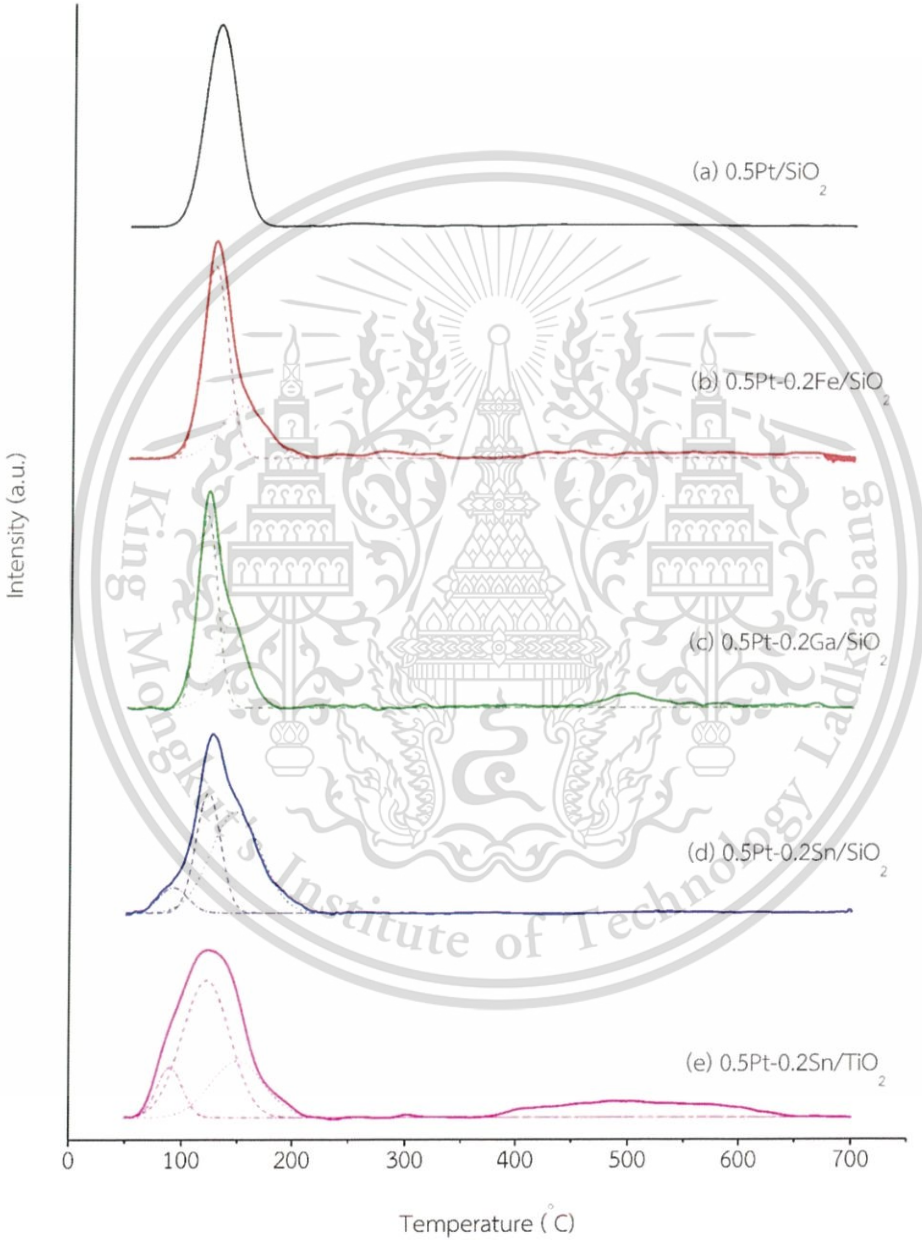

Figure 4.2 TPR profiles of (a) $0.5Pt/SiO_2$, (b) $0.5Pt\text{-}0.2Fe/SiO_2$, (c) $0.5Pt\text{-}0.2Ga/SiO_2$, (d) $0.5Pt\text{-}0.2Sn/SiO_2$, and (e) $0.5Pt\text{-}0.2Sn/TiO_2$.

It was found that the 0.5Pt/SiO_2 catalyst (Figure 4.2 (a)) showed only a single reduction peak at the peak temperature T_p of 125 °C, corresponding to the reduction of Pt^{2+} to Pt [76]. When the second metal was incorporated, the reduction peak shift to a higher temperature suggesting to the bimetallic Pt-M formation.

The formation of bimetallic Pt-M results in the overlap of reduction peaks in all cases. For 0.5Pt-0.2Fe/SiO_2 catalyst (Figure 4.2 (b)), the H_2 consumption can be deconvoluted into two components. The first peak was found at T_p of 125 °C and corresponded to the reduction of Pt^{2+} specie, while the latter peak (T_p of 150 °C) is assigned to the reduction of bimetallic Pt-Fe specie [79]. This reduction temperature for bimetallic Pt-Fe specie is drastically different from the reduction of Fe_2O_3 (T_p ; 250 – 750 °C) [80]. Hence, the formation of bulk Fe_2O_3 in 0.5Pt-0.2Fe/SiO_2 can be excluded.

For the 0.5Pt-0.2Ga/SiO_2 catalyst (Figure 4.2 (c)), the H_2 consumption can also be deconvoluted into two components. The first peak at T_p of 125 °C was again corresponded to the reduction of Pt^{2+} specie, while the latter peak at T_p of 145 °C is assigned to the reduction of bimetallic Pt-Ga specie [81]. However, the reduction peak at T_p = 500 °C (assigned to the reduction of Ga_2O_3 [81]), suggests that Ga_2O_3 is retained in the catalyst, and the actual amount of Ga alloying with Pt could be lower than the expected amount.

The TPR profile of 0.5Pt-0.2Sn/SiO_2 catalyst (Figure 4.2 (d)) can be deconvoluted into three components. The first (T_p = 90 °C) and second (T_p = 125 °C) peaks were assigned to the reduction of Pt^{2+} as above. This result suggests that disaggregation of some Pt into smaller particle took places. Hence, the reduction of Pt^{2+} specie is promoted at relatively low temperature (90 °C) when Sn was added. The last peak at T_p = 150 °C is assigned to the reduction of bimetallic Pt-Sn specie [76].

Furthermore, the effect of support toward the reduction of Pt^{2+} specie can be seen from the 0.5Pt-0.2Sn/TiO_2 TPR profile (Figure 4.2 (e)). Although, the same temperature region of Pt^{2+} and bimetallic Pt-Sn reduction peak were observed, as compared to the 0.5Pt-0.2Sn/SiO_2 (Figure 4.2 (d)), a relatively low reduction

temperature of TiO_2 support was found at 450-700 °C in TPR, in comparison to 600-900 °C typically observed for the reduction of TiO_2 without Pt [18]. Moreover, the H_2 consumption (Table 4.2) were larger for the 0.5Pt-0.2Sn/TiO_2 (0.046 mmol/g), as compared to 0.5Pt-0.2Sn/SiO_2 (0.038 mmol/g). In other words, this amount of H_2 consumed over 0.5Pt-0.2Sn/TiO_2 is much higher than that required (0.038 mmol/g) to reduce all Pt-Sn oxide particles to bimetallic Pt-Sn. Assuming that the initial oxidation state of Pt-Sn in the 0.5Pt-0.2Sn/TiO_2 samples is the same as that in 0.5Pt-0.2Sn/SiO_2, this amount of H_2 consumption is likely the combination of the reduction of bimetallic Pt-Sn, and also of Ti^{4+} to Ti^{3+} on the TiO_2 surface via hydrogen spillover mechanism, [81].

Since bimetallic Pt with oxophillic metal (Fe, Sn, or Ga) can be readily obtained with Sn, the effect of the Sn loading further investigated as shown in Figure 4.3.

The increase Sn content to 0.3 (0.5Pt-0.3Sn/SiO_2; Figure 4.3 (c)) leads to lower reduction temperature of Pt^{2+} at low temperature (T_p shift from 125 to ~ 100 °C) suggesting that Pt is better dispersed over 0.5Pt-0.3Sn/SiO_2 catalyst. In addition, the amount of hydrogen consumption of PtSn phase (T_p ~ 145 °C) is increased. Moreover, the reduction temperature at T_p ~ 170 °C were observed, which is attributed to the formation Pt_2Sn_3 phase [76]. These results suggest that the increase Sn ratio in bimetallic Pt-Sn does not only inhibit the aggregation of Pt particle, but also facilitate the formation of other bimetallic Pt-Sn phase (PtSn, Pt_2Sn_3). Since no reduction peak for SnO_2 (T_p ~ 500 °C) was detected [76], the bulk SnO_2 is not present in these catalysts. Especially, even when an equal amount of Pt and Sn was employed (i.e., x = 0.5; Figure 4.3 (d)), neither isolated Pt nor Sn reduction was not observed. In turn, a new $PtSn_2$ phase appeared at high reduction temperature (T_p ~ 225 °C) [76]. These results suggest that bimetallic Pt and Sn were completely formed in 0.5Pt-0.5Sn/SiO_2.

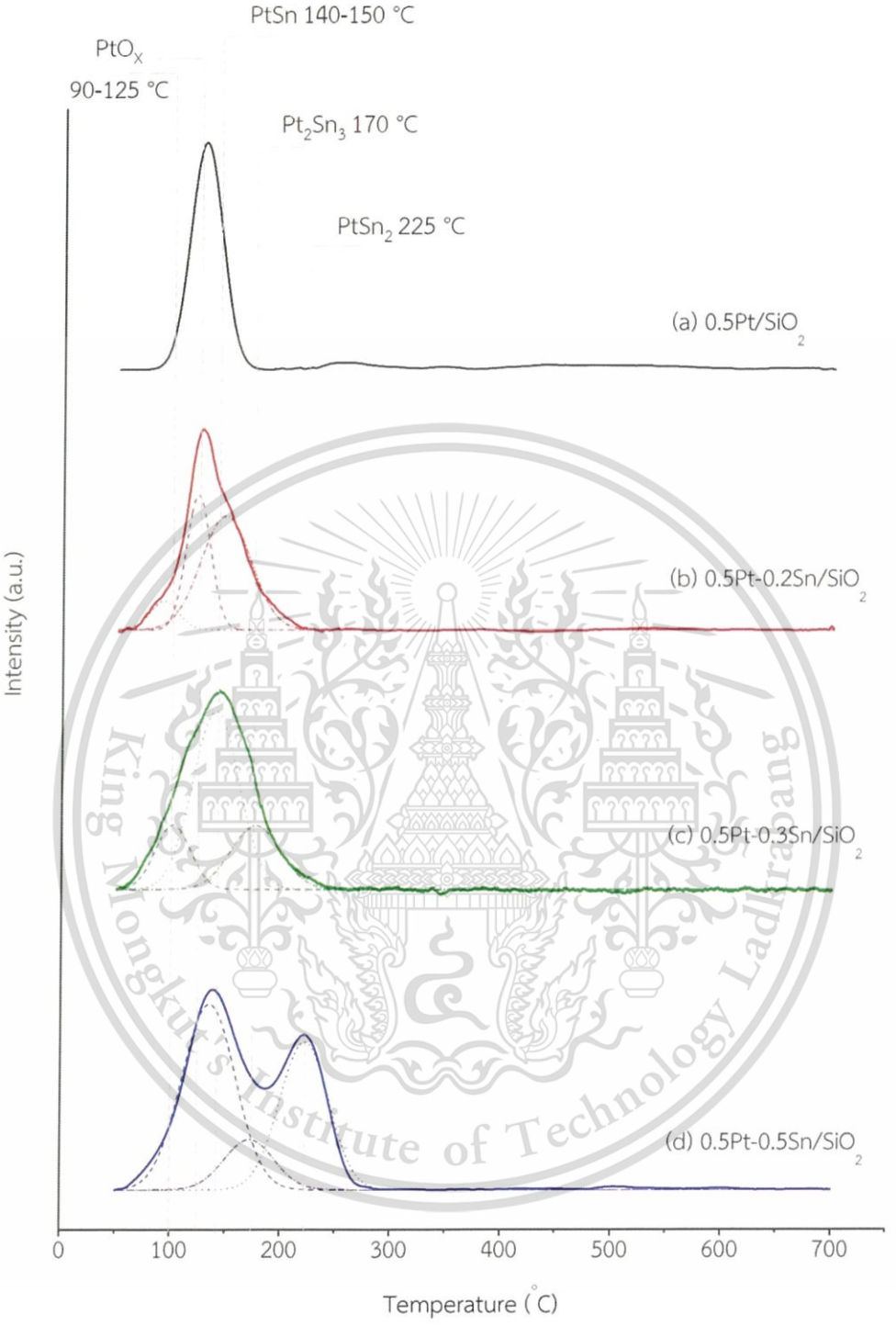

Figure 4.3 TPR profiles of (a) 0.5Pt/SiO_2, (b) 0.5Pt-0.2Sn/SiO_2, (c) 0.5Pt-0.3Sn/SiO_2, and (d) 0.5Pt-0.5Sn/SiO_2.

The H_2-consumption of Pt/SiO_2 and all bimetallic Pt-M catalysts as discussed earlier is summarized in Table 4.2. The amount of reducible metal can be estimated from the H_2-consumption per gram of the catalyst.

Table 4.2 The H_2-consumption of all catalysts.

Sample	T_p (°C)	Assignment	H_2-consumption (mmol/g) Actual	Total	Theoretical[a]
$0.5Pt/SiO_2$	125	$Pt^{2+} \rightarrow Pt$	0.024	0.024	0.024
$0.5Pt\text{-}0.2Fe/SiO_2$	125	$Pt^{2+} \rightarrow Pt$	0.023	0.035	0.035
	150	$PtFeO_x \rightarrow Pt\text{-}Fe$	0.012		
$0.5Pt\text{-}0.2Ga/SiO_2$	125	$Pt^{2+} \rightarrow Pt$	0.025	0.036	0.036
	145	$PtGaO_x \rightarrow Pt\text{-}Ga$	0.009		
	500	$Ga_2O_3 \rightarrow Ga$	0.002		
$0.5Pt\text{-}0.2Sn/SiO_2$	90	$Pt^{2+} \rightarrow Pt$	0.003	0.038	0.038
	125	$Pt^{2+} \rightarrow Pt$	0.013		
	150	$PtSnO_x \rightarrow PtSn$	0.022		
$0.5Pt\text{-}0.2Sn/TiO_2$	90	$Pt^{2+} \rightarrow Pt$	0.004	0.046	0.038
	125	$Pt^{2+} \rightarrow Pt$	0.022		
	150	$PtSnO_x \rightarrow PtSn$	0.011		
	500	$Ti^{4+} \rightarrow Ti^{3+}$	0.009		
$0.5Pt\text{-}0.3Sn/SiO_2$	100	$Pt^{2+} \rightarrow Pt$	0.007	0.040	0.040
	145	$PtSnO_x \rightarrow PtSn$	0.024		
	170	$PtSnO_x \rightarrow Pt_2Sn_3$	0.009		
$0.5Pt\text{-}0.5Sn/SiO_2$	140	$PtSnO_x \rightarrow PtSn$	0.023	0.046	0.046
	170	$PtSnO_x \rightarrow Pt_2Sn_3$	0.006		
	225	$PtSnO_x \rightarrow PtSn_2$	0.017		

[a] *Estimated data from the amount of metal loading (Appendix A).*

4.2 Hydrodeoxygenation of *n*-heptanoic acid and *n*-heptanal over 0.5Pt/SiO_2

The catalytic hydrodeoxygenation over supported Pt catalysts is attempted for the conversion of fatty acids to hydrocarbons via decarboxylation and decarbonylation. These reactions were studied using two model compounds: *n*-heptanoic acid and *n*-heptanal.

n-Heptanoic acid is a small fatty acid found in typical bio-derived feedstocks, while *n*-heptanal is a potential intermediate for the decarbonylation of *n*-heptanoic acid to 1-hexene.

4.2.1 Product distribution

The product distributions obtained from the reaction of *n*-heptanoic acid at various contact times (*W/F*) are shown in Figure 4.4.

It can be seen that the conversion of *n*-heptanoic acid is increased with the contact time (*W/F*). This result can be reasonably understood considering that the activity of the catalyst toward the formation of products depends on the number of the active metal sites (which is proportional to *W/F*). It was also observed that both hexene and *n*-hexane are the major products at all contact times while 2,4-hexadiene, hexanal and 7-tridecanone were the minor products. (In this work, "hexene" refers to a combination of 1- and 2-hexene.) The yield of all products was increased with *W/F*, except for *n*-heptanal which was present only at a low contact time. This result suggests that *n*-heptanal may be an intermediate for hexene or *n*-hexane. Hence, the reaction of heptanal was tested to compare with *n*-heptanoic acid. The product distribution from the reaction with different feed at the same contact time is summarized in Table 4.3.

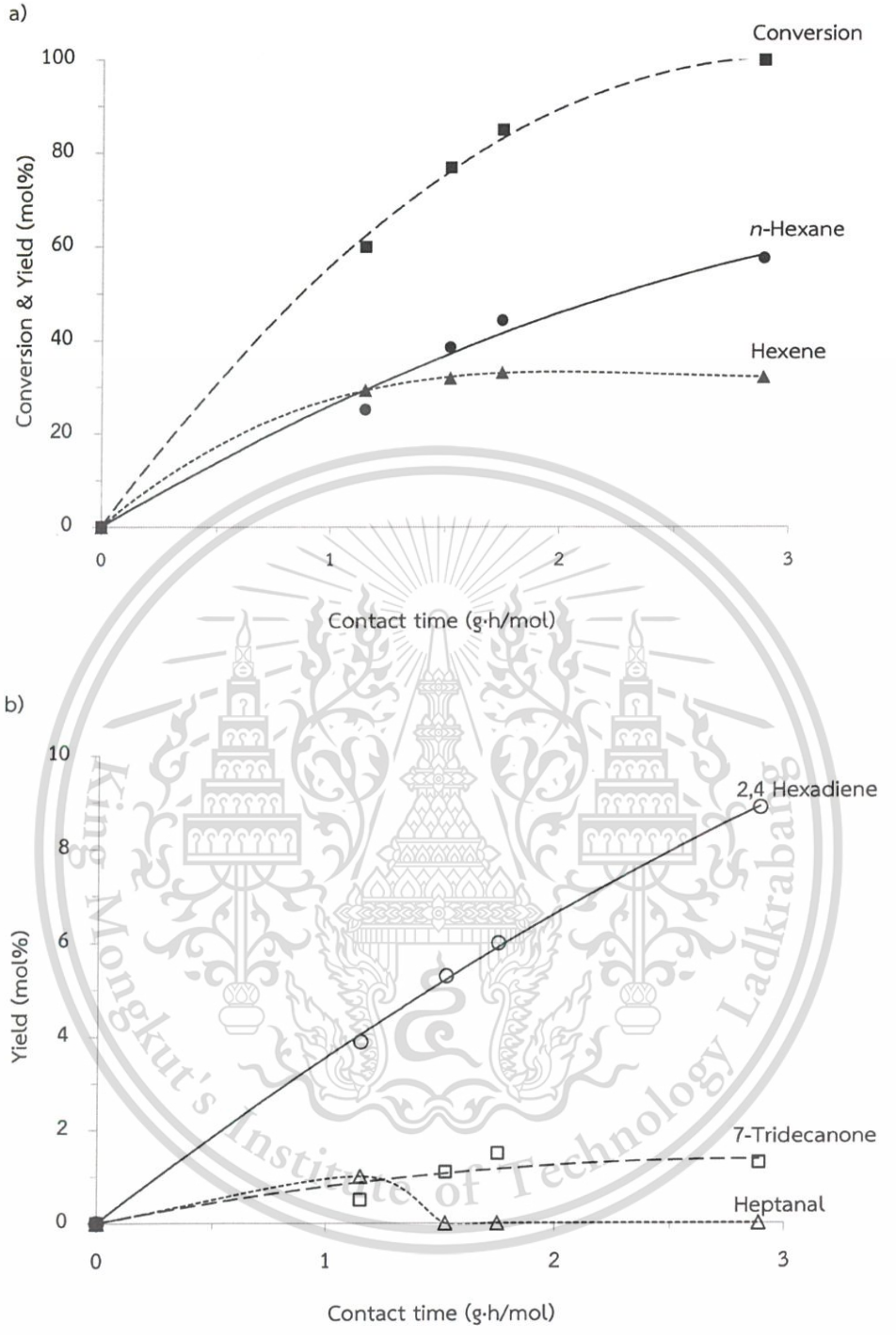

Figure 4.4 The effect of contact time on *n*-heptanoic hydrodeoxygenation over 0.5Pt/SiO_2; a) Conversion and yield of major products (hexene and *n*-hexane); b) yield of minor products (2,4-hexadiene, 7-tridecanone and *n*-heptanal).

Reaction conditions: reaction temperature (T_{react}) 400 °C, reduction temperature (T_{red}) 400 °C, flow rate of H_2 carrier gas (F_{H2}) 100 mL/min, atmospheric pressure, contact time (W/F) 1.15-2.89 g·h/mol. The values shown were initial values extrapolated to the time on stream (TOS) of zero.

Table 4.3 Conversion and the product distribution over $0.5Pt/SiO_2$ using different feeds.

	Contact time	Conversion	Product yield (mol%)				
	(g·h/mol)	(mol%)	Hexene[c]	*n*-Hexane	2,4-Hexadiene	*n*-Heptanal	7-Tridecanone
Feed							
n-Heptanoic acid [a]	1.15	21.4	8.2	8.2	2.6	0.3	2.1
n-Heptanal [b]	1.15	34.2	17.3	13.9	3.0	-	0.0

Reaction condition: T_{react} = 400 °C, T_{red} = 400 °C, F_{H2} = 100 mL/min, atmospheric pressure. *The values shown were taken at 60 min time on stream.*

[a] *Feed: 15 wt% n-heptanoic acid in n-octane*

[b] *Feed: 100 wt% n-heptanal*

[c] *Hexene: 1-Hexene & 2-Hexene*

From Table 4.3, when *n*-heptanal was used as feed, a higher conversion was obtained while the product distributions are similar to that observed with *n*-heptanoic acid. (Details of the conversion of *n*-heptanal and products distribution as a function of time on stream can be found in Appendix B). As *n*-heptanal is observed only at low *W/F*, it is likely that *n*-heptanal is the primary product from reduction of *n*-heptanoic acid, as shown in Scheme 4.1.

Scheme 4.1 Hydrogenation of *n*-heptanoic acid.

Since hexene is presented as major product of heptanal, it is suggested that *n*-heptanal can be converted to *n*-hexene via decarbonylation [83], as shown in Scheme 4.2.

Scheme 4.2 Decarbonylation of heptanal.

n-Hexane was also found as the major product in both *n*-heptanoic acid and *n*-heptanal feeds over the $0.5Pt/SiO_2$ catalyst. The formation of *n*-hexane might be produced via either (i) the direct decarboxylation of *n*-heptanoic acid (Scheme 4.3), or (ii) the hydrogenation of hexene (Scheme 4.4) that is formed via decarbonylation.

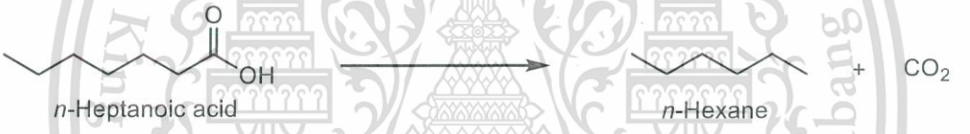

Scheme 4.3 Direct decarboxylation of *n*-heptanoic acid.

Scheme 4.4 Hydrogenation of 1-hexene.

However, in the reaction with *n*-heptanal, *n*-hexane cannot be produced from direct decarboxylation. Therefore, the observed *n*-hexane would be virtually derived from hydrogenation of hexene produced.

It is noted that a small amount of 2,4-hexadiene is also obtained from the reaction (from either *n*-heptanoic acid or *n*-heptanal feed). This formation suggests that some small amount of *n*-hexane may also be derived from hydrogen transfer, as demonstrated in Scheme 4.5.

Scheme 4.5 Hydrogen transfer of 1-hexene.

To verify the extent of hexene hydrogenation and hydrogen transfer, the reaction with co-feeding *n*-heptanoic acid/hexene is tested, as shown in Table 4.4.

Table 4.4 Conversion and the products distribution in the mixed feed.

Catalyst		$0.5Pt/SiO_2$
Feed (mol%)		
n-Heptanoic acid	100	55.0
Hexene	-	45.0
Outlet yield (mol%)		
n-Heptanoic acid	30.0	16.7
Hexene	33.0	36.9
n-Hexane	30.6	34.8
2,4-Hexadiene	4.7	9.4
n-Heptanal	0.7	0.0
7-Tridecanone	1.0	2.2
Conversion (mol%)	70.0	69.6
Contact time (g·h/mol)	3.35	1.77

Reaction condition: T_{react} = 400 °C, T_{red} = 400 °C, F_{H2} = 100 mL/min, atmospheric pressure. *The values shown were taken at 60 min time on stream (steady state).*

It can be clearly seen that, at a similar level of conversion, the yield of hexene in the mixed feed (36.9%) is lower than starting composition (45.0%). Moreover, the *n*-hexane yield (34.8%) in the mixed-feed was higher than that obtained over the single feed (30.6%) as well. This result suggests that the hydrogenation of hexene to *n*-hexane was particularly promoted over 0.5Pt/SiO_2 catalyst. Moreover, the higher yield of 2,4-hexadiene is also obtained. This result suggests that the hydrogen transfer of hexene to 2,4-hexadiene was also promoted. It might be deduced that the production of *n*-hexane yield is from two main routes: (i) the direct decarboxylation of *n*-heptanoic acid (as discussed previously), and also from (ii) the hydrogenation of hexene.

In addition to hydrocarbon balance, 7-tridecanone is only detected when *n*-heptanoic acid was used as the feed (Table 4.3 and 4.4). It is suggested that this product was formed from ketonization of *n*-heptanoic acid over SiO_2 support (Scheme 4.6). Hence, no 7-tridecanone is observed when heptanal is used as feed.

Scheme 4.6 Ketonization of *n*-heptanoic acid.

From the above observations and discussion, the overall reaction pathway for the hydrodeoxygenation of *n*-heptanoic acid over Pt/SiO_2-based catalysts can be proposed, as demonstrated in Scheme 4.7.

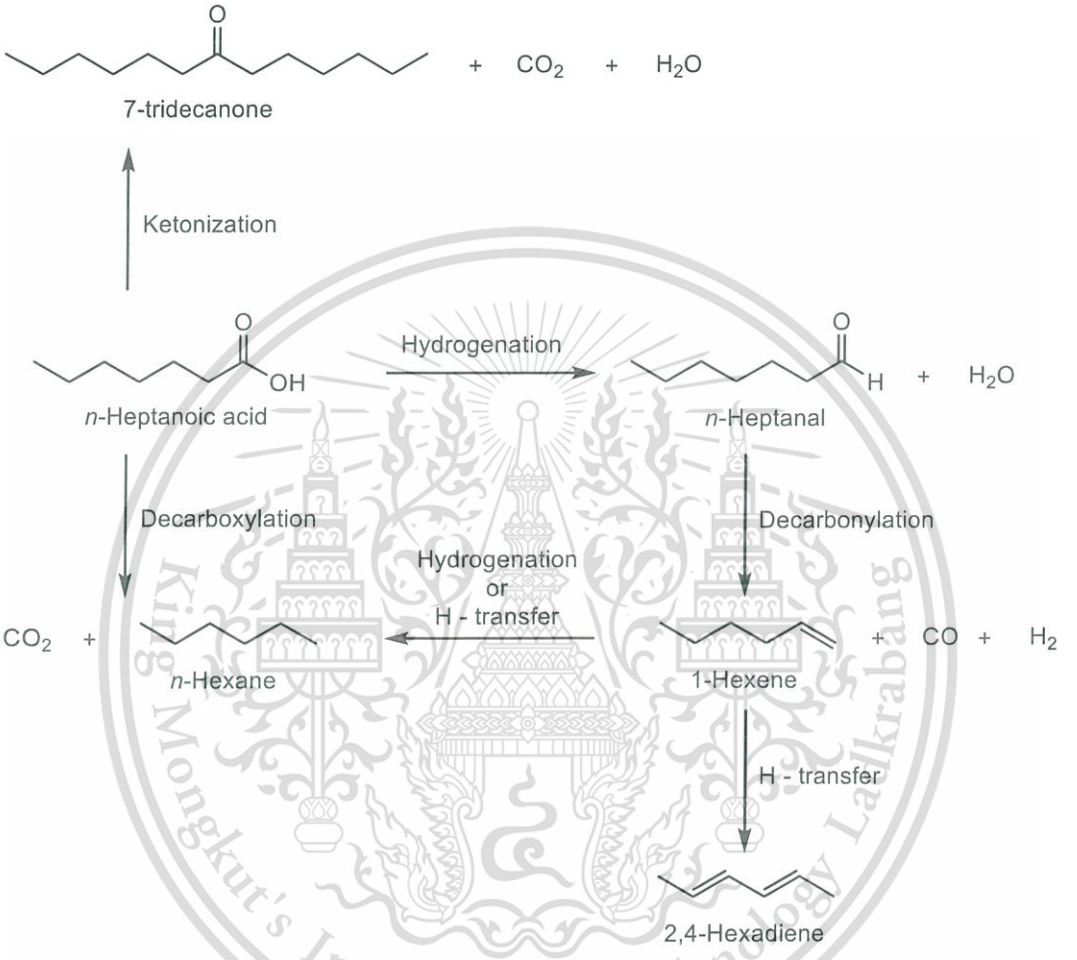

Scheme 4.7 The reaction pathway for the conversion of *n*-heptanoic acid over $0.5Pt/SiO_2$-based catalysts studied in this work.

4.2.2 Effect of pretreatment on catalyst

It is well known that preliminary treatments have a strong influence on the structure and activity of supported Pt catalysts [84]. The pretreatment experiments in this work were carried out using 0.5Pt/SiO_2 as an example. The catalyst was heated in flowing hydrogen at 400 °C for 2 h to reduce any platinum cationic species to the metallic Pt particles. In another sample, 0.5Pt/SiO_2 was calcined in air-zero at 400 °C for 2 h, followed by reduction, as described previously. The comparison of the activity and selectivity of the catalysts with these two pretreatment conditions ("reduced" and "calcined/reduced") were shown in Table 4.5.

Table 4.5 The effect of pretreatment conditions on the deoxygenation of *n*-heptanoic acid over 0.5Pt/SiO_2

Catalyst	0.5Pt/SiO_2	
Pretreatment condition	Reduced	Calcined/Reduced
Conversion (mol%)	54.0	30.8
Selectivity (mol%)		
Hexene[a]	40.3	40.2
n-Hexane	40.5	38.7
2,4-Hexadiene	12.1	13.6
n-Heptanal	0.0	0.0
7-Tridecanone	7.1	7.5

Reaction condition: T_{react} = 400 °C, T_{red} = 400 °C, F_{H2} = 100 mL/min, atmospheric pressure, W/F = 2.89 g·h/mol. *The values shown were taken at 60 min time on stream (steady state).*

From Table 4.5, the calcined/reduced 0.5Pt/SiO_2 showed lower activity while maintaining the same products selectivity. This result suggests that some active sites were lost by calcination. TEM images in Figure 4.5 show that there are relatively large particles with the diameter of 2-6 nm (presumably Pt particles) in the calcined/reduced 0.5Pt/SiO_2 catalyst, likely due to sintering induced by calcination. This number could be compared to 1-3 nm for the reduced 0.5Pt/SiO_2 catalyst. With large particles, some

metal atoms are not exposed to the surfaces but remain encapsulated in the core of the particles. So, these metal atoms would not show any catalytic activity. Since Pt generally has poor interaction with the silica support, calcination would activate its migration that leads to sintering of the Pt particle. Hence, the overall activity is relatively dropped.

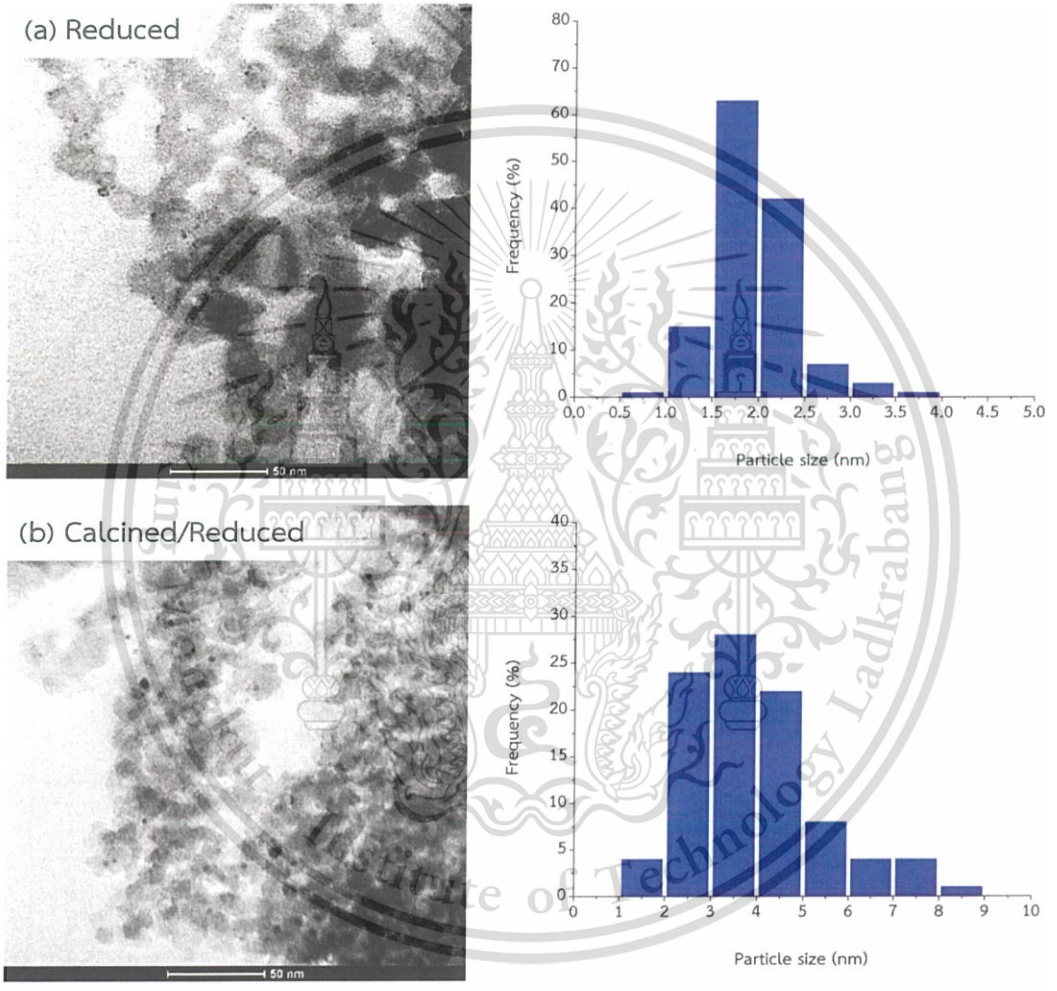

Figure 4.5 TEM images of Pt/SiO_2: (a) after reduction, and (b) after calcination-reduction at 400 °C.

Examination of changes in particle size by TEM and changes in catalytic activity due to the pretreatment conditions indicate that, the reduction at 400 °C is sufficient to activate the $0.5Pt/SiO_2$ catalyst for hydrodeoxygenation of *n*-heptanoic acid.

4.2.3 Effect of reaction temperature on decarbonylation of *n*-heptanal

According to Scheme 4.7, *n*-heptanal (produced from the reduction of *n*-heptanoic acid) is an intermediate for hydrodeoxygenation of the *n*-heptanoic acid to both hexene and *n*-hexane. In order to evaluate only the decarbonylation and hydrogenation activity of Pt/SiO_2-based catalysts (disregard the direct decarboxylation and reduction of *n*-heptanoic acid) the conversion of *n*-heptanal as a feed model was investigated. Since it is well known that the hydrodeoxygenation activity is thermodynamically favored at high reaction temperature [85], catalytic activities at different reaction temperatures (320 – 400 °C) were conducted and the results are shown in Figure 4.6.

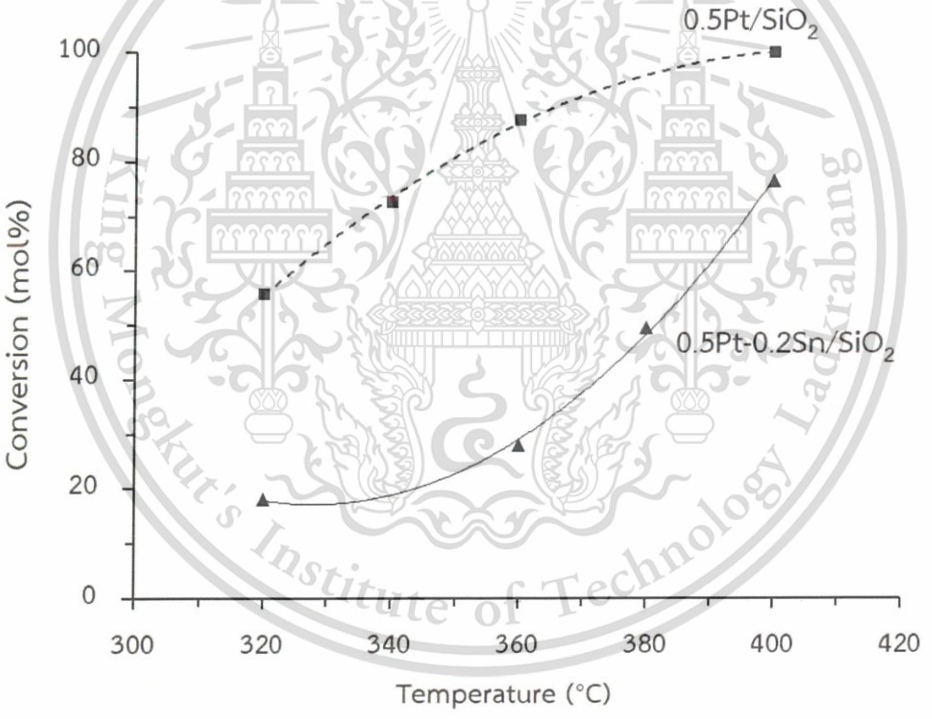

Figure 4.6 The *n*-heptanal hydrodeoxygenation activity over $0.5Pt/SiO_2$ and $0.5Pt\text{-}0.2Sn/SiO_2$ in the effect of the reaction temperature.

Reaction condition: T_{react} = 400 °C, T_{red} = 400 °C, F_{H2} = 100 mL/min, atmospheric pressure, W/F = 2.89 g·h/mol. *The values shown were taken at 60 min time on stream (steady state).*

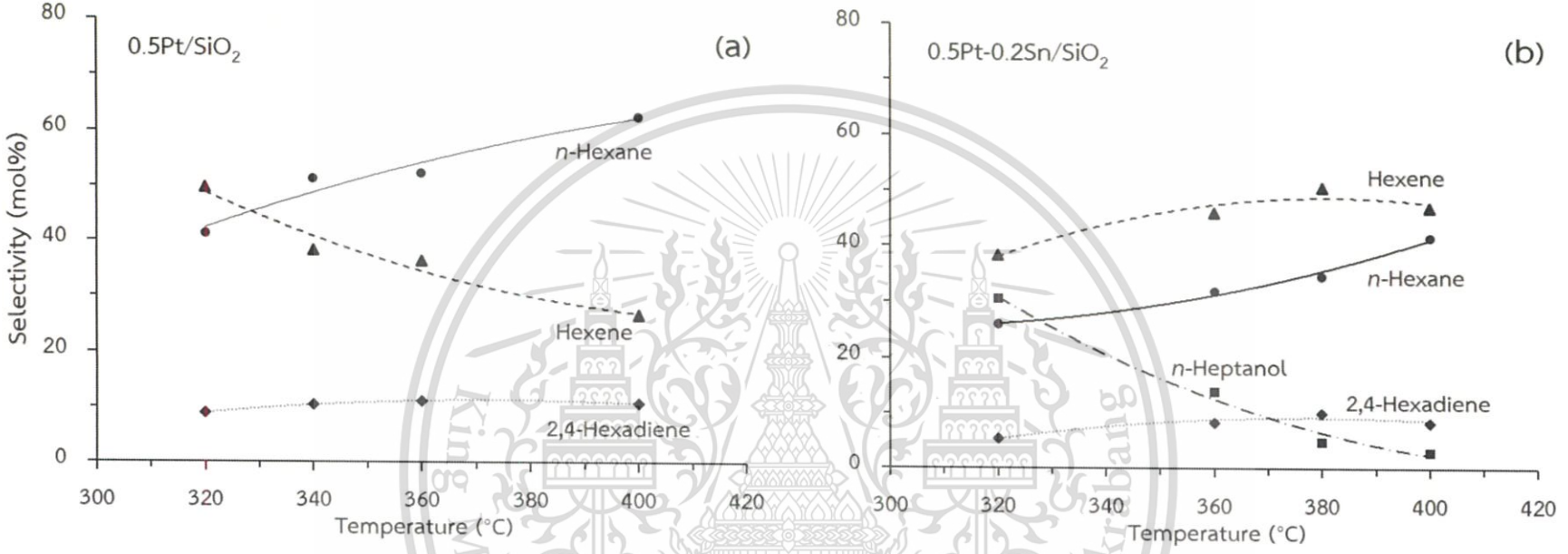

Figure 4.7 The selectivity of (a) 0.5Pt/SiO_2 and (b) 0.5Pt-0.2Sn/SiO_2 as a function of reaction temperature.

Reaction condition: T_{react} = 320-400 °C, T_{red} = 400 °C, F_{H2} = 100 mL/min, atmospheric pressure, W/F = 2.89 g·h/mol. The values shown were at 60 min of time on stream (steady state).

From Figure 4.6, the increase in the reaction temperature over 0.5Pt/SiO_2 resulted in the increase in conversion from 33% to 88% with *n*-hexane and hexene as the main products. Figure 4.7 shows in more detail the selectivity to hexene and *n*-hexane as a function of the reaction temperature. Over 0.5Pt/SiO_2 (Figure 4.7 (a)), it can be seen that with increasing temperature, the selectivity of hexene (derived from decarbonylation) is decreased from 67% to 49%, while the selectivity to *n*-hexane (obtained from hydrogenation of hexene) is proportionally increased from 33% to 51%. This result indicates that the reaction temperature does not only affect the decarbonylation of heptanal to hexene, but also the hydrogenation of hexene to *n*-hexane. Accordingly, the produced hexene from heptanal would subsequently convert to *n*-hexane, particularly at high temperature.

When Sn is present (0.5Pt-0.2Sn/SiO_2), the overall activity of the bimetallic Pt-Sn catalyst is lower than that of the 0.5Pt/SiO_2. This result suggests that the incorporation of Sn reduced the decarbonylation activity. This behavior was ascribed to the electropositive nature of Sn, which result in a lower stability of the di-sigma surface aldehyde species η^2(C,O)-heptanal, as compared to that on the pure Pt surface. The bimetallic Pt-Sn surface also hinders the formation of η^1(C)-acyl species, involved in the decarbonylation reaction, as shown in Scheme 4.8 [85].

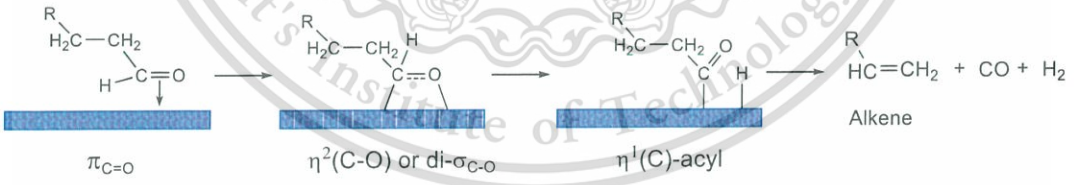

Scheme 4.8 Decarbonylation of *n*-heptanal.

Nevertheless, the increase in the reaction temperature promotes the conversion especially 400 °C. This result might be reasonably understood considering that the formation of bimetallic Pt-Sn required a higher temperature to activate the decarbonylation, as compared to that for the monometallic Pt. In other words, activation energy for the decarbonylation over bimetallic Pt-Sn is higher than that over pure Pt catalyst [76].

Besides the activity, the differences in product distribution were also observed when Sn was incorporated into the $0.5Pt/SiO_2$ catalyst, as seen in Figure 4.7 (b). The main products over bimetallic Pt-Sn catalyst are hexene, *n*-hexane, and *n*-heptanol. The hexene and *n*-hexane selectivity increase with temperature and the higher hexene yield over $0.5Pt\text{-}0.2Sn/SiO_2$ suggests that the Sn addition dramatically hinders hexene hydrogenation to *n*-hexane. This might be explained considering the interaction between Sn and Pt, which decreases the electron density on Pt, resulting in a lower efficiency of hydrogen adsorption and dissociation. In consistent, the reduction of Pt-Sn species shifts to the higher temperature, as shown in TPR profiles (Figure 4.2). This Pt-Sn interaction also results in a lower extent of back-donation from the alloy surface to the chemisorbed olefin, i.e., weakening of the hexene-bimetallic (Pt-Sn alloy) surface bonding [18]. Hence, the hydrogenation activity was dropped, as clearly seen in Figure 4.7 (b).

The presence of *n*-heptanol over $0.5Pt\text{-}0.2Sn/SiO_2$ is remarkable since it is not observed over $0.5Pt/SiO_2$. It is well known that *n*-heptanol is produced from hydrogenation of the *n*-heptanal adsorb exclusively in the $\eta^1(O)$ configuration [85], as shown in Scheme 4.9.

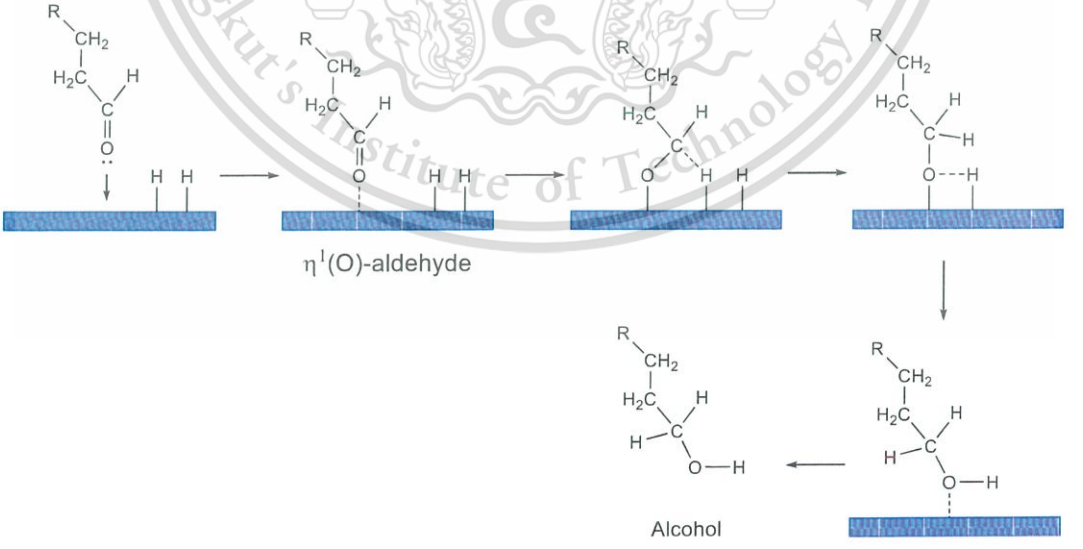

Scheme 4.9 Hydrogenation of *n*-heptanal.

As the stability of the di-sigma η^2(C,O)-heptanal species is decreased when Sn is incorporated, the η^1(O) configuration would be favored. In this configuration, the *n*-heptanal is bonded to the surface through the oxygen lone pair orbital of the carbonyl, acting as a Lewis base [85]. The η^1(O)-heptanal intermediate can be readily hydrogenated to *n*-heptanol. Hence, high selectivity of the *n*-heptanol was observed when Sn is presented in the bimetallic catalyst, particularly at low temperature (~320 °C).

While the hexene selectivity was gradually increased, the selectivity to *n*-heptanol was rapidly decreased as a function of temperature. This is due to a more favorable of the decarbonylation, as compared to the hydrogenation at high temperature.

From these observations, the temperature at 400 °C was selected for further studies on the bimetallic Pt-M catalysts since it especially shows high activity and high hexene selectivity.

4.2.4 Effect of the metal incorporation and the type of support on the hydrodeoxygenation of *n*-heptanoic acid

As the bimetallic Pt-Sn catalyst provided high hexene selectivity, other bimetallic Pt with electropositive metal were evaluated in the hydrodeoxygenation of *n*-heptanoic acid, and the results are summarized in Table 4.6. Detailed results showing the conversion and the products selectivity as a function of time on stream can be found in Appendix C.

It was found that bimetallic Pt-M/SiO_2 (M = Fe, Sn, or Ga) catalysts generally exhibit a lower activity for the hydrodeoxygenation of *n*-heptanoic acid, as compared to 0.5Pt/SiO_2 at the same experimental conditions. This might be explained considering the interaction between a second (alloying) metal and platinum as discussed previously (Section 4.2.3).

Interestingly, the incorporation of Fe or Sn on to Pt/SiO_2 catalyst show the higher selectivity to hexene, as compared to other catalysts. This behavior was ascribed to the electropositive nature of Fe and Sn, which suppresses hydrogenation, as discussed previously. According to TPR results, these catalysts show high H_2-consumption of bimetallic Pt-M phase without residue Fe/Sn oxide phase. That is, both Fe and Sn can be completely formed with Pt. Hence, the electron density at Pt is particularly decreased such that the adsorption of hexene (and its hydrogenation to *n*-hexane) is reduced.

On the other hand, the 0.5Pt-0.2Ga/SiO_2 shows a low selectivity to hexene and shows hexene/*n*-hexane ratio (~1) similar to that over 0.5Pt/SiO_2 catalyst. This suggests that Ga may not be completely bimetallic formed with Pt. This is confirmed by the TPR results in Figure 4.2 showing the isolated reduction peak for Ga_2O_3. This Ga_2O_3 is known as inactive phase for both decarbonylation and hydrogenation [18]. Moreover, the remaining Pt phase in 0.5Pt-0.2Ga/SiO_2 catalyst readily promoted the hexene hydrogenation, resulting in the higher *n*-hexane selectivity. Furthermore, a high selectivity of 2,4-hexadiene was observed over 0.5Pt-0.2Ga/SiO_2. This product is most

likely produced via hydrogen transfer of hexene over a Lewis acid site in the catalyst, derived from the presence of Ga_2O_3 phase [18]. In addition, the ketonization of *n*-heptanoic acid to 7-tridecanone can also be promoted over Lewis acid sites.

Interestingly, *n*-heptanal can be detected for all reactions over bimetallic Pt-M catalysts, while it was not observed over $0.5Pt/SiO_2$. This result suggests that *n*-heptanal (produced from the hydrogenation of *n*-heptanoic acid) is not completely converted to hexene via decarbonylation because the bimetallic Pt-M possess a lower activity, as compared to the Pt alone (Section 4.2.3).

As, $Pt\text{-}Sn/SiO_2$ catalysts show a relatively higher both activity and selectivity of hexene, as compared to others bimetallic catalysts, the $0.5Pt\text{-}0.2Sn/TiO_2$ was prepared in order to reduce the electron density of the metal active site via a strong metal-support interaction (SMSI) [82].

However, it is shown in Table 4.6 that a very low conversion of *n*-heptanoic acid and high selectivity to a ketone (7-tridecanone) was observed over $0.5Pt\text{-}0.2Sn/TiO_2$. This is presumably because the active sites of $0.5Pt\text{-}0.2Sn/TiO_2$ were deactivated by the strong adsorption of the high molecular weight intermediate such as ketone. It is likely that 7-tridecanone is formed via ketonization of *n*-heptanoic acid over Lewis acid support, as mentioned above. The ketonization of an acid over TiO_2 is well known to involve defects such as the oxygen vacancy sites from the hydrogen spillover [66]. The H_2 molecules are first chemically adsorbed and dissociated into atomic species over bimetallic Pt-Sn surface; then they migrate to nearby TiO_2 supports and reduce TiO_2 to titania suboxides (TiO_x) [66], providing active species (oxygen vacancy sites) for ketonization reaction. Although $0.5Pt\text{-}0.2Sn/TiO_2$ gives the very high hexene/*n*-hexane ratio (~2.5), it is not an appropriate catalyst since the high selectivity of the ketone product was obtained.

Table 4.6 Summary of the catalytic activities of Pt and Pt-alloy catalysts in the deoxygenation of *n*-heptanoic acid.

Catalyst	$0.5Pt/SiO_2$	$0.5Pt\text{-}0.2Fe/SiO_2$	$0.5Pt\text{-}0.2Ga/SiO_2$	$0.5Pt\text{-}0.2Sn/SiO_2$	$0.5Pt\text{-}0.2Sn/TiO_2$
Conversion (mol%)	54.0	49.4	45.3	51.6	26.7
Selectivity (mol%)					
Hexene	40.3	44.8	37.0	46.5	3.8
n-Hexane	40.5	31.7	38.1	26.6	1.5
2,4-Hexadiene	12.1	8.2	10.5	7.7	0.5
n-Heptanal	0.0	8.4	4.2	12.1	3.5
7-Tridecanone	7.1	6.9	10.2	7.1	90.7
Hexene/*n*-Hexane	1.0	1.4	1.0	1.7	2.5

Reaction condition: T_{react} = 400 °C, T_{red} = 400 °C, F_{H2} = 100 mL/min, atmospheric pressure, W/F = 2.89 g·h/mol. *The values shown were at 60 min of time on stream (steady state).*

4.2.5 Effect of Sn content on the Pt-Sn/SiO_2 catalyst

To further investigate the role of Sn, the 0.5Pt-xSn/SiO_2 (x = 0, 0.2, 0.3 and 0.5) catalysts were prepared and their catalytic activities evaluated for *n*-heptanoic acid hydrodeoxygenation in the presence of H_2 and at 400 °C, as compared with the monometallic Pt catalyst as shown in Table 4.7. In these experiments, the contact time was varied such that a similar conversion (~ 50%) was obtained over all catalysts.

Table 4.7 Conversion and the products distribution in effect of Sn content (wt%) on *n*-heptanoic acid deoxygenation over 0.5Pt-xSn/SiO_2 (x = 0 - 0.5).

Sn content (wt%)	0	0.2	0.3	0.5
Contact time ($g \cdot hmol^{-1}$)	2.89	2.89	3.70	6.07
Conversion (mol%)	54.0	51.6	50.4	51.5
Selectivity (mol%)				
Hexene	40.3	46.5	50.1	50.7
n-Hexane	40.5	26.6	23.2	15.7
2,4-Hexadiene	12.1	7.7	8.0	6.6
n-Heptanal	0.0	12.1	12.2	14.9
7-Tridecanone	7.1	7.1	6.5	9.4
Hexene/*n*-Hexane	1.0	1.7	2.2	3.2

Reaction condition: T_{react} = 400 °C, T_{red} = 400 °C, F_{H2} = 100 mL/min, atmospheric pressure, *The values shown were at 60 min of time on stream (steady state).*

It is important to note that the activity was in fact lower as the Sn content is increased. This is seen from the higher contact time employed to obtain a similar level of conversion. The catalyst with relatively low amount of Sn (0.5Pt-0.2Sn/SiO_2) showed a higher hexene selectivity of 46%, as compared to 0.5Pt/SiO_2 (40.3%). Upon increasing the Sn content, the selectivity to both hexene and *n*-heptanal are increased, while the selectivity to *n*-hexane and 2,4-hexadiene are noticeably decreased. Moreover, the selectivity to 7-tridecanone is slightly increased with Sn addition. This is because the increasing Sn ratio would increase Pt-Sn alloy phase, as shown by an increase in

the hydrogen consumption and also T_p (Table 4.3). It is well known that the alloy will suppress decarbonylation and hydrogenation activity of catalyst by the decreasing of electron density of Pt metal by incorporated with Sn. A decreased in electron density of Pt can be evidenced by XPS as shown in Figure 4.8.

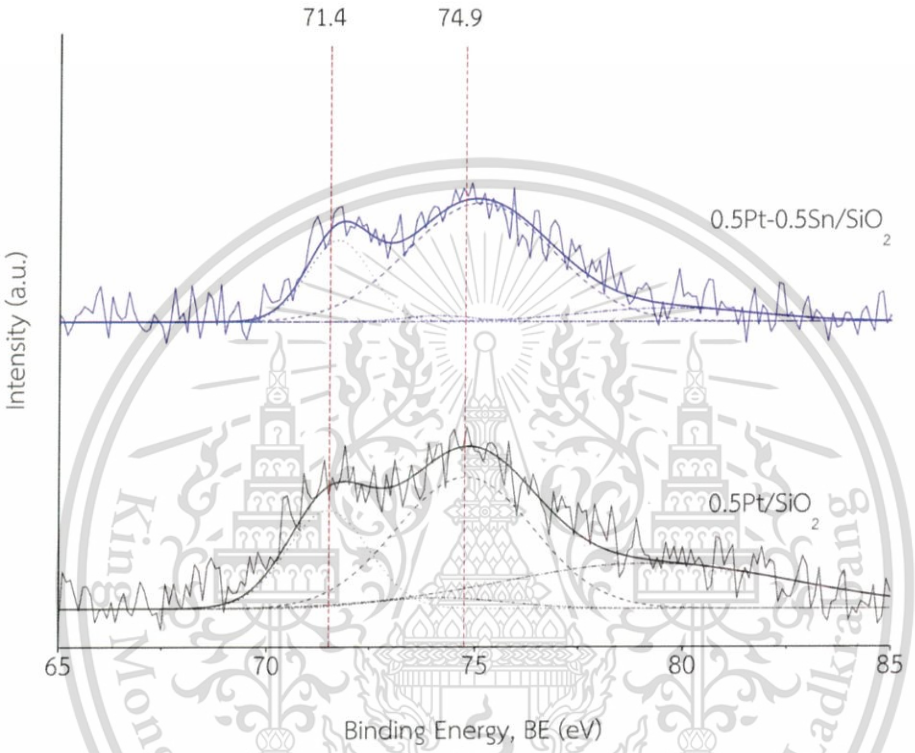

Figure 4.8 XPS spectra for the Pt region (Pt 4f) of $0.5Pt/SiO_2$ vs $0.5Pt\text{-}0.5Sn/SiO_2$.

The XPS shows a shift to a high-binding energy state for Pt 4f in bimetallic Pt-Sn catalyst (71.4 and 74.9 eV to 71.6 and 75.2, respectively). These higher binding energy of the core levels in the alloy indicate an extensive degree of Pt-Sn interaction and confirm that Sn incorporated decreases the electron density in d orbitals of the platinum. It causes a lower extent of π-back-donation from d orbitals and hence, a weaker adsorption strength of an adsorbate such as aldehyde or alkene over bimetallic Pt-Sn surface. Theoretical studies showed that the lowering of d-band center of $PtSn_X$ in comparison to Pt also resulted in a lower binding energy of an olefinic adsorption through a η^2(C,C) type over the catalyst surface [86]. These effects from Sn

incorporation results in a lower efficient of decarbonylation and hydrogenation activity, as compared to Pt alone, as discussed earlier.

Moreover, it can be seen from Table 4.7 that when Sn is presented in the catalyst, the *n*-hexane yield dramatically dropped more significantly, while hexene is slightly increased. If *n*-hexane was produced solely from hexene hydrogenation, one could expect a similar extent of decreasing *n*-hexane with an increasing hexene. However, the significant suppression of *n*-hexane selectivity observed in this case, suggests that Sn could not only reduce the hexene hydrogenation, but also inhibit the direct decarboxylation of heptanoic acid.

To verify the effect of Sn on the hydrogenation activity, the reaction with co-feeding *n*-heptanoic acid/hexene is also tested, as shown in Table 4.8.

Table 4.8 Conversion and the products distribution in the mixed feed.

Catalyst	0.5Pt-0.5Sn/SiO_2	
Feed (mol%)		
n-Heptanoic acid	100	55.0
Hexene	-	45.0
Outlet yield (mol%)		
n-Heptanoic acid	30.0	16.5
Hexene	37.0	48.8
n-Hexane	17.0	20.5
2,4-Hexadiene	7.5	8.7
n-Heptanal	4.5	3.3
7-Tridecanone	4.0	2.2
Conversion (mol%)	70.0	70.0
Contact time (g·h/mol)	7.30	4.03

Reaction condition: T_{react} = 400 °C, T_{red} = 400 °C, F_{H2} = 100 mL/min, atmospheric pressure, *The values shown were at 60 min of time on stream (steady state).*

The experiments using co-fed heptanoic acid/hexene over 0.5Pt-0.5Sn/SiO_2 catalyst gives a higher yield of hexene (48.8 mol%), as compared to the starting composition (45.0 mol%) at the similar level of conversion. This result clearly confirms that the bimetallic Pt-Sn catalyst mainly suppresses the hydrogenation of hexene to *n*-hexane, despite hexene is originally present in the feed.

4.2.6 Effect of hydrogen partial pressure

In the presence of hydrogen over Pt-Sn/SiO_2 catalyst, *n*-heptanoic acid could be decarbonylated to hexene and the produced hexene could be hydrogenated to an undesired product as *n*-hexane. For this reason, the effect of hydrogen partial pressure was investigated to reduce the hydrogen consumption and to produce a higher amount of more valuable hexene as the major product. The carrier gas in this experiment is the mixture of H_2/N_2 in several proportions. Results are shown in Figure 4.9 and Table 4.9.

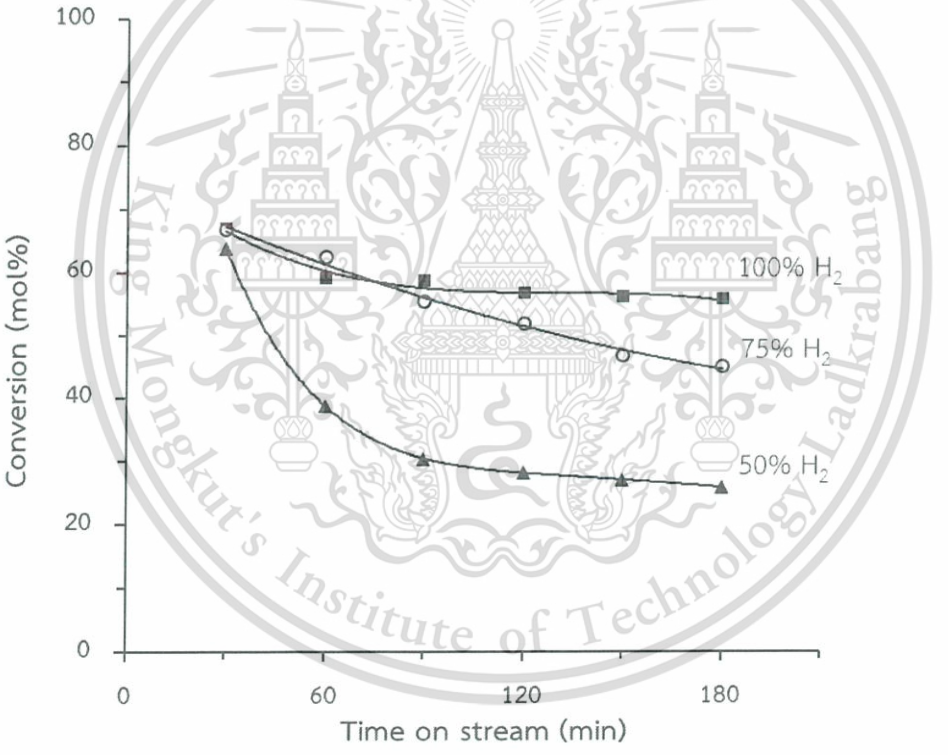

Figure 4.9 The effect of H_2 partial pressure on the conversion of *n*-heptanoic acid over 0.5Pt-0.5Sn/SiO_2.

Reaction condition: T_{react} = 400 °C, T_{red} = 400 °C, F_{H2+N2} = 100 mL/min, atmospheric pressure, W/F = 3.01 g·h/mol.

From Figure 4.9, all experiments initially offered the high conversion of *n*-heptanoic acid. However, a gradual decrease in activity is observed after 30 minutes on stream. The decrease in the conversion is more pronounced as the H_2 partial pressure is reduced. This is probably due to the strong adsorption of *n*-heptanoic acid to the active sites when hydrogen is limited, inhibiting the dissociative adsorption of H_2 on the active sites. The decrease in the conversion is later stabilized. This result suggests that the remaining active site is available at a later stage depending on the coverage of H_2/heptanoic acid on the surface. Although Table 4.9 shows that the reduction in the hydrogen partial pressure results in a significant decrease in the catalyst activity at steady state, the products distribution is unchanged. This is because the hydrogen partial pressure not affected to the nature of the available active sites resulting in the similar selectivity of all products.

Table 4.9 The effect of H_2 partial pressure on the deoxygenation of *n*-heptanoic acid over 0.5Pt-0.5Sn/SiO_2.

Hydrogen (vol%)	100	75	50
Conversion (mol%)	56.1	46.7	27.1
Selectivity (mol%)			
Hexene	56.1	55.4	55.9
n-Hexane	19.9	18.6	17.6
2,4-Hexadiene	8.8	8.7	8.5
n-Heptanal	8.2	9.9	9.3
7-Tridecanone	7.0	7.4	8.7

Reaction condition: T_{react} = 400 °C, T_{red} = 400 °C, F_{H2+N2} = 100 mL/min, atmospheric pressure, W/F = 3.01 g·h/mol. The values shown were at 150 min of time on stream (steady state).

The hypothesis that heptanoic acid competitively adsorb against H_2 was tested by the reaction using *n*-heptanal as the feed, as shown in Figure 4.10.

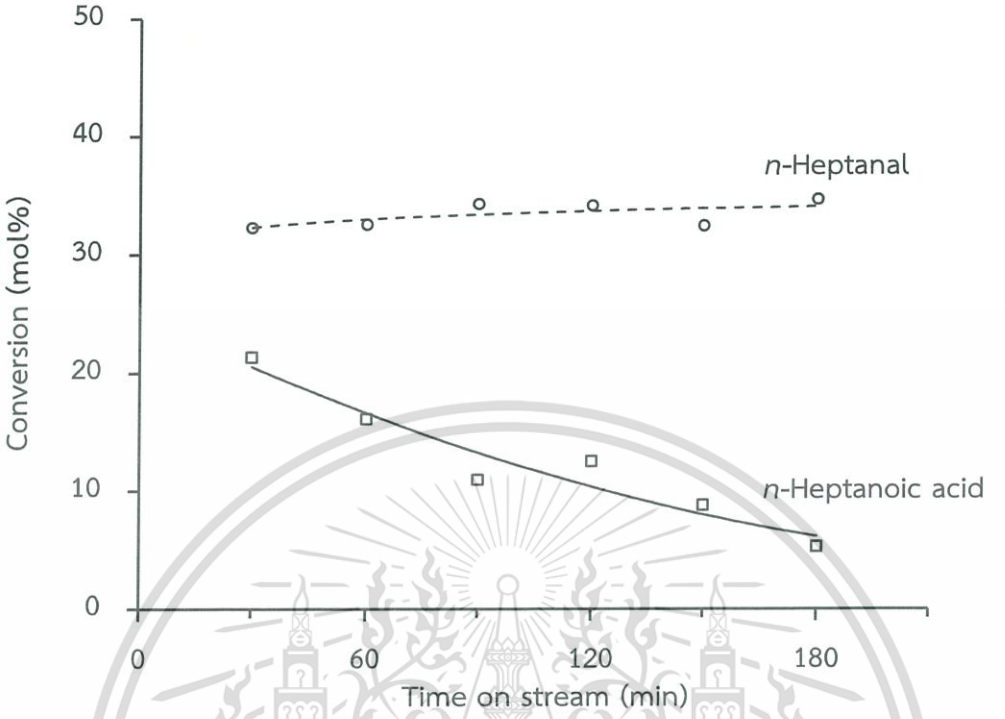

Figure 4.10 Conversion of *n*-heptanoic acid and *n*-heptanal deoxygenation over 0.5Pt/SiO_2.

Reaction condition: T_{react} = 400 °C, T_{red} = 400 °C, F_{H2} = 100 mL/min, atmospheric pressure, W/F = 1.15 g·h/mol.

It can be seen that the activity of 0.5Pt/ SiO_2 is more stable with *n*-heptanal in comparison to *n*-heptanoic acid. This suggests that only the carboxylic group of *n*-heptanoic acid possesses strong interaction to the metal surfaces of 0.5Pt/ SiO_2 Moreover, the TGA results (Figure 4.11) confirm the hypothesis that the strongly adsorbed *n*-heptanoic acid is the cause of declining activity, but not the coke formation. The first TGA cycle in N_2 of spent 0.5Pt-0.5Sn/SiO_2 in nitrogen atmosphere shows that one major mass loss of the octane solvent at 150 °C (corresponding to its boiling point), and a small amount of the strongly adsorped *n*-heptanoic acid at 330 °C (*bp* 220 °C). The TGA second cycle in air does not show any mass loss due to decomposition of a coke deposit. This result suggests that coke precursors is not present in 0.5Pt-0.5Sn/SiO_2.

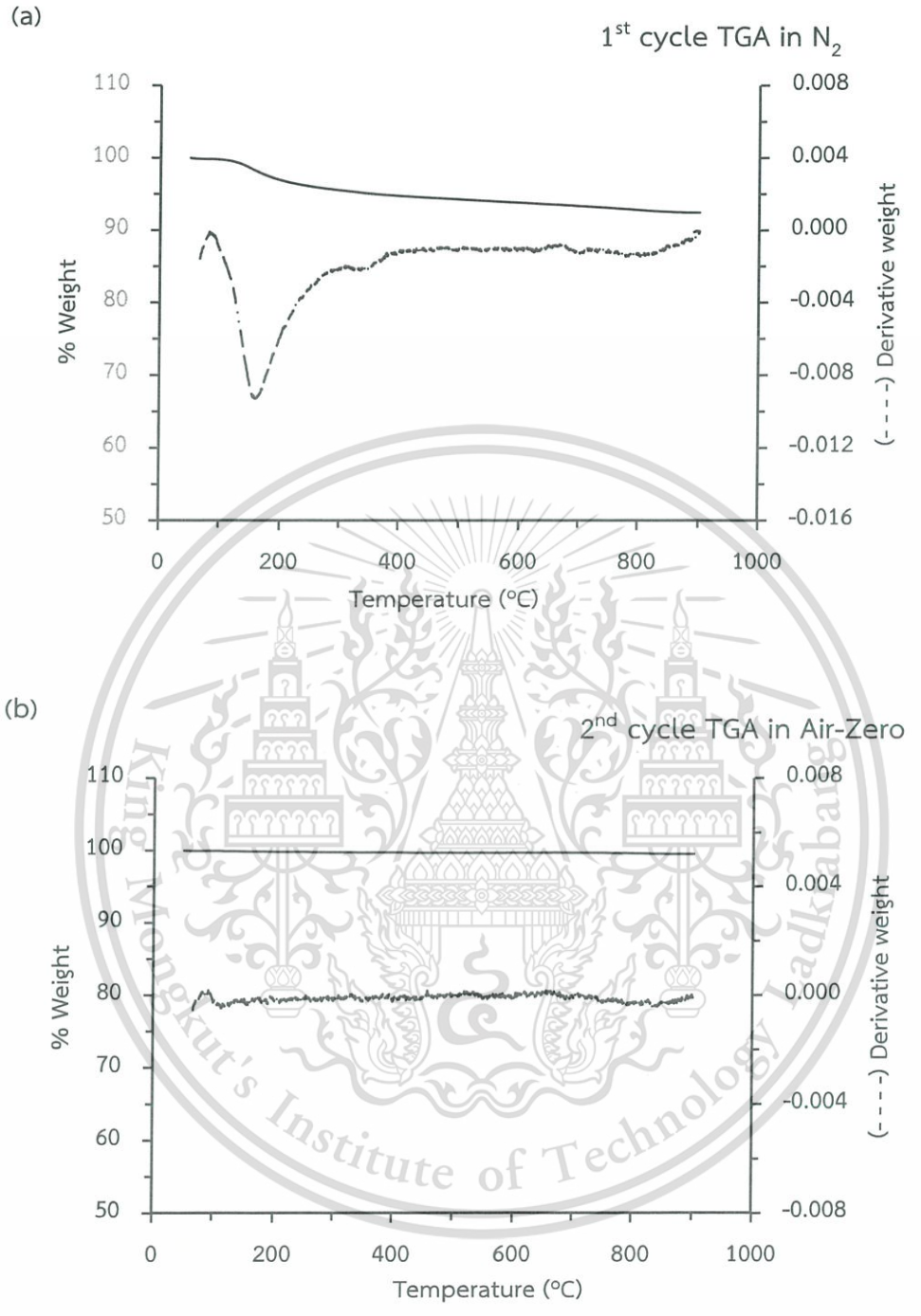

Figure 4.11 The mass loss curve of the 0.5Pt-0.5Sn/ SiO_2 spent catalyst (50% H_2/ 50% N_2): (a) 1st cycle run in nitrogen and (b) 2nd cycle run in air.

Chapter 5
Conclusions and Suggestions

5.1 Conclusions

The catalytic hydrodeoxygenation of *n*-heptanoic acid to 1-hexene was conducted as a model reaction for the production of α-olefins from fatty acids. Silica (or titania)-supported Pt (0.5 wt%), including the bimetallic Pt-M catalysts with M = Fe, Ga, and Sn (0.2 wt% each) were evaluated at 400 °C and atmospheric pressure of H_2 in a fixed bed flow reactor. It was found that the $0.5Pt/SiO_2$ catalyst exhibits not only the decarbonylation activity (to produce hexene, via *n*-heptanal intermediate), but also the direct decarboxylation and hexene hydrogenation activity (to produce *n*-hexane). Moreover, the presence of 2,4-hexadiene, *n*-hexanal and 7-tridecanone as the minor products, suggested that the H-transfer, the hydrogenation of heptanoic acid, and the ketonization of heptanoic acid, respectively, have occurred as well.

The study on reaction temperature (320-400 °C) over Pt-based catalysts using *n*-heptanal intermediate as the feed, indicated that the decarbonylation was a more favorable than the hydrogenation at high temperature. Nevertheless, the undesirable hydrogenation to *n*-hexane was obtained (~67% selectivity) over $0.5Pt/SiO_2$. The incorporation of Sn onto Pt/SiO_2 to produce the bimetallic Pt-Sn catalyst enhanced the selectivity to desirable hexane, since olefin hydrogenation was particularly suppressed. Over the bimetallic Pt-Sn catalyst, the formation of *n*-heptanol, which is a minor product produced via the hydrogenation of η^1(O)-heptanal surface intermediate, also decreased with the temperature.

As the formation of the bimetallic Pt-Sn catalyst was completed, the $0.5Pt\text{-}0.2Sn/SiO_2$ catalyst showed the higher hexene selectivity (~47%), as compared to other catalysts (Pt-Fe, ~45%; Pt-Ga, ~37%; and Pt, ~40%) in the conversion of heptanoic acid. In addition, the increase in Sn content (0.2 to 0.5 wt%)

resulted in the formation of several bimetallic Pt-Sn phases (PtSn, Pt_2Sn_3 and $PtSn_2$) which can suppress the hydrogenation of hexene to *n*-hexane, leading to the high hexene selectivity (up to ~50% at 50% conversion). This is due to the electropositive nature of Sn which destabilizes the η^2(C,C)-hexene surface species, which is a precursor for hexene hydrogenation to *n*-hexane, and reduces the efficiency of hydrogen adsorption/dissociation over the active site.

The 0.5Pt-0.2Sn/TiO_2 also gave high hexene/*n*-hexane ratio through the SMSI effect. However, the high selectivity of the ketone product (~91%, likely through the Lewis acid character of the oxygen vacancy sites in TiO_2) was not desirable. When hydrogen was limited, the strong adsorption of *n*-heptanoic acid inhibited the H_2 adsorption and dissociation on the active sites. Hence, the catalyst stability largely depended on H_2 partial pressure.

The overall results suggested that the 0.5Pt-0.5Sn/SiO_2 catalyst was effective for the conversion of fatty acids to the high value hydrocarbons such as the α-olefin in the presence of H_2 atmospheric pressure at 400 °C.

5.2 Suggestions

1. The formation of some bimetallic Pt-M catalysts (e.g., Pt-Ga) should be driven to completion in order to increase the α-olefin productivity.

2. The bimetallic Pt-M incorporating other oxophilic or electropositive metals (i.e., Co, Mo) should be investigated, to further verify the effect of the electronic structure of the second metal on the yield and selectivity of the α-olefin product.

3. The bimetallic Pt-M catalyst over TiO_2 support could be modified such that its Lewis acid character is reduced, so as to decrease the ketone formation and to increase the overall activity.

4. The hydrodeoxygenation of high molecular weight fatty acids or natural fatty acids over the bimetallic Pt-M catalysts under hydrogen atmosphere should be investigated, in order to test the potential of this technology for a further development into an industrial process.

Reference

[1] Amin, M.A., Mohsen, Q., Mostafa, N.Y., El-Bagoury, N., Al-Refaie, A., Bairamov, A.K., Al-Maaesab, S., Murill, E.M. and Al-Qahtani, S.A. 2014. "Case study: Corrosion behavior of constructive alloys in linear alpha olefin environment." *Int. J. Electrochem. Sci.* 9 : 2631-2648

[2] Organization of the Petroleum Exporting Countries. 2013. **World Oil Outlook.** [Online]. Available : http://www.opec.org/opec_web/static_files_project/ media/downloads/ publications/ WOO2012.pdf

[3] Santillan-Jimene, E. Morgan, T. Lacny, J. Mohapatra, S. and Crocker, M. 2013. "Catalytic deoxygenation of triglycerides and fatty acids to hydrocarbons over carbon-supported nickel." *Fuel* 103 : 1010–1017.

[4] Sari, E. Kim, M. Salley, S.O. and Ng, K.Y.S. 2013. "A highly active nanocomposite silica-carbon supported palladium catalyst for decarboxylation of free fatty acids for green diesel production: correlation of activity and catalyst properties." *Appl. Catal. A.-Gen.* 467 : 261–269.

[5] Ping, E.W. Venkatasubbaiah, K. Fuller, T.F. and Jones, C.W. 2010. "Oxidative heck coupling using Pd(II) supported on organosilane-functionalized silica mesocellular Foam." *Topics in Catalysis* 53 : 1048-1054.

[6] Ping, E.W. Pierson, J. Wallace, R. Miller, J.T. Fuller, T.F. and Jones, C.W. 2011. "On the nature of the deactivation of supported palladium nano particle catalysts in the decarboxylation of fatty acids." *Appl. Catal. A.-Gen.* 396 : 85–90.

[7] Shi, H. Chen, J. Yang, Y. and Tian, S. 2014. "Catalytic deoxygenation of methyl laurate as a model compound to hydrocarbons on nickel phosphide catalysts: remarkable support effect." *Fuel Process. Technol.* 118 : 161–70.

[8] Chen, J. Yang, Y. Shi, H. Li, M. Chu, Y. and Pan, Z. 2014. "Regulating product distribution in deoxygenation of methyl laurate on silica-supported Ni–Mo phosphides: effect of Ni/Mo ratio." *Fuel* 129 : 1–10.

[9] Kalnes, T. Marker, T. and Shonnard, D.R. 2007. "Greendiesel: a second generation Biofuel." *Int. J. Chem. React. Eng.* 5 : 1542–1580.

[10] Yang, Y. Wang, Q. Zhang, X. Wang, L. and Li, G. 2013. "Hydrotreating of C_{18} fatty acids to hydrocarbons on sulphided $NiW/SiO_2–Al_2O_3$." *Fuel Process. Technol.* 116 : 165–174.

[11] Srifa, A. Faungnawakij, K. Itthibenchapong, V. Viriya-empikul, N. Charinpanitkul, T. and Assabumrungrat, S. 2014. "Production of bio-hydrogenated diesel by catalytic hydrotreating of palm oil over $NiMoS_2/\gamma$-Al_2O_3 catalyst." *Bioresour. Technol.* 158 : 81–90.

[12] Lestari, S. Maki-Arvela, P. Beltramini, J. Lu, G.Q.M. and Murzin, D.Y. 2009. "Transforming triglycerides and fatty acids into biofuels." *ChemSusChem.* 2 : 1109–1119.

[13] Thomas, Y. Suljo, L. and Phillip, E. S. 2014 "Deactivation of Pt Catalysts during Hydrothermal Decarboxylation of Butyric Acid." *ACS Sustainable Chem. Eng.* 2 : 2399-2406.

[14] Juan, A. Lopez, R. and Robert, J. D. 2014. "Decarbonylation of heptanoic acid over carbon-supported platinum nanoparticles." *Green Chem.* 16 : 683-694.

[15] Masoudeh, A. Eugenia, E. M. Jacek, B. J. Paul, R. and Moises, A. C. 2014. "Decarboxylation and further transformation of oleic acid over bifunctional, Pt/SAPO-11 catalyst and Pt/chloride Al_2O_3 catalysts." *J. Mol. Catal. A: Chem.* 386 : 14-19.

[16] Jie, F. Xiuyang, L. and Phillip, E. S. 2011. "Hydrothermal Decarboxylation and Hydrogenation of Fatty Acids over Pt/C." *ChemSusChem.* 4 : 481-486.

[17] Thomas, M. Y. Ryan, L. H. Suljo, L. and Phillip, E. S. 2015. "Hydrothermal decarboxylation of unsaturated fatty acids over $PtSn_x$/C catalysts." *Fuel* 156 : 219-224.

[18] Plomp, A. J. van Asten, D. M. P. van der Eerden, A. M. J. Mäki-Arvela, P. Murzin, D. Y. de Jonga, K. P. and Bittera, J. H. 2009. "Catalysts based on platinum–tin and platinum–gallium in close contact for the selective hydrogenation of cinnamaldehyde." *J. Catal.* 263 : 146-154.

[19] David, K. Jan, H. Michal, S. Roman, B. Arnošt, Z. and Iva, K. 2014. "Effect of support-active phase interactions on the catalyst activity and selectivity in deoxygenation of triglycerides." *Appl. Catal., B.* 145 : 101-107.

[20] Rohm and Haas Company. 2009. **Esterification of fatty acids.** [Online]. Available : http://www.amberlyst.com/fatty_acids.htm.

[21] Jerry L. Sarquis. 2010. **Fats and Fatty Acids.** [Online]. Available : http://www.chemistryexplained.com/Di-Fa/Fats-and-Fatty-Acids.html.

[22] Aparadh, V.T. and Karadge, B.A. 2010. "Fatty acid composition of seed oil from some *Cleome* species." *Pharmacognosy Journal.* 2(10) : 324-327.

[23] Shahidi, F. 2005. **Baily's Industrial Oil and Fat Products.** German : John Wiley & Sons.

[24] Świzdor, A. Panek, A. Milecka-Tronina, N. and Kołek, T. 2012. "Biotrans-formations utilizing *β*-oxidation cycle reactions in the synthesis of natural compounds and medicines." *Int. J. Mol. Sci..* 13(12) : 16514-16543.

[25] Glinski, M. and Kijenski, J. 2000. "Decarboxylative coupling of heptanoic acid. Manganese, cerium and zirconium oxides as catalysts." *Appl. Catal. A-Gen.* 190(1-2) : 87–91.

[26] Lappin, G.R. and Sauer, J.D. 1989. **Alpha Olefins Applications Handbook.** USA : Marcel Dekker.

[27] Ian H. 2009. **Decarboxylation Reaction.** [Online]. Available : http://www.chem.ucalgary.ca/courses/350/Carey5th/Ch19/ch19-3-4.html.

[28] Hartwig, J. F. 2010. **Organotransition Metal Chemistry, from Bonding to Catalysis.** New York : University Science Books.

[29] Condrad, W. F. Harold, W. and Robert, E. V. 1979. "Ethylene: The organic chemical industry's most important building block." *J. Chem. Educ.* 56(6) : 385.

[30] Micheal, R. 2005. "Ketonization of Carboxylic Acids by Decarboxylation : Mechanism and Scope." *Eur. J. Org. Chem.* 2005(6) : 979-988.

[31] Wikipedia 2016. **Ketonic decarboxylation.** [Online]. Available : https://en.wikipedia.org/wiki/Ketonic_decarboxylation#cite_ref-2

[32] Gaertner, C. A. Serrano-Ruiz, J. C. Braden, D. J. and Dumesic, J. A. 2009. "Catalytic coupling of carboxylic acids by ketonization as a processing step in biomass conversion." *J. Catal.* 266(1) : 71–78.

[33] Lenntech, B.V. 1998. **Platinum.** [Online]. Available : http://www.lenntech.com/periodic/elements/pt.htm

[34] Hershel Friedman and Minerals.net. 2016 **Platinum Gemstone.** [Online]. Available : http://www.minerals.net/gemstone/platinum_gemstone.aspx

[35] Wang, C. Daimon, H. Onodera, T. Koda, T. Sun, S. 2008. "A general approach to the size- and shape-controlled synthesis of platinum nanoparticles and their catalytic reduction of oxygen." *Angew. Chem. Int. Ed.* 47(19) : 3588–3591.

[36] Bond, G. C. F.R.I.C. and Sercombe, E. J. 1965. *Platinum Metals Rev.* 9(3) : 74

[37] Watanabe, M. Motoo, S. 1975. "Electrocatalysis by ad-atoms: Part III. Enhancement of the oxidation of carbon monoxide on platinum by ruthenium ad-atoms." *J. Electroanal. Chem., Interfacial Electrochem.* 60(3) : 275-283.

[38] Ponec, V.and Bond, G.C. 1995. "Catalysis by Metals and Alloys." *Studies in Surface Science and Catalysis*. 95 : 437–447.

[39] Ma, Z. and Zaera, F. 2006. **Encyclopedia of Inorganic Chemistry.** John Willey.

[40] Tauster, S. J. Fung, S. C. and Garten, R. L. 1978. "Strong metal-support interactions Group 8 noble metals supported on titanium dioxide." *J. Am. Chem. Soc.* 100(1) : 170-175.

[41] Beltonn, D. N. Sun, Y. M. and White, M. J. 1984. "Metal-support interactions on rhodium and platinum/titanium dioxide model catalysts." *J. Phys. Chem.* 88(22) : 5172-5176.

[42] Takatani, S. and Chung, Y. W. 1984. "Strong metal-support interaction in $NiTiO_2$: Auger and vibrational spectroscopy evidence for the segregation of TiO_x ($x \approx -1$) on Ni and its effects on CO chemisorption." *J. Catal.* 90(1) : 75-83.

[43] Baker, R. T. K. Prestridge, E. B. and Murrell, L. L. 1983. "Electron microscopy of supported metal particles: III. The role of the metal in an SMSI interaction." *J. Catal.* 79(2) : 348-358.

[44] Michaleson, H. E. 1977. "The work function of the elements and its periodicity." *J. Appl. Phys.* 48(11) : 4729.

[45] Gates, B.C. 1992. **Catalytic chemistry**. New York : John Wiley & Sons.

[46] George, L. 1989. **Alpha Olefins Applications Handbook**. [Online]. Available : http://en.wikipedia.org/wiki/Linear_alpha_olefin.

[47] Ineosoligomers. 2016 **Polyalpha Olefin (PAO).** [Online]. Available : http://www.ineosoligomers.com/126-Products.htm.

[48] Chevron Phillips Chemical Company. 2016. **Normal Alpha Olefins.** [Online]. Available : http://www.cpchem.com/enu/nao_a_applications.asp.

[49] Sadrameli, S.M. and Alex, E.S. Green. 2007. "Systematics of renewable olefins from thermal cracking of canola oil." *J. Anal. Appl. Pyrolysis.* 78 : 445–451.

[50] Snåre, M. Kubičková, I. Mäki-Arvela, P. Eränen , K. and Murzin, D. Y. 2006. "Heterogeneous Catalytic Deoxygenation of Stearic Acid for Production of Biodiesel." *Ind. Eng. Chem. Res.* 45(16) : 5708–5715.

[51] Lestari, S. Mäki-Arvela, P. Bernas, H. Simakova, O. Sjöholm, R. Beltramini, J. Lu, G. Q. M. Myllyoja, J. Simakova, I. and Murzin, D. Y. 2009. "Catalytic Deoxygenation of Stearic Acid in a Continuous Reactor over a Mesoporous Carbon-Supported Pd Catalyst." *Energy Fuels*. 23(8) : 3842–3845.

[52] Miller, J. A. Nelson, J. A. and Byrne, M. P. 1993. "A highly catalytic and selective conversion of carboxylic acids to 1-alkenes of one less carbon atom." *J. Org. Chem.* 58(1) : 18–20.

[53] Maier, W. F. Roth, W. Thies, I. and Ragué Schleyer, P. v. 1982. "Hydrogenolysis, IV. Gas phase decarboxylation of carboxylic acids." *Chem. Ber.* 115(2) : 808–812.

[54] Gaertner, C. A. Serrano-Ruiz, J. C. Braden, D. J. and Dumesic, J. A. 2010. "Ketonization Reactions of Carboxylic Acids and Esters over Ceria–Zirconia as Biomass-Upgrading Processes." *Ind. Eng. Chem. Res.* 49(13) : 6027–6033.

[55] Snåre, M. Kubičková, I. Mäki-Arvela, P. Chichova, D. Eranen, K. and Murzin, D. Y. 2008. "Catalytic deoxygenation of unsaturated renewable feedstocks for production of diesel fuel hydrocarbons." *Fuel* 87(6) : 933–945.

[56] Pham, H. N. Pagan-Torres, Y. J. Serrano-Ruiz, J. C. Wang, D. Dumesic, J. A. and Datye, A. K. 2011. "Improved hydrothermal stability of niobia-supported Pd catalysts." *Appl. Catal. A.-Gen* 397(1-2) : 153–162.

[57] Bernas, H. Eränen, K. Simakova, I. Leino, A. Kordás, K. Myllyoja, J. Mäki-Arvela, P. Salmi, T. and Yu, D. 2010. "Deoxygenation of dodecanoic acid under inert atmosphere Original Research Article." *Fuel*. 89(8) : 2033–2039.

[58] Ford, J. P. Immer, J. G. and Lamb, H. H. 2012. "Palladium Catalysts for Fatty Acid Deoxygenation: Influence of the Support and Fatty Acid Chain Length on Decarboxylation Kinetics." *Top. Catal.* 55(3-4) : 175–184.

[59] Snåre, M., Kubičková, I., Mäki-Arvela, P., Eränen, K., Wärnå, J., and Murzin, D. Y. 2007 "Production of diesel fuel from renewable feeds : Kinetics of ethyl stearate decarboxylation." *Chem. Eng. J.* 134 : 29–34.

[60] Simakova, I., Rozmysłowicz, B., Simakova, O. A., Mäki-Arvela, P., Simakov, A. and Murzin, D. Y. 2011 "Catalytic Deoxygenation of C18 Fatty Acids Over Mesoporous Pd/C Catalyst for Synthesis of Biofuels." *Top. Catal.* 54(8-9) : 460–466.

[61] Mäki-Arvela, P. Kubičková, I. Snåre, M. Eränen, K. and Murzin, D. Y. 2007 "Catalytic Deoxygenation of Fatty Acids and Their Derivatives." *Energ. Fuel.* 21(1) : 30–41.

[62] Immer, J. G. and Lamb, H. H., 2010, "Fed-Batch Catalytic Deoxygenation of Free Fatty Acids," Energ. Fuel. 130(10) : 5291–5299.

[63] Immer, J. G. Kelly, M. J. and Lamb, H. H. 2010 "Catalytic reaction pathways in liquid-phase deoxygenation of C18 free fatty acids." *Appl. Catal. A-Gen.* 375(1) : 134–139.

[64] Lugo-José, Y. K. Monnier, J. R. and Williams, C. T. 2014. "Gas-Phase, Catalytic Hydrodeoxygenation of Propanoic Acid Over Supported Group VIII Noble Metals: Metal and Support Effects." *Appl. Catal. A-Gen.* 469 : 410–418.

[65] Alotaibi, M. A. Kozhevnikova, E. F. and Kozhevnikov, I. V. 2012. "Deoxygenation of propionic acid on heteropoly acid and bifunctional metal-loaded heteropoly acid catalysts: Reaction pathways and turnover rates." *Appl. Catal A-Gen.* 447-448 : 32–40.

[66] Boda, L. Onyestyák, G. Solt, H. Lónyi, F. Valyon, J. and Thernesz, A. 2010. "Catalytic hydroconversion of tricaprylin and caprylic acid as model reaction for biofuel production from triglycerides." *Appl Catal A-Gen.* 374(1-2) : 158–169.

[67] Lestari, S. Mäki-Arvela, P. Bernas, H. Simakova, O. Sjöholm, R. Beltramini, J. Lu, G. Q. M. Myllyoja, J. Simakova, I. and Murzin, D. Y. 2009. "Catalytic Deoxygenation of Stearic Acid in a Continuous Reactor over a Mesoporous Carbon-Supported Pd Catalyst." *Energ Fuel.* 23(8) : 3842–3845.

[68] Mäki-Arvela, P. Snåre, M. Eränen, K. Myllyoja, J. and Murzin, D. Y. 2008. "Continuous decarboxylation of lauric acid over Pd/C catalyst." *Fuel.* 87(17-18) : 3543–3549.

[69] Rozmysłowicz, B. Mäki-Arvela, P. Lestari, S. Simakova, O. A. Eränen, K. Simakova, I. L. Murzin, D. Y. and Salmi, T. O. 2010. "Catalytic Deoxygenation of Tall Oil Fatty Acids Over a Palladium-Mesoporous Carbon Catalyst : A New Source of Biofuels." *Top Catal.* 53(15-18) : 1274–1277.

[70] Ma, H.Y. and Wang, G. C. 2011. "Theoretical study of 1,3-cyclohexadiene dehydrogenation on Pt (111), Pt_3Sn/Pt (111), and Pt_2Sn/Pt (111) surfaces." *J Catal.* (281) : 63–75.

[71] Yang, M. L. Zhu, Y. A. Zhou, X. G. Sui, Z. J. and Chen, D. 2012. "First-principles calculations of propane dehydrogenation over PtSn catalysts." *ACS Catal.* (2) : 1247–58.

[72] Iglesias-Juez, A. Beale, A. M. Maaijen, K. Weng, T. C. Glatzel, P and Weckhuysen, B. M. 2010. "A combined in situ time-resolved UV-Vis, Raman and high-energy resolution X-ray absorption spectroscopy study on the deactivation behavior of Pt and PtSn propane dehydrogenation catalysts under industrial reaction conditions." *J Catal.* (276) : 268–79.

[73] Miguel, S. Castro, A. Scelza, O. Fierro, J. and Soria, J. 1996. "FTIR and XPS study of supported PtSn catalysts used for light paraffins dehydrogenation." *Catal Lett.* (36) : 201–206.

[74] Grolier, V. and Schmid-Fetzer, R. 2008. "Thermodynamic analysis of the Pt–Sn system." *J Alloys Compd.* (450) : 264–271.

[75] Vu, B. K. Song, M. B. Ahn, I. Y. Suh, Y. W. Suh, D. J. and Kim, W. I. 2011. "Pt–Sn alloy phases and coke mobility over Pt–Sn/Al_2O_3 and Pt–Sn/$ZnAl_2O_4$ catalysts for propane dehydrogenation." *Appl Catal. A-Gen* (400) : 25–33.

[76] Chiappero, M. Do, P. T. M. Crossley, S. Lobban, L. L. and Resasco, D. E. 2011. "Direct conversion of triglycerides to olefins and paraffins over noble metal supported catalysts." *Fuel.* (90) : 1155–1165.

[77] de Lange, M.W. 2000. "Selective deoxygenation of carboxylic acid." Innovation Oriented reseach Programme on Catalysis.

[78] Liu, H. Ma, H. T. Li, X. Z. Li, W. Z. Wu, M. and Bao, X. H. 2003. "The enhancement of TiO_2 photocatalytic activity by hydrogen thermal treatment." *Chemosphere* 50 : 39-46.

[79] Julieta, P. S. Patricia, D. Z. Sergio, R. de M. Osvaldo, A. S. 2013. "Formation of different promoted metallic phases in PtFe and PtSn catalysts supported on carbonaceous materials used for selective hydrogenation." *J Catal.* 306 : 11–29.

[80] Meisheng, L. Wenkai, K. Kechang X. 2009. "Comparison of reduction behavior of Fe_2O_3, ZnO and $ZnFe_2O_4$ by TPR technique." *J Nat Gas Chem.* 18 : 110–113.

[81] Yu, C. C. Xuan, Z. J. 2005. "Supported platinum–gallium catalysts for selective hydrodechlorination of CCl_4." *J Mol Catal A-Chem.* 242 : 119–128.

[82] Martin, E. Andreas, J. Johannes, A. L. 1997. "Structure Sensitivity of the Hydrogenation of Crotonaldehyde over Pt/SiO_2 and Pt/TiO_2." *J Catal.* 166 : 25–35.

[83] Doughty, D. H. McGuiggan, M. F. Wang, H. Pignolet, L. H. 1979. "Catalytic Decarbonylation of Aldehydes Using Cationic Complexes of Rhodium(I) with Chelating Diphosphine Ligands." *Fundamental Research in Homogeneous Catalysis.* : 909–919.

[84] Peter, C. F, Sieghard E. W. 1975. "Effect of pretreatment and adsorption conditions on gas adsorption by supported metal catalysts." *Can. J. Chem. Eng.* 53 : 636–640.

[85] Surapas, S. Daniel, E. R. 2011. "Hydrodeoxygenation of Furfural Over Supported Metal Catalysts: A Comparative Study of Cu, Pd and Ni." *Catal Lett.* 141 : 784–791.

[86] Andrea, B. M. Bruno, F. M. Virginia, V. Joaquim, L. F. Mónica, L. C. 2010. "$PtSn/SiO_2$ catalysts prepared by surface controlled reactions for the selective hydrogenation of cinnamaldehyde." *Appl Catal A-Gen.* 383 : 43–49.

APPENDICES

APPENDIX A

CALCULATION

Example 1: Calculations of catalytic parameters

W/F, conversion, yield and selectivity

Example 2: Calculations of reducibility

H_2 consumption

Calculations of catalytic parameters

W/F

$$W/F = \frac{\text{Weight of catalyst (g)}}{\text{Reactant feed rate (mol/h)}}$$

In the reaction using 0.0045 mol/h of *n*-heptanoic acid in feed and using 0.0121 grams of catalyst, the *W/F* is calculated as follow:

$$W/F = \frac{0.0121\ (g)}{0.0045(mol/h)}$$

$$= 2.71\ g{\cdot}h/mol$$

In a similar manner; *W/F* of catalysts with different catalyst weight and different feed rate are calculated.

Calculation of % yield from gas chromatography

From the chromatogram, the peaks of hydrocarbon samples were identified using of reference standard for comparison. The peak area of hydrocarbon (or oxygenated compounds) which possesses the equal number of carbon was summarized. The example of the peak area obtained from chromatogram of a mixture reactor outlet is shown in Table A1.

Table A1 The example of the peak area for reactor outlet.

Chemicals	Peak area	Corrected peak area	RF
Hexene	1,692	745	2.27
n-Hexane	659	290	2.27
2,4-Hexadiene	292	129	2.27
n-Heptanal	202	150	1.35
n-Heptanoic acid	920	920	1.00
7-Tridecanone	177	109	1.62
Total	3,942	2,343	-

$$\text{Corrected peak area in each product} = \frac{\text{Peak area of sample}}{\text{RF}}$$

Where RF is the response factor of the analyzed sample showing in Table A1.

For example;

$$\text{Corrected peak area of hexene} = \frac{1{,}692}{2.27}$$

$$= 745$$

In the normalization method, the areas of all eluted peak were compute after correcting these areas for differences in the detector response (RF) to different compound types. After correcting areas, the concentration of the analyzed was found from the ratio of its area to the total area of all peaks.

Calculate the percent yield of each component in sample as follows:

$$\%\text{Yield in each product} = \frac{\text{Corrected peak area of sample x 100}}{\text{Total corrected area}}$$

For example;

$$\%\text{Yield of hexene} = \frac{745 \times 100}{2{,}343}$$

$$= 31.8$$

The percent yield of each sample which is obtained from above calculation is shown in Table A2.

Table A2 % yield derived by normalization method.

Chemicals	%Yield of sample
Hexene	31.8
n-Hexane	12.4
2,4-Hexadiene	5.5
n-Heptanal	6.4
n-Heptanoic acid	39.3
7-Tridecanone	4.6
Total	100.0

Conversion

%Conversion can be calculated from the following equation.

$$\%\text{Conversion} = 100 - (\%\text{Yield of heptanoic acid left in product})$$

For example;

$$\%\text{Conversion} = 100 - 39.3$$

$$= 60.7$$

Selectivity

%Selectivity can be obtained from the following equation.

$$\%\text{Selectivity in each product} = \frac{\%\text{ Yield in each product}}{\%\text{ Conversion}} \times 100$$

For example;

$$\%\text{Selectivity of hexene} = \frac{31.8}{60.7} \times 100$$

$$= 52.3$$

Calculations of reducibility

The electronic signal from the TCD detector during TPR analysis is converted to mmol H_2, employing CuO as a standard. Here, CuO is used because it is a highly-reducible metal with clean and well-known reduction giving Cu metal as a final product following the equation;

$$CuO\ (s) + H_2\ (g) \rightarrow Cu\ (s) + H_2O\ (g)$$

An example of TPR profile of CuO is shown in **Figure A1**.

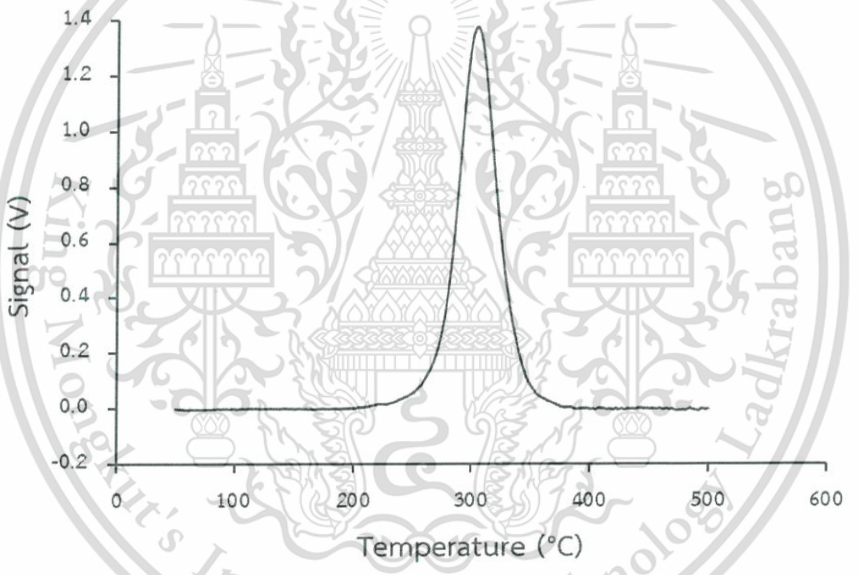

Figure A1 TPR profile of CuO

A few runs were performed by variation of the mass of CuO. Then, the peak area (integrated with **Origin Pro 8.0**) in the range T = 50-500 °C is plotted against the mole of CuO. The resulting plot (**Figure A2**) serves as a calibration curve where the mmol H_2 of any sample could be calculated from the peak area as shown below.

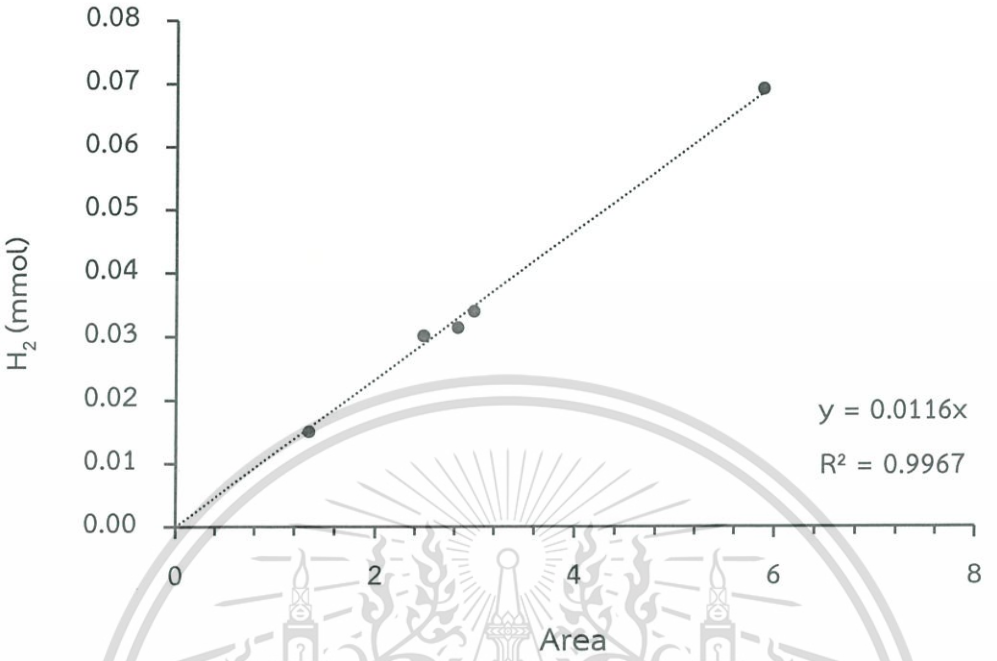

Figure A2 Standard curve of CuO; peak area *vs* the amount of H_2 consumption

From TPR results, the 0.5Pt/SiO_2 (0.2500 g) sample gives the peak area of 0.5500. Substituting this number into the equation in **Figure A2** gives;

$$y = 0.0117x$$

$$y = 0.0117\ (0.5500)$$

$$y = 0.06435 \text{ mmol}$$

As the mole ratio of PtO to H_2 is 1:1, the number of mmol of H_2 consumed by 0.5Pt/SiO_2 equals 0.06435 mmol as well. So, the reducibility of 0.5Pt/SiO_2 is;

0.06435 mmol / 0.2500 g = 1.2600 mg of Pt / 2.5000 g of sample

= 0.5 g of Pt / g of sample

= 0.5 wt%

Theoretical H_2-consumption

For example; 0.5Pt/SiO_2 (0.58%wt of Pt)

As the mole ratio of Pt to H_2 is 1:1, the number of consumed H_2 equal to mole of Pt in a sample as well. So, the H_2-consumption of 0.58%wt Pt (from ICP/MS) over SiO_2 support is;

Amount of Pt in 1 g of sample		Theoretical H_2-consumption
Weight (g)	Mole (mmol)	(mmol/g)
0.0058	0.024	0.024

Table A3 The theoretical H_2-consumption

Sample	Amount of metal in 1 g of sample (mmol)		Theoretical H_2-consumption (mmol/g)
	Pt	2nd metal	
0.5Pt/SiO_2	0.024	-	0.024
0.5Pt-0.2Fe/SiO_2	0.022	0.008[a]	0.035
0.5Pt-0.2Ga/SiO_2	0.023	0.008[b]	0.036
0.5Pt-0.2Sn/SiO_2	0.024	0.007[c]	0.038
0.5Pt-0.3Sn/SiO_2	0.022	0.009[c]	0.040

[a] mole ratio of Fe^{3+} to H_2 is 2:3

[b] mole ratio of Ga^{3+} to H_2 is 2:3

[c] mole ratio of Sn^{4+} to H_2 is 1:2

Appendix B

GC CONDITIONS

Prior to analysis, the products were identified by GC-MS (Gas chromatography equipped with Mass Spectrometer detector). Then, quantitative analysis was carried out with GC-FID (Gas chromatography equipped with Flame Ionization Detector). The analytical conditions of products from the deoxygenation of heptanoic acid is shown in **Table B1**.

Table B1 GC conditions for product analysis

Column	DB-1, 30 m × 0.32 mm i.d., 5 μm
Temperature program	40 °C for 5 min to 280 °C at rate 15 °C /min for 24 min
Carrier gas	Nitrogen gas 1.2 mL/min (39 cm/sec)
Injector	265 °C (split ratio 45:1)
Injection volume	250 microliter (gas sampling loop)
Detector	FID (275 °C)

The products from heptanoic acid were identified by comparing the retention time as listed in **Table B2**.

Table B2 Retention time of the products from heptanoic acid

Chemical	Retention time (min)
1-hexene	8.2
n-hexane	8.5
Heptanal	13.7
Heptanoic acid	15.8
7-Tridecanone	20.0

APPENDIX C

REACTION DATA

1. Effect of activation

Table C1 The heptanoic acid conversion and yield of products over 0.5Pt/SiO_2 as non-calcined

	Time on stream (min)					
	30	60	90	120	150	180
Conversion of heptanoic acid	72.9	54.0	45.5	42.0	34.7	32.9
Yield (%)						
Hexene	30.3	21.8	19.5	19.5	16.7	15.7
n-Hexane	32.7	21.9	16.9	14.2	11.0	9.9
2,4-Hexadiene	6.8	6.5	5.3	4.4	2.8	2.4
Heptanal	0	0	0	0	0	0
7-Tridecanone	3.1	3.8	3.8	3.9	4.2	4.9

Reaction condition: T_{react} = 400 °C, T_{red} = 400 °C, F_{H2} = 100 mL/min, atmospheric pressure, W/F = 2.89 g·h/mol.

Table C2 The heptanoic acid conversion and yield of products over 0.5Pt/SiO_2 as calcined under air-zero at 400 °C for 2 h

	Time on stream (min)					
	30	60	90	120	150	180
Conversion of heptanoic acid	39.0	30.8	23.7	20.1	17.6	16.1
Yield (%)						
Hexene	14.1	12.4	12.3	10.9	9.3	8.4
n-Hexane	15.5	11.9	7.1	5.1	4.3	3.9
2,4-Hexadiene	6.0	4.2	1.3	0.9	0.7	0.5
Heptanal	0	0	0	0	0	0
7-Tridecanone	3.4	2.3	3.0	3.2	3.3	3.3

Reaction condition: T_{react} = 400 °C, T_{red} = 400 °C, F_{H2} = 100 mL/min, atmospheric pressure, W/F = 2.89 g·h/mol.

2. Effect of contact time

Table C3 The heptanoic acid conversion and yield of products over 0.5Pt/SiO_2 at contact time of 1.15 g.h/mol

	Time on stream (min)					
	30	60	90	120	150	180
Conversion of heptanoic acid	38.1	21.4	16.1	11.0	12.6	8.8
Yield (%)						
Hexene	17.7	8.2	6.2	3.6	4.4	2.5
n-Hexane	15.3	8.2	4.7	2.3	2.6	1.4
2,4-Hexadiene	3.5	2.6	1.6	0.7	0.7	0.3
Heptanal	0.2	0.3	0.4	0.4	0.6	0.5
7-Tridecanone	1.4	2.1	3.2	4.0	4.3	4.1

Reaction condition: T_{react} = 400 °C, T_{red} = 400 °C, F_{H2} = 100 mL/min, atmospheric pressure

Table C4 The heptanoic acid conversion and yield of products over 0.5Pt/SiO_2 at contact time of 1.51 g.h/mol

	Time on stream (min)					
	30	60	90	120	150	180
Conversion of heptanoic acid	51.1	25.9	26.0	24.4	22.2	17.6
Yield (%)						
Hexene	19.2	8.6	10.9	11.1	10.5	6.8
n-Hexane	20.3	9.4	8.5	7.4	6.6	4.0
2,4-Hexadiene	4.5	2.9	2.8	2.1	1.6	0.9
Heptanal	0	0	0	0	0	1.1
7-Tridecanone	7.1	5.0	3.8	3.8	3.5	4.8

Reaction condition: T_{react} = 400 °C, T_{red} = 400 °C, F_{H2} = 100 mL/min, atmospheric pressure

Table C5 The heptanoic acid conversion and yield of products over 0.5Pt/SiO_2 at contact time of 1.75 g.h/mol

	Time on stream (min)					
	30	60	90	120	150	180
Conversion of heptanoic acid	62.7	33.0	28.4	24.6	23.4	12.9
Yield (%)						
Hexene	24.2	14.1	12.4	10.8	9.5	2.6
n-Hexane	30.3	10.8	8.2	6.1	5.1	1.2
2,4-Hexadiene	5.1	3.7	2.3	1.5	1.1	0.3
Heptanal	0.5	0.7	1.5	1.6	1.8	0.7
7-Tridecanone	2.6	3.7	4.0	4.6	5.9	8.1

Reaction condition: T_{react} = 400 °C, T_{red} = 400 °C, F_{H2} = 100 mL/min, atmospheric pressure

Table C6 The heptanoic acid conversion and yield of products over 0.5Pt/SiO_2 at contact time of 2.89 g.h/mol

	Time on stream (min)					
	30	60	90	120	150	180
Conversion of heptanoic acid	76.7	54.0	45.5	42.0	34.7	32.9
Yield (%)						
Hexene	25.7	20.3	19.6	19.5	16.7	15.7
n-Hexane	40.1	23.7	16.8	14.2	11.0	9.9
2,4-Hexadiene	8.7	6.9	5.3	4.4	2.8	2.4
Heptanal	0	0	0	0	0	0
7-Tridecanone	2.2	3.1	3.8	3.9	4.2	4.9

Reaction condition: T_{react} = 400 °C, T_{red} = 400 °C, F_{H2} = 100 mL/min, atmospheric pressure

Table C7 Product distribution from reaction of heptanal over 0.5Pt/SiO_2 at contact time of 1.15 g.h/mol

	Time on stream (min)					
	30	60	90	120	150	180
Conversion of heptanoic acid	32.3	34.2	34.3	33.6	32.5	34.7
Yield (%)						
Hexene	16.1	17.3	17.3	16.8	16.6	18.1
n-Hexane	13.4	13.9	14.0	14.0	13.3	13.9
2,4-Hexadiene	2.8	3.0	3.0	2.8	2.6	2.7
Heptanal	0	0	0	0	0	0
7-Tridecanone	0	0	0	0	0	0

Reaction condition: T_{react} = 400 °C, T_{red} = 400 °C, F_{H2} = 100 mL/min, atmospheric pressure

3. Effect of temperature

Table C8 The heptanal conversion and yield of products over 0.5Pt/SiO_2 at 320 °C

	Time on stream (min)					
	30	60	90	120	150	180
Conversion of heptanal	58.0	55.7	51.5	52.4	49.5	47.5
Yield (%)						
Hexene	23.2	21.3	21.3	23.4	22.2	23.2
n-Hexane	28.8	28.6	24.8	23.5	22.6	19.9
2,4-Hexadiene	6.0	5.8	5.4	5.5	4.7	4.4
Heptanol	0	0	0	0	0	0
7-Tridecanone	0	0	0	0	0	0

Reaction condition: T_{red} = 400 °C, F_{H2} = 100 mL/min, atmospheric pressure, W/F = 2.89 g·h/mol.

Table C9 The heptanal conversion and yield of products over 0.5Pt/SiO_2 at 340 °C

	Time on stream (min)					
	30	60	90	120	150	180
Conversion of heptanal	75.1	72.8	59.5	57.3	55.8	48.5
Yield (%)						
Hexene	30.4	26.5	23.4	20.2	22.9	20.9
n-Hexane	36.3	38.1	29.4	30.3	26.8	22.5
2,4-Hexadiene	8.4	8.2	6.7	6.8	6.1	5.1
Heptanol	0	0	0	0	0	0
7-Tridecanone	0	0	0	0	0	0

Reaction condition: T_{red} = 400 °C, F_{H2} = 100 mL/min, atmospheric pressure, W/F = 2.89 g·h/mol.

Table C10 The heptanal conversion and yield of products over 0.5Pt/SiO_2 at 360 °C

	Time on stream (min)					
	30	60	90	120	150	180
Conversion of heptanal	92.1	87.7	74.2	69.2	67.7	64.1
Yield (%)						
Hexene	25.4	23.3	27.2	28.3	27.0	23.8
n-Hexane	56.3	54.9	38.7	33.0	32.9	33.0
2,4-Hexadiene	10.4	9.5	8.3	7.8	7.7	7.3
Heptanol	0	0	0	0	0	0
7-Tridecanone	0	0	0	0	0	0

Reaction condition: T_{red} = 400 °C, F_{H2} = 100 mL/min, atmospheric pressure, W/F = 2.89 g·h/mol.

Table C11 The heptanal conversion and yield of products over 0.5Pt/SiO_2 at 400 °C

	Time on stream (min)					
	30	60	90	120	150	180
Conversion of heptanal	100	100	100	100	100	100
Yield (%)						
Hexene	13.3	26.6	36.6	37.0	39.4	40.1
n-Hexane	64.9	62.6	52.1	51.9	49.3	48.9
2,4-Hexadiene	9.5	10.8	11.3	11.1	11.3	11.0
Heptanol	0	0	0	0	0	0
7-Tridecanone	0	0	0	0	0	0

Reaction condition: T_{red} = 400 °C, F_{H2} = 100 mL/min, atmospheric pressure, W/F = 2.89 g·h/mol.

Table C12 The heptanal conversion and yield of products over 0.5Pt-0.2Sn/SiO_2 at 320 °C

	Time on stream (min)					
	30	60	90	120	150	180
Conversion of heptanal	21.8	18.1	16.2	15.6	15.3	15.5
Yield (%)						
Hexene	7.8	6.9	6.0	5.7	5.5	5.4
n-Hexane	6.5	4.7	4.2	4.1	4.0	3.7
2,4-Hexadiene	1.0	1.0	0.8	0.8	0.8	0.8
Heptanol	6.5	5.5	5.2	5.0	5.0	5.6
7-Tridecanone	0	0	0	0	0	0

Reaction condition: T_{red} = 400 °C, F_{H2} = 100 mL/min, atmospheric pressure, W/F = 2.89 g·h/mol.

Table C13 The heptanal conversion and yield of products over 0.5Pt-0.2Sn/SiO_2 at 360 °C

	Time on stream (min)					
	30	60	90	120	150	180
Conversion of heptanal	30.7	28.1	21.9	22.6	21.7	20.8
Yield (%)						
Hexene	13.5	12.9	9.2	9.4	9.1	8.7
n-Hexane	9.7	8.9	6.3	6.5	6.3	6.1
2,4-Hexadiene	2.8	2.4	2.8	3.2	2.8	2.5
Heptanol	4.7	3.9	3.6	3.5	3.5	3.5
7-Tridecanone	0	0	0	0	0	0

Reaction condition: T_{red} = 400 °C, F_{H2} = 100 mL/min, atmospheric pressure, W/F = 2.89 g·h/mol.

Table C14 The heptanal conversion and yield of products over 0.5Pt-0.2Sn/SiO_2 at 380 °C

	Time on stream (min)					
	30	60	90	120	150	180
Conversion of heptanal	55.4	49.5	43.6	40.0	41.8	38.6
Yield (%)						
Hexene	27.5	25.2	22.1	20.9	21.2	19.6
n-Hexane	20.3	17.1	14.5	12.8	13.7	12.7
2,4-Hexadiene	5.5	4.9	4.3	3.8	4.1	3.7
Heptanol	2.1	2.3	2.7	2.5	2.8	2.6
7-Tridecanone	0	0	0	0	0	0

Reaction condition: T_{red} = 400 °C, F_{H2} = 100 mL/min, atmospheric pressure, W/F = 2.89 g·h/mol.

Table C15 The heptanal conversion and yield of products over 0.5Pt-0.2Sn/SiO_2 at 400 °C

	Time on stream (min)					
	30	60	90	120	150	180
Conversion of heptanal	81.7	76.6	71.7	68.4	66.5	65.7
Yield (%)						
Hexene	37.2	36.1	36.9	33.3	32.6	32.6
n-Hexane	35.4	31.9	25.0	25.6	24.9	24.1
2,4-Hexadiene	7.1	6.3	7.6	7.2	6.8	6.7
Heptanol	2.0	2.3	2.2	2.3	2.2	2.3
7-Tridecanone	0	0	0	0	0	0

Reaction condition: T_{red} = 400 °C, F_{H2} = 100 mL/min, atmospheric pressure, W/F = 2.89 g·h/mol.

4. Effect of metal alloy and support

Table C16 The heptanoic acid conversion and yield of products over 0.5Pt-0.2Fe/SiO_2

	Time on stream (min)					
	30	60	90	120	150	180
Conversion of heptanoic acid	49.9	49.4	49.1	46.6	46.3	47.6
Yield (%)						
Hexene	20.2	22.1	22.0	20.0	20.9	21.3
n-Hexane	19.6	15.7	16.1	16.4	14.3	15.0
2,4-Hexadiene	4.7	4.1	4.3	4.0	3.5	3.6
Heptanal	2.3	4.1	3.8	3.1	4.5	4.6
7-Tridecanone	3.1	3.4	2.9	3.1	3.1	3.1

Reaction condition: T_{react} = 400 °C, T_{red} = 400 °C, F_{H2} = 100 mL/min, atmospheric pressure, W/F = 2.89 g·h/mol.

Table C17 The heptanoic acid conversion and yield of products over 0.5Pt-0.2Ga/SiO_2

	Time on stream (min)					
	30	60	90	120	150	180
Conversion of heptanoic acid	49.3	45.3	31.7	37.9	34.3	33.6
Yield (%)						
Hexene	17.6	16.8	13.0	16.4	14.5	14.4
n-Hexane	19.2	17.2	8.9	11.0	8.6	7.7
2,4-Hexadiene	5.3	4.8	2.5	2.8	2.1	1.9
Heptanal	1.2	1.9	2.8	4.1	4.7	5.4
7-Tridecanone	6.0	4.6	4.5	3.6	4.4	4.2

Reaction condition: T_{react} = 400 °C, T_{red} = 400 °C, F_{H2} = 100 mL/min, atmospheric pressure, W/F = 2.89 g·h/mol.

Table C18 The heptanoic acid conversion and yield of products over 0.5Pt-0.2Sn/SiO_2

	Time on stream (min)					
	30	60	90	120	150	180
Conversion of heptanal	45.4	51.6	52.8	53.4	53.0	45.8
Yield (%)						
Hexene	20.3	24.0	24.5	25.8	24.9	21.8
n-Hexane	12.3	13.7	14.1	13.7	13.2	11.0
2,4-Hexadiene	3.6	4.0	4.0	3.9	3.7	3.1
Heptanal	4.8	6.2	7.0	6.9	7.8	6.7
7-Tridecanone	4.4	3.7	3.3	3.2	3.4	3.3

Reaction condition: T_{react} = 400 °C, T_{red} = 400 °C, F_{H2} = 100 mL/min, atmospheric pressure, W/F = 2.89 g·h/mol.

Table C19 The heptanoic acid conversion and yield of products over 0.5Pt-0.2Sn/TiO_2

	Time on stream (min)					
	30	60	90	120	150	180
Conversion of heptanoic acid	30.5	26.7	26.4	29.2	29.2	30.6
Yield (%)						
Hexene	0.3	1.1	0.8	0.9	2.4	2.1
n-Hexane	0.2	0.4	0.3	0.3	0.8	0.7
2,4-Hexadiene	0.1	0.1	0.1	0.1	0.1	0.2
Heptanal	0.5	0.9	0.8	0.9	1.8	1.7
7-Tridecanone	29.4	24.2	24.4	27.0	24.1	25.9

Reaction condition: T_{react} = 400 °C, T_{red} = 400 °C, F_{H2} = 100 mL/min, atmospheric pressure, W/F = 2.89 g·h/mol.

5. Effect of Sn content

Table C20 The heptanoic acid conversion and yield of products over 0.5Pt-0.3Sn/SiO_2

	Time on stream (min)					
	30	60	90	120	150	180
Conversion of heptanoic acid	44.9	50.4	51.6	55.8	59.3	54.6
Yield (%)						
Hexene	15.6	25.3	25.3	27.0	28.5	26.3
n-Hexane	18.8	11.7	13.1	14.6	15.8	14.8
2,4-Hexadiene	4.4	4.0	4.5	4.9	5.1	5.0
Heptanal	0	6.1	5.4	5.6	5.8	5.1
7-Tridecanone	6.1	3.3	3.3	3.7	4.1	3.4

Reaction condition: T_{react} = 400 °C, T_{red} = 400 °C, F_{H2} = 100 mL/min, atmospheric pressure, W/F = 3.70 g·h/mol.

Table C21 The heptanoic acid conversion and yield of products over 0.5Pt-0.5Sn/SiO_2

	Time on stream (min)					
	30	60	90	120	150	180
Conversion of heptanoic acid	61.3	51.5	51.8	51.4	52.4	50.4
Yield (%)						
Hexene	32.3	27.1	26.9	26.4	26.9	25.8
n-Hexane	12.7	8.5	8.6	8.7	8.6	8.4
2,4-Hexadiene	5.4	3.4	3.7	3.2	3.1	2.8
Heptanal	6.3	7.7	7.5	8.2	9.4	9.2
7-Tridecanone	4.6	4.8	5.1	4.9	4.4	4.2

Reaction condition: T_{react} = 400 °C, T_{red} = 400 °C, F_{H2} = 100 mL/min, atmospheric pressure, W/F = 6.07 g·h/mol.

6. Effect of hydrogen partial pressure

Table C22 The heptanoic acid conversion and yield of products over 0.5Pt-0.5Sn/SiO_2 at H_2 carrier gas: 100 mL/min

	Time on stream (min)					
	30	60	90	120	150	180
Conversion of heptanoic acid	66.9	59.2	58.7	56.8	56.1	55.7
Yield (%)						
Hexene	34.2	31.5	30.7	29.6	33.2	29.5
n-Hexane	14.3	11.8	11.7	11.5	11.8	11.8
2,4-Hexadiene	5.9	4.2	4.9	4.5	5.2	5.1
Heptanal	6.9	5.8	5.8	5.1	4.9	4.6
7-Tridecanone	5.6	5.9	5.6	5.4	4.1	4.7

Reaction condition: T_{react} = 400 °C, T_{red} = 400 °C, F_{H2} = 100 mL/min, atmospheric pressure, W/F = 3.01 g·h/mol.

Table C23 The heptanoic acid conversion and yield of products over 0.5Pt-0.5Sn/SiO_2 at H_2 carrier gas: 75 mL/min

	Time on stream (min)					
	30	60	90	120	150	180
Conversion of heptanoic acid	66.7	62.5	55.5	51.9	46.7	45.1
Yield (%)						
Hexene	36.9	34.6	31.9	28.7	26.5	25.9
n-Hexane	12.5	12.3	9.2	8.9	7.9	6.2
2,4-Hexadiene	5.8	6.1	4.2	4.0	3.8	3.0
Heptanal	6.6	5.3	6.2	6.4	4.7	6.8
7-Tridecanone	4.9	4.2	4.0	3.9	3.8	3.2

Reaction condition: T_{react} = 400 °C, T_{red} = 400 °C, F_{H2} = 100 mL/min, atmospheric pressure, W/F = 3.01 g·h/mol.

Table C24 The heptanoic acid conversion and yield of products over 0.5Pt-0.5Sn/SiO_2 at H_2 carrier gas: 50 mL/min

	Time on stream (min)					
	30	60	90	120	150	180
Conversion of heptanoic acid	63.8	38.9	30.5	28.2	27.1	25.9
Yield (%)						
Hexene	36.8	21.3	17.9	16.8	15.9	15.0
n-Hexane	12.5	4.5	3.5	2.6	2.5	2.1
2,4-Hexadiene	8.6	2.7	2.3	1.5	1.4	1.2
Heptanal	0	6.4	3.4	4.5	4.6	5.0
7-Tridecanone	5.9	4.0	3.4	2.8	2.7	2.6

Reaction condition: T_{react} = 400 °C, T_{red} = 400 °C, F_{H2} = 100 mL/min, atmospheric pressure, W/F = 3.01 g·h/mol.

APPENDIX D

XRD PATTERN

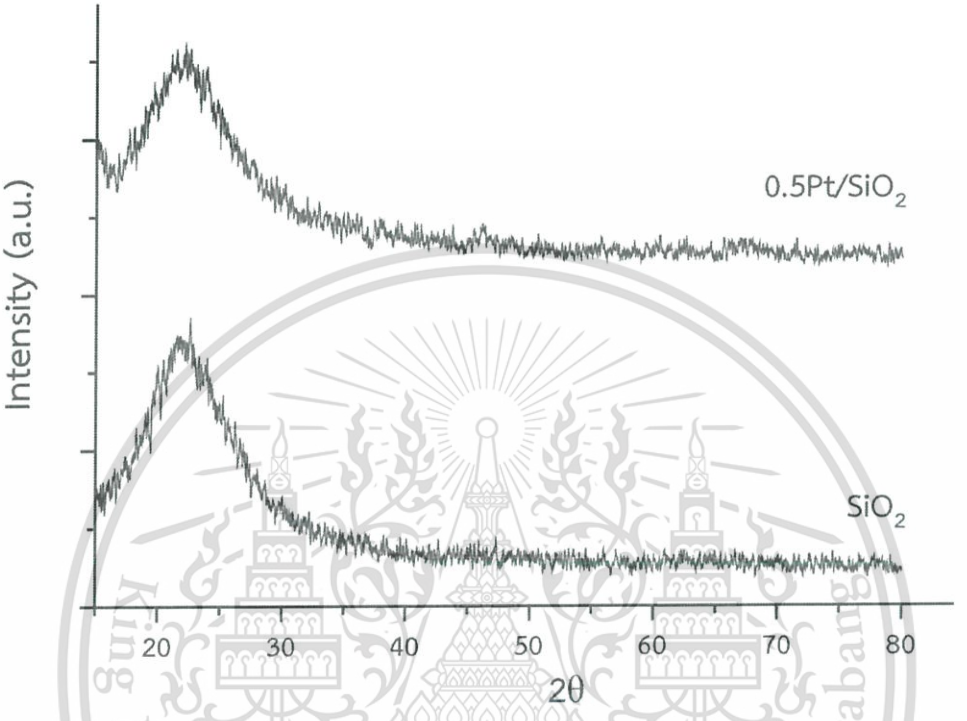

Figure D1 XRD patterns of $0.5Pt/SiO_2$ vs SiO_2.

APPENDIX E

XPS SPECTRUM

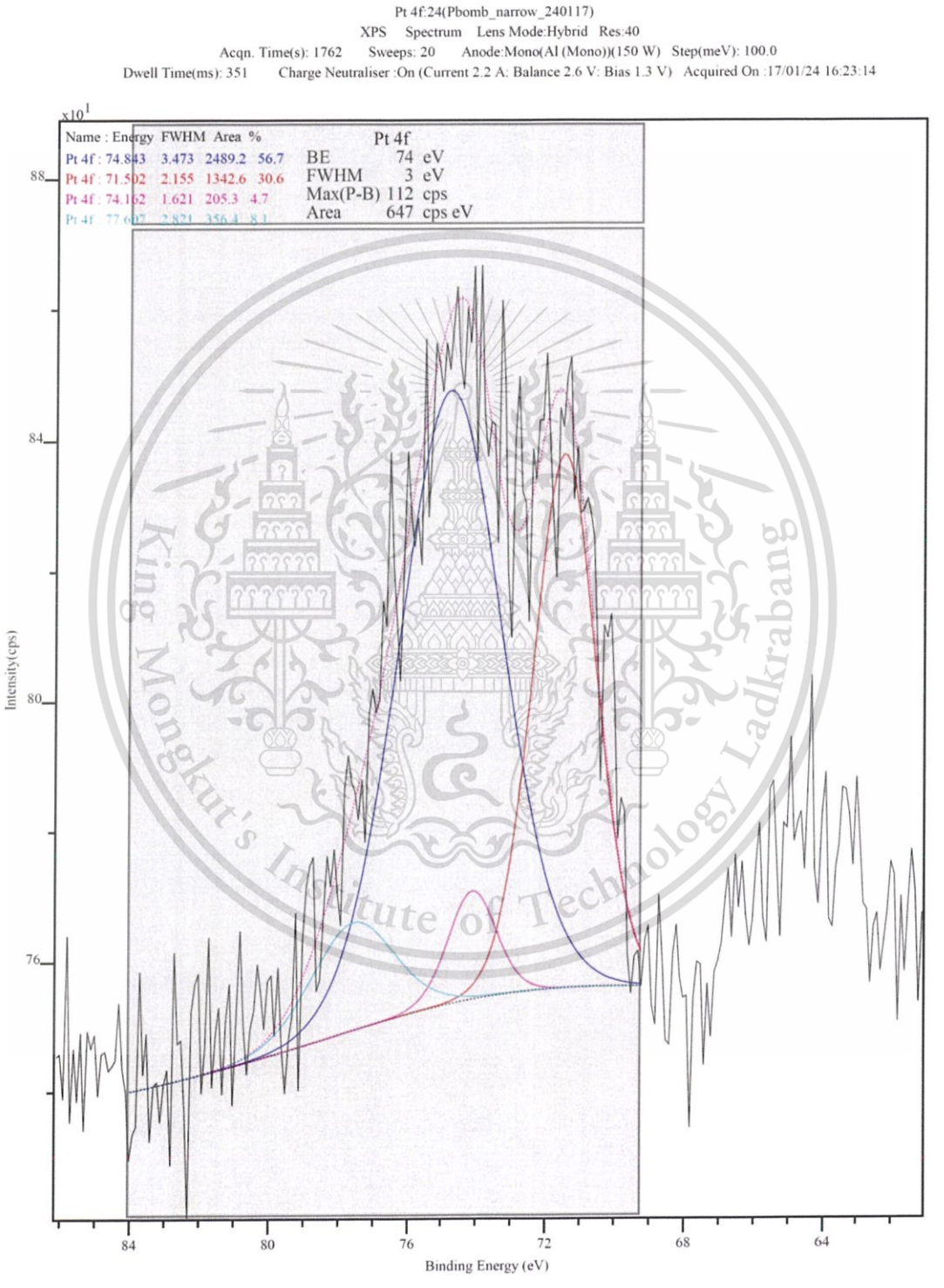

Figure E1 XPS spectrum of 0.5Pt-0.5Sn/SiO_2

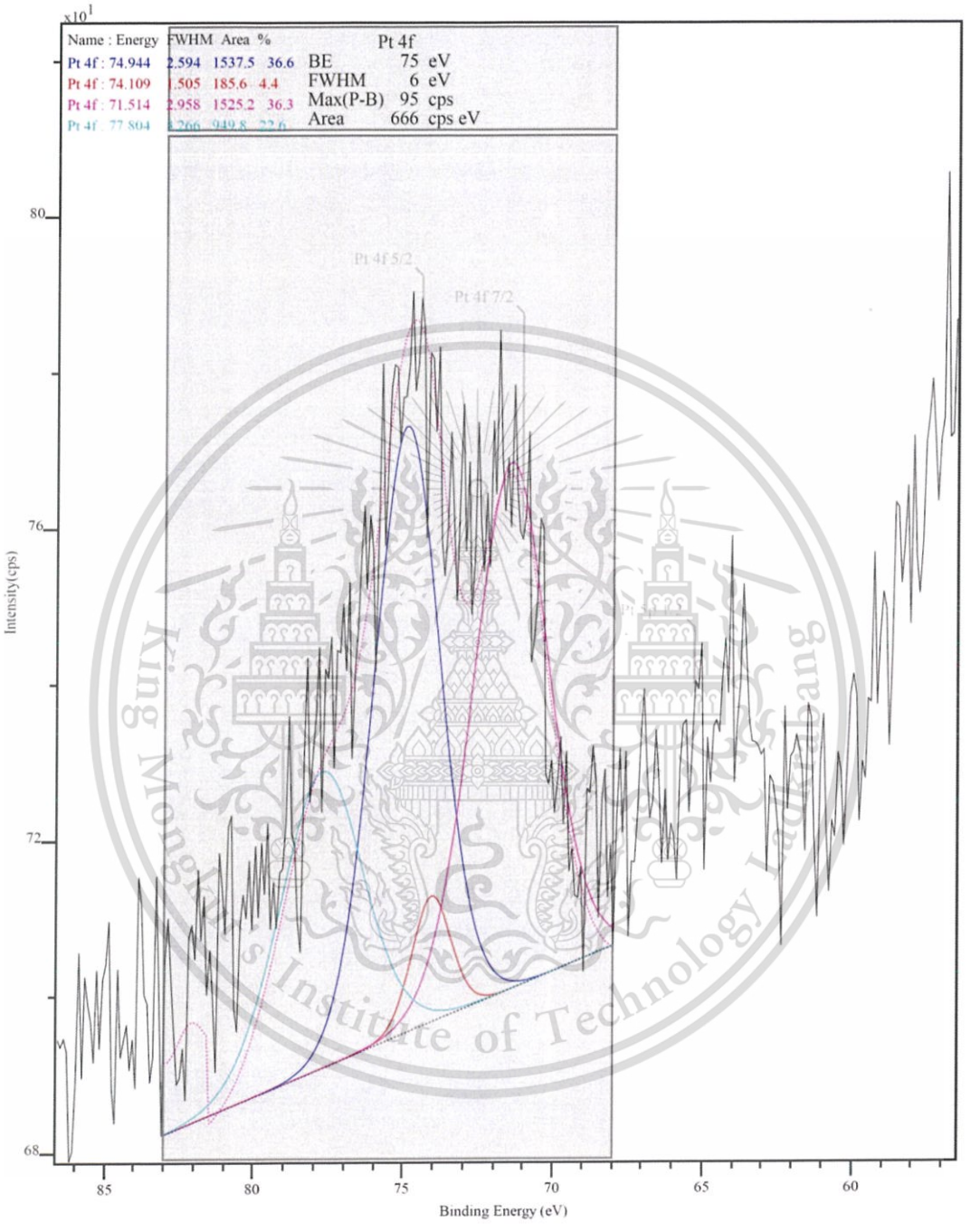

Figure E2 XPS spectrum of 0.5Pt/SiO_2

AUTHOR BIOGRAPHY

Miss Patcharee Jutalikitwong was born on July 22th, 1992 in Bangkok. She graduated a Senior High school in Science and Mathematics (Gifted program) from Mahaprutaram Girls' school (under the Royal Patronage of her Majesty the Queen) and a Bachelor degree in Industrial Chemical Science from the Department of Chemical, Faculty of Science, King Mongkut's Institute of Technology Ladkrabang in 2015. She has been a graduate student in Petrochemicals and Hydrocarbon Chemistry program of Faculty of Science, King Mongkut's Institute of Technology Ladkrabang, since 2015.

Work experiences:

Mar – Apr 2014	Internship at IRPC Public Company Limited.
2015 –2017	Teacher Assistant, King Mongkut's Institute of Technology Ladkrabang.

Conferences

2017 **Patcharee Jutaliketwong,** Tosapol Maluangnont, and Tawan Sooknoi, "Deoxygenation of heptanoic acid over alloyed-Pt catalysts: Model of terminal olefins production from fatty acids", Poster presentation, Pure and Applied Chemistry International Conference 2017 (PACCON 2017), February 2-3, 2017, Centra Government Complex Hotel & Convention Centre Bangkok, Thailand.

Publication

2017 **Patcharee Jutaliketwong,** Tosapol Maluangnont, and Tawan Sooknoi, 2017. "Deoxygenation of heptanoic acid over alloyed-Pt catalysts: Model of terminal olefins production from fatty acids.", *PACCON 2017 Conference Proceedings*. : 1311–1315.

PUBLICATION

Deoxygenation of heptanoic acid over alloyed-Pt catalysts: Model of terminal olefins production from fatty acids

Patcharee Jutaliketwong[1], Tosapol Maluangnont[2, 3] and Tawan Sooknoi[1, 2]*

[1]*Department of Chemistry, Faculty of Science, KMITL, Bangkok 10520, Thailand*
[2]*Catalytic Chemistry Research Unit, Faculty of Science, KMITL, Bangkok 10520, Thailand*
[3]*College of Nanotechnology, KMITL, Bangkok, 10520 Thailand*

*e-mail: kstawan@gmail.com

Abstract: Terminal olefins (1-alkenes) are of importance for several industrial applications. In this work, the catalytic deoxygenation of heptanoic acid to 1-hexene was conducted at 400 °C under atmospheric H_2 in a fixed bed flow reactor. Heptanoic acid was employed as the model compound for the production of terminal olefins from fatty acids. Silica (titania)-supported Pt catalysts (0.5%), including the Pt alloyed with Sn (0.5%Pt, 0.2%Sn), were synthesized by spray impregnation using H_2PtCl_6 (and $SnCl_2$) as the corresponding metallic precursors. It was found that the Pt/SiO_2 catalyst exhibited decarboxylation activity, producing *n*-hexane as the main product. In contrast, the alloying of Pt by Sn suppresses the decarboxylation and hydrogenation activities, while promoting the decarbonylation activity. So, 1-hexene can be selectively produced (29% selectivity at 50% conversion). On the other hand, over the $0.5\%Pt/TiO_2$, only the ketonization product (7-tridecanone, 95% selectivity) was produced at similar conversion of heptanoic acid.

1. Introduction

Terminal olefins (1-alkenes) are prominent substrate for the production of daily life chemicals such as detergent, alcohols, plasticizers, polymers, surfactants and lubricants.[1] However, the growing energy requirement combined with declining fossil fuel reserves stimulates the use of alternative renewable resources. Potential feedstocks include vegetable oils since they provide high energy density and they are structurally similar to petroleum-based fuels.[2]

The vegetable oil feeds consist of triglycerides, which can be easily converted to fatty acids. Catalytic deoxygenation of obtained fatty acids can produce terminal olefins via the removal the carboxylic group without breaking the hydrocarbon chains.[3] Two plausible pathways for the deoxygenation of carboxylic acids have been identified to be (i) decarboxylation which yields CO_2 and an *n*-alkane, and (ii) decarbonylation which yields CO, water and the corresponding alkene.[4]

Recent work on the decarboxylation and decarbonylation of carboxylic acids over supported noble metal catalysts (Cu, Ni, Pd or Pt) are often performed in the presence of hydrogen to inhibit catalyst deactivation.[5-8] While it has been suggested that decarbonylation has taken place (from the evolution of gaseous CO), mostly paraffinic products were obtained likely because of the rapid hydrogenation of any alkenes formed in the process.[9, 10]

Therefore, it is important to selectively obtain olefins by suppressing its hydrogenation to paraffins. This work presents a catalyst exhibiting high selectivity to alkene products (especially terminal olefins), while maintaining relatively high activity with minimal deactivation. Incorporation of a tin promoter as metal alloys to supported Pt catalysts, is a promising route. In addition,

the product distribution could well be influenced by the nature of the support.

2. Experimental Methods

2.1. Catalyst Preparation

Supported platinum catalysts (Pt/SiO_2 and Pt/TiO_2) and platinum-metal alloyed catalysts ($Pt\text{-}Sn/SiO_2$) were used in this study. Pt/SiO_2 and Pt/TiO_2 were prepared by sprayed-incipient wetness impregnation using the aqueous solution prepared from chloroplatinic acid hexahydrate ($H_2PtCl_6 \cdot 6H_2O$, Sigma Aldrich) to obtain a 0.5 wt.% Pt loading into SiO_2 (CARLO ERBA) or TiO_2 (P25, Degussa). $Pt\text{-}Sn/SiO_2$ catalyst was similarly prepared by sprayed-impregnation, using the co-ethanolic precursor solutions prepared from hexa-chloroplatinic acid and tin chloride ($SnCl_2 \cdot 2H_2O$, QRëC) with required concentrations to obtain 0.5 wt.% Pt and 0.5 wt.% Sn loadings. After impregnation, the catalysts were dried overnight in an oven at 110 °C.

2.2 Catalyst Characterization

The reducibility of the metal/alloyed metal catalysts can be determined by a temperature-programmed reduction under H_2 gas (H_2-TPR). Prior to an analysis, the sample (approximately 0.1 g) was treated in nitrogen (flow rate of 30 mL/min) at 200 °C (10 °C/min) for 1 h. The TPR experiments were carried out under 10% H_2 in Ar at the heating rate of 10 °C/min, from 50 to 700 °C. The effluent gases were analyzed using an online VICI thermal conductivity detector (TCD).

2.3 Catalyst Activity

Gas-phase catalytic conversion of heptanoic acid was investigated in a continuous fixed bed reactor. The 15 wt.% heptanoic acid in *n*-octane was continuously vaporized into the reactor inlet at a feed rate of 5 mL(liq)/h using a syringe pump. The catalyst (sieved into 250-450 μm diameter) was placed in a glass tube reactor and sandwiched by glass wool and glass bead. Reaction conditions were as follows: temperature, 400 °C; ambient pressure; carrier gas, H_2 (100 mL/min); contact time (W/F), 2 $g \cdot h \cdot mol^{-1}$. Products were analyzed by online by an HP6890 gas chromatography (GC) equipped with a DB-1 column (30 m × 0.32 mm) and FID detector.

3. Results & Discussion

3.1 Temperature programmed reduction

Figure 1 shows the reducibility obtained by TPR measurements. The $0.5\%Pt/SiO_2$ catalyst showed only a single reduction peak above 130 °C corresponding to Pt reduction.[11] The H_2 consumption at 400–600 °C were larger for the $0.5\%Pt/TiO_2$ (0.202 μmol/g) than for $0.5\%Pt/SiO_2$ (0.173 μmol/g), and were much higher than that required to reduce all PtO particles to metallic Pt. Assuming that the initial oxidation state of Pt in the Pt/TiO_2 samples is the same as that in $0.5\%Pt/SiO_2$, this amount of H_2 consumption is likely the combination of the reduction of PtO to metallic Pt, and also of Ti^{4+} to Ti^{3+} on the TiO_2 samples via hydrogen spillover mechanism.[12-14]

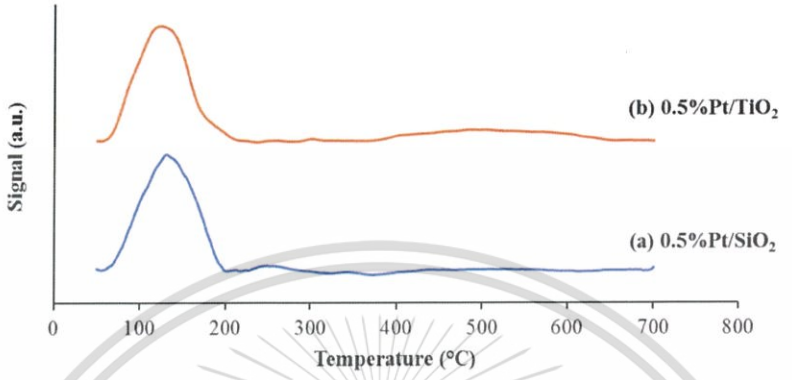

Figure 1. H_2–TPR profile of 0.5%Pt/SiO_2 and 0.5%Pt/TiO_2 catalysts.

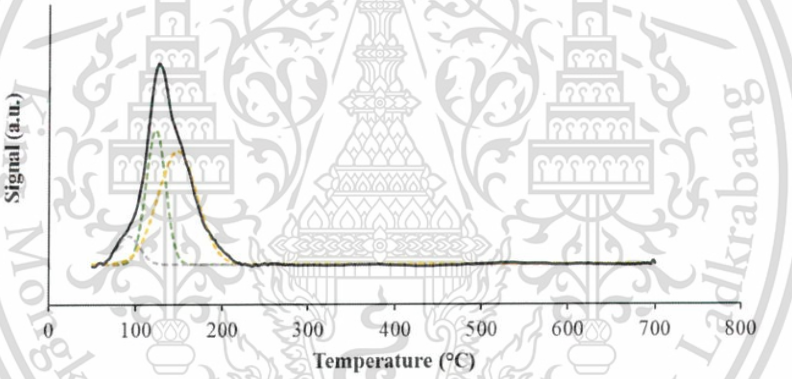

Figure 2. H_2–TPR profile of 0.5%Pt-0.2%Sn/SiO_2.

For the 0.5%Pt-0.2%Sn/SiO_2 catalyst (Figure 2), the H_2 consumption can be deconvoluted into three components. The first and second peak were found at around 90–120 °C and corresponded to the reduction of platinum-oxide species, while the latter peak at about 150 °C is assigned to the reduction of Pt-Sn alloy.

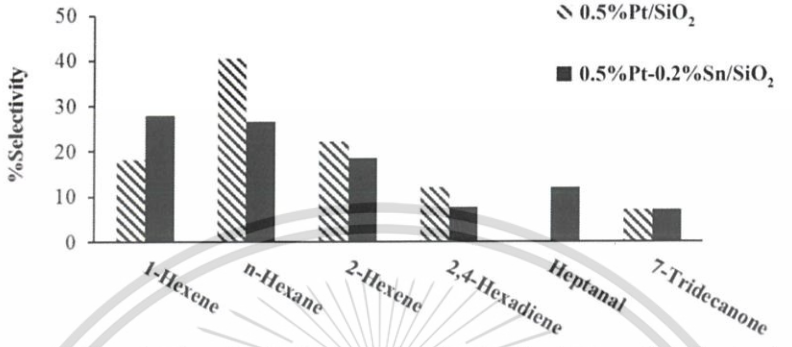

Figure 3. Effect of catalyst alloying. Products selectivity from the deoxygenation of heptanoic acid over 0.5%Pt/SiO_2 and 0.5%Pt-0.2%Sn/SiO_2.

3.2. Catalytic conversion of heptanoic acid

The deoxygenation of heptanoic acid at 400 °C under 100 % H_2 was investigated over 0.5%Pt/SiO_2 and 0.5%Pt/TiO_2. As shown in Table 1, the conversion and yields were very different. The Pt/SiO_2 proceeds selectively via the decarbonylation and decarboxylation pathway producing 1-hexene and hexanes. On the other hand, the ketonization pathway is dominant for heptanoic acid when over Pt/TiO_2, producing 7-tridecanone.

Table 1. Product distribution from reaction of heptanoic acid over 0.5%Pt/SiO_2 and 0.5%Pt/TiO_2 catalysts.

	Catalyst	
	0.5%Pt/SiO_2	0.5%Pt/TiO_2
W/F (g·h/mol)	2.9	2.9
Conversion (%)	54.0	26.6
Yield (%)		
1-Hexene	7.5	0.7
n-Hexane	23.7	0.4
2-Hexane	12.8	0.3
2,4-Hexadiene	6.8	0.1
Heptanal	-	1.0
7-Tridecanone	3.2	24.1

Figure 3 shows that while Pt is active for the deoxygenation, isomerization to internal olefins, the hydrogenation of olefinic products to paraffins is also significant. The addition of tin to make the alloy has a positive effect regarding terminal olefin content (28.5% for Pt-Sn vs. 18.7% for Pt), while reducing the undesirable paraffin content (28.0% for Pt-Sn vs. 40.1% for Pt). As reported in the literature,[15-17] tin can function both as a structural (geometric) and an electronic promoter. It is proposed that the addition of tin modifies catalyst activity by reducing platinum ensemble size and by altering heats of adsorption.

Cortright and Dumesic[16] used micro-calorimetric studies to show that addition of tin decreases the number of sites that strongly interact with hydrogen. So, the hydrogenation of olefins products to paraffins is then dramatically shutdown.

4. Conclusion

The type of support is shown to have a significant effect on the deoxygenation pathway of heptanoic acid. That is, Pt/SiO_2 catalysts are active in the deoxygenation whereas Pt/TiO_2 catalysts are more selective to ketonization. The addition of tin to the Pt/SiO_2 monometallic catalyst produced a remarkable shift in the product distribution to the desired terminal olefin. Importantly, since Sn itself does not dissociate H_2, it does not possess intrinsic hydrogenation properties. So, the simultaneous increase of both activity and selectivity indicates the formation of a new type of active site in the alloyed catalyst which is different in nature when compared with the original Pt.

Acknowledgements

The assistance of the Catalytic Chemistry Research Unit and the Department of Chemistry, Faculty of Science, KMITL are acknowledged. This work is financially supported by the Thailand Research Fund TRG5780160 (*Malhuangnont, T.*) and by the Basic Research Grant BRG568007 (*Sooknoi, T.*).

References

1. Amin, M. A.; Mohsen, Q.; Mostafa, N. Y.; El-Bagoury, N.; Al-Refaie, A.; Bairamov, A. K.; Al-Maaesab, S.; Murill, E. M.; Al-Qahtani, S. A. *Int. J. Electrochem. Sci.* **2014**, 9, 2631–2648.
2. Gosselink, R. W.; Hollak, S. A. W.; Chang, S.-W.; Haveren, J. van; de Jong, K. P.; Bitter, J. H.; van Es, D. S. *ChemSusChem* **2013**, 6, 1576–1594.
3. Lilis, H.; Ahmad Z. A.; Abdul, R. M. *RENEW SUST ENERG REV* **2015**, 42, 1223–1233.
4. Gwen, J. S. D.; Elinor, L. S.; Jérôme, L. N.; Johan, P. M. S.; Johannes, H. B.; *Green Chem* **2015**, 17, 3231–3250.
5. Boda, L.; Onyestyak, G.; Solt, H.; Lonyi, F.; Valyon, J.; Thernesz, A. *Appl. Catal. A* **2010**, 374, 158–169.
6. Madsen, A. T.; Ahmed, E. H.; Christensen, C. H.; Fehrmann, R.; Riisager, A.; *Fuel* **2011**, 90, 3433–3438.
7. Peng, B.; Yuan, X.; Zhao, C.; Lercher, J. A. *J. Am. Chem. Soc.* **2012**, 134, 9400–9405.
8. Berenblyum, A. S.; Shamsiev, R. S.; Podoplelova, T. A.; Danyushevsky, V. Y. *Russ. J. Phys. Chem.* **2012**, 86, 1199–1203.
9. Snåre, M.; Kubickova, I.; Mäki-Arvela, P.; Eränen, K.; Murzin, D. Y. *Ind. Eng. Chem. Res.* **2006**, 45, 5708–5715.
10. Immer, J.G.; Kelly, M.J.; Lamb, H. H. *Appl. Catal. A* **2010**, 375, 134–139.
11. De Miguel, S. R.; Román-Martınez, M. C.; Cazorla-Amorós D.; Jablonski E. L.; Scelza O. A. *Catal Today* **2001**, 66, 289–95.
12. Huizinga, T.; Prins, R. *J. Phys. Chem.* **1981**, 85, 2156.
13. Conesa, J. C.; and Sofia, J. *J. Phys. Chem.* **1984**, 86, 1392.
14. Conesa, J. C.; Malet, P.; Munuera, G.; Sanz, J.; Soria, J. *J. Phys. Chem.* **1984**, 88, 2986.
15. Arteaga, J. G.; Anderson, J. A.; Rochester, C. H. *J Catal* **1999**,187, 219–229.
16. Cortright R. D.; Dumesic J. A. *J Catal* **1994**,148, 771–778.
17. Verbeek H.; Sachtler W. M. H. *J Catal* **1976**, 42, 257–267.